# Evolutionary games and population dynamics

Vlastimil Křivan

Department of Theoretical Ecology, Biology Center, Academy of Sciences of the Czech Republic, and Department of Mathematics and Informatics, Faculty of Science, University of South Bohemia, Branišovská 31, 370 05 České Budějovice, Czech Republic. E-mail: vkrivan@seznam.cz

Lecture notes for Seminar in Differential Equations – Kamenice nad Lipou, May 19-23, 2008

Version of June 2, 2008

# Contents

# Chapter 1

# Evolutionarily game theory

Evolutionarily game theory assumes a population where individuals can use different strategies. These strategies are interpreted as different phenotypes. There are two distinct possibilities: either all individuals use the same strategy in which case the population is monomorphic, or population is polymorphic, if population consists of several phenotypes. The classical evolutionarily game theory started with the assumption that the population is monomorphic (Maynard Smith and Price 1973). The theory assumes that phenotypes are inherited by offsprings, which is realistic in the case of clonal reproduction but questionable in the case of sexual reproduction. Payoff to an individual adopting some strategy is called fitness which is assumed to be proportional to the expected number of offsprings. As phenotypes with a higher fitness produce more offsprings, these phenotypes will spread in the population replacing those with a lower fitness. Evolutionarily game theory aims to study the stable equilibria of evolution and it became one of the major methodologies to study evolution. One of the problem with the theory since it was conceived by Maynard Smith and Price (1973) was the fact that this theory aims to explain the outcome of an inherently dynamical process without actually specifying the underlying dynamics. This shortcoming was pointed out by Taylor and Jonker (1978). However, it is quite surprising that even if some evolutionary dynamics are introduced, the corresponding equilibrium often is that which corresponds to the one defined by Maynard Smith and Price (1973). Many articles therefore try to reconciliate the relation between the classical evolutionarily game theory with the results when some particular dynamics are used (Cressman 1992).

Another complication with the evolutionarily game theory is the fact that this name is used for two different types of games. The first type are so called pairwise contest games where a given individual plays against an opponent that was randomly chosen from the population. These games are then formally the same as those from the classical two-person game theory. However, there is

another type of games, so called games against the field in which there is no specific opponent for a given individual. In this case the individual payoff depends on what everyone in the population is doing.

I will start with the classical example introduced by Maynard Smith and Price (1973) that laid foundations of evolutionarily stability.

## 1.1 Hawk-Dove game

One of the first evolutionarily games was invented to understand evolution of aggressiveness among animals (Maynard Smith and Price 1973). Although many species have strong weapons (e. g., teeth, horns), it is puzzling observation that in many cases the antagonistic encounters do not result in fight. In fact, such encounters often result in a complicated series of behaviors, but without causing serious injuries. For example, in contests between male red deers, the two contestants first approach each other, and provided one does not withdraw, the contest escalates to roar contest and to so called parallel walk. Only if this does not lead to withdrawal of one deer, fight follows. It was observed (Maynard Smith 1982) that out of 50 encounters, only 14 resulted in fight. The obvious question is why do not animals always end up in the fight? As it is good for an individual to get the resource, Darwinian selection seems to suggest that individuals should fight whenever possible. One possible answer to this question is that such a behavior is for the good of the species, because any species following this aggressive strategy would die out quickly. Then we should accept that the unit of selection is not an individual, and abandon Darwinian "survival of the fittest".

Hawk-Dove model explains animal contest behavior from the Darwinian point of view. This model considers two strategies, that differ in the level of aggressiveness, in a single species population. The highly aggressive strategy (or phenotype) is called Hawk and the strategy with low level of aggressiveness is called Dove. The question is, what should be distribution of these two strategies in a population? Should all individuals use Hawk strategy, Dove strategy, or a mixture of these two? These model assumes pairwise contests in which exactly two individuals are involved. To quantify these two strategies we need to specify how Darwinian fitness increases (decreases) after each encounter between two opponents. Change in fitness $W$ depends on the strategy the two opponents use. For Hawk-Dove game there are four possibilities:

- When an individual playing strategy $H$ encounters an individual playing strategy $D$ it always wins and its fitness increases by $V$ units. I write $W(H, D) = V$.

- When an individual playing strategy $D$ encounters an individual playing strategy $H$ it always withdraws and its fitness does not change. I write $W(D, H) = 0$.

- An encounter between two individuals playing strategy $H$ will always lead to fight. One individual will win and its fitness increases by $V$, one individual will loose and it fitness decreases by $C$ units. In average, the change in fitness is equal to $W(H,H) = (V-C)/2$.

- An encounter between two individuals playing strategy $D$ does not lead to fight and both contestants share the reward equally, i. e., $W(D,D) = V/2$.

The above evaluation of each strategy lead to the following payoff table that specifies the payoff for the raw player. The payoffs for the column player are assumed to be symmetric, which is why such games are called symmetric games in the literature.

|   | $H$ | $D$ |
|---|-----|-----|
| $H$ | $\frac{V-C}{2}$ | $V$ |
| $D$ | $0$ | $\frac{V}{2}$ |

Here, the payoff of the player one that uses strategy H against the second (column) player that uses say strategy D is equl to V and so on.

Now, I want to know which of the two strategies is better and will spread in the population. First, let us consider a resident population where all individuals use strategy $D$. Now, consider a mutant with strategy $H$ in this population. Because fitness of such a mutant will be higher than is the fitness of residents

$$W(H,D) = V > W(D,D) = 0$$

this mutant will, initially (i. e., when at low density) spread in the resident population. Thus, it seems that strategy $H$ is better than is strategy $D$. Can mutants that use strategy $D$ spread in the resident population where all individuals use strategy $H$? Because

$$W(D,H) = 0$$

and

$$W(H,H) = \frac{V-C}{2}$$

there are two possibilities. If $C < V$, then $W(H,H) > W(D,H)$ and mutants (playing strategy D) cannot spread in the population. In this case, strategy $H$ is resistant with respect to invasions of mutants that use strategy $D$. If $C > V$, then $W(D,H) > W(H,H)$ and strategy $D$ can spread in the resident population where all individuals use strategy $H$.

It follows that it is a priori impossible to say which of the two strategies is better then the other. I remark that neither strategy $D$ nor strategy $H$ is superior. To proceed, I consider mixed strategies where individuals play $H$ with probability $p$ and $D$ with probability $1-p$. Such a mixed strategy will be denoted as $pH + (1-p)D$.

Fitness of strategies $H$ and $D$ in the population that plays the mixed strategy is

$$W(H, pH + (1-p)D) = pW(H, H) + (1-p)W(H, D) = V - \frac{p}{2}(V + C)$$

and

$$W(D, pH + (1-p)D) = pW(D, H) + (1-p)W(D, D) = (1-p)\frac{V}{2}.$$

If $p < V/C$, then $W(H, pH + (1-p)D) > W(D, pH + (1-p)D)$ and the strategy $H$ increases in the population. If $p > V/C$, then $W(H, pH + (1-p)D) < W(D, pH + (1-p)D)$ and strategy $D$ spreads in the population.

The mixed strategy $p = V/C$ resists invasions of both strategies $H$ and $D$ and it is called the evolutionarily stable strategy (ESS). Parameter $C$ measures the damage one individual can cause to his opponent. The model predicts that if this cost $C$ is high then aggressiveness in the population will be low. In other words, the species that pose strong weapons (e.g., antlers in deers) should solve conflicts without direct fights. The level of aggressiveness in species that do not have such weapons should be much higher and conflicts end often in fight where one of the opponents is killed or seriously injured. For example, biological doves are known to be very aggressive when caged. A similar reasoning lead to "arms race" during the Cold war as it was generally believed that weapons of mass destruction can prevent the opponent to strike first.

## 1.2   Darwinian evolution vs. group selection

Darwinism assumes that selection operates at the level of an individual, maximizing individual fitness. However, this is not the only possibility. Some biologists (e. g., Gilpin 1975) postulated that selection operates on a larger unit, a group, maximizing the benefit of this unit (e. g., a population, a species etc.). This approach was termed group selection. Some others suggested that selection operates on a lower gene level (Dawkins 1976). The Hawk-Dove game allows to show clearly the difference between the group and Darwinian selection.

Let us consider a mixed strategy in the Hawk-Dove game. If individuals are monomorphic the individual fitness and the average fitness in the population is the same

$$W(pH+(1-p)D, pH+(1-p)D) = pW(H, pH+(1-p)D)+(1-p)W(D, pH+(1-p)D) = \frac{V}{2} - \frac{C}{2}p^2.$$

Thus, the group selection should maximize this average fitness, which implies $p = 0$. In other words, the level of aggressiveness in the population should be zero and individual fitness equals $V/2$.

On the contrary, at the evolutionarily stable equilibrium $p = V/C$, individual fitness is

$$\frac{V}{C}W(H, pH + (1-p)D) + (1 - \frac{V}{C})W(D, pH + (1-p)D) = \frac{V}{2}(1 - \frac{V}{C}),$$

thus always smaller than $\frac{V}{2}$.

We observe that when selection operates on an individual level, fitness is lower than in the case of group selection. However, in the case of group selection, the population is not resistant to invasions of aggressive mutants and such a strategy cannot be considered as an end point of evolution.

## 1.3 Normal form games

In these notes I will mainly use so called normal form games. These games consists of players, a finite number of elementary strategies $e_1, \ldots, e_n$ and a payoff matrix $U$.

DEFINITION 1 *A mixed strategy* $p = (p_1, \ldots, p_n)$ *defines probabilities* $p_i$, *with which elementary strategies* $e_1, \ldots, e_n$ *are played. The set of all mixed strategies is the probability simplex*

$$S_n = \{p \in R^n \mid p_i \geq 0, \ \sum_{i=1}^{n} p_i = 1\}.$$

I remark that the elementary strategy $e_i$ can be also written as a mixed strategy $e_i = \{0, \ldots, 1, \ldots 0\}$ where 1 is at the $i$-th place.

DEFINITION 2 *Matrix* $U = (u_{ij})_{i,j=1}^{n}$, *where* $u_{ij}$ *is the expected payoff of the elementary strategy* $e_i$ *when played against* $e_j$, *is called the payoff matrix.*

EXAMPLE 1 *In the Hawk-Dove game there are two elementary strategies:* $e_1 = (1, 0)$ *denotes Hawk strategy and* $e_2 = (0, 1)$ *Dove strategy. A mixed strategy* $p = (p_1, p_2) \in S_2$, *where* $p_1$ *is the probability of playing Hawk and* $p_2$ *is the probability of playing Dove. The payoff table for the Hawk-Dove game defines the payoff matrix for the first player:*

$$U = \begin{pmatrix} \frac{V-C}{2} & V \\ 0 & \frac{V}{2} \end{pmatrix}.$$

*The payoff matrix for the second player is the transposed matrix because this game is symmetric.*

### 1.3.1 Fitness for mixed strategies

The payoff matrix defines fitness for a player that uses one of his elementary strategies against another player that also uses one of his elementary strategies. Now the question is how to compute fitness of a player that uses a mixed strategy against another player that can use a mixed strategy

as well. If the first player uses an elementary strategy $e_i$ and his opponent uses a mixed strategy $q = \{q_1, \ldots, q_n\}$ then the payoff of the first player is

$$W(e_i, q) = \sum_{j=1}^{n} u_{ij} q_j = \langle e_i, Uq \rangle,$$

where $\langle \cdot, \cdot \rangle$ denotes the scalar product in $R^n$. If the first player uses also a mixed strategy $p = (p_1, \ldots, p_n)$, then his payoff is

$$W(p, q) = \langle p, Uq \rangle = \sum_{i,j=1}^{n} p_i u_{ij} q_j.$$

DEFINITION 3  *Let $p = (p_1, \ldots, p_n) \in S_n$ be a mixed strategy. Then*

$$supp(p) = \{i \mid 1 \le i \le N, \ p_i > 0\}$$

*denotes the set of elementary strategies that are used in the mixed strategy p.*

### 1.3.2   Nash equilibrium

DEFINITION 4  *Strategy $p = (p_1, \ldots, p_n) \in S_n$ is called an equilibrium if*

$$W(p, p) = W(e_i, p) \ \text{ for every } \ i \in supp(p).$$

Thus, every elementary strategy is an equilibrium by definition. At the equilibrium $p$, every elementary strategy when played against $p$ has the same payoff.

EXAMPLE 2  *The Hawk-Dove game has three equilibria: Elementary strategies $H$ and $D$, and the mixed strategy $(V/C, 1 - V/C)$.*

DEFINITION 5 (NASH EQUILIBRIUM)  *Strategy $p = (p_1, \ldots, p_n) \in S_n$ for which*

$$W(p, p) \ge W(q, p)$$

*for all strategies $q = (q_1, \ldots, q_n) \in S_n$ is called the Nash equilibrium (NE).*
   *If*

$$W(p, p) > W(q, p)$$

*for every other strategy $q \ne p$, then $p$ is a strict Nash equilibrium.*

In words, the NE $p$ is "the best response against itself". The question is, under which conditions a NE for a given game exists. Let $W : S_n \times S_n \mapsto R$ and $b : S_n \rightsquigarrow S_n$ be the best response map, i. e.,

$$b(x) = \{y \in S_n \mid W(y, x) = \sup_{z \in S_n} W(z, x)\}.$$

Here the sign $\rightsquigarrow$ indicates that the mapping is set-valued, i. e., $b(x) \subset S_n$. Then, the Nash equilibrium $p$ is the best response against itself, i. e.,

$$p \in b(p).$$

For matrix games with a payoff matrix $U$, the best response is

$$b(x) = \arg \max_{y \in S_n} \langle y, Ux \rangle = \{ y \in S_n : \langle y, Ux \rangle = \max_{z \in S_n} \langle z, Ux \rangle \}.$$

The question of the existence of a NE is thus reduced to the existence of a fixed point for the best response mapping. To answer this, we need an extension of continuity and the Brower fixed point for multivalued maps.

DEFINITION 6 (UPPER SEMICONTINUOUS SET-VALUED MAP) *Let $F : X \mapsto Y$ be set-valued map with non-empty values. We say that $F$ is upper semicontinuous at a point $x$, if for any open set $N$ containing $F(x)$ there exists an open set $M$ containing $x$ such that $F(M) \subset N$.*

PROPOSITION 1 (THE KAKUTANI FIXED POINT THEOREM, AUBIN AND CELLINA (1984)) *Let $K$ be a compact convex subset of a Banach space $X$ and let $F$ be an upper semicontinuous set-valued map from $K$ into its compact convex subsets. Then $F$ has a fixed point, i. e., there exists $x$ such that $x \in F(x)$.*

PROPOSITION 2 (EXISTENCE OF THE NE) *Let $W : S_n \times S_n \mapsto R$ be continuous. Then at least one Nash equilibrium exists.*

*Proof.* It is enough to prove that the best response map $x \rightsquigarrow b(x)$ has a fixed point is $S_n$. Because the best response map is upper semicontinuous (Aubin and Cellina 1984) with non-empty, convex and compact values, the existence of a fixed point follows from the Kakutani fixed point theorem.

$\square$

REMARK 1 *The above proposition implies that every matrix game has a NE.*

The next Proposition is used when calculating the NE.

PROPOSITION 3 *Let $p = (p_1, \ldots, p_n)$ be a Nash equilibrium. Then $W(e_i, p) = W(p, p)$ for every elementary strategy $e_i$, $i \in supp(p)$.*

*Proof.* For every elementary strategy $e_i$, $i \in \text{supp}(p)$, $W(p, p) \geq W(e_i, p)$ by definition. If for some $e_i$, $W(p, p) > W(e_i, p)$ then

$$W(p, p) = \sum_{j=1}^{n} p_j W(e_j, p) < W(p, p),$$

a contradiction.

□

PROPOSITION 4 *Let $U = (u_{ij})_{i,j=1}^n$ be a payoff matrix. If there exists $i$ such that $u_{ii} \geq u_{ji}$ for $j = 1, \ldots, n$, then elementary strategy $e_i$ is the Nash equilibrium. If $u_{ii} > u_{ji}$ for $j = 1, \ldots, n$, $j \neq i$ then elementary strategy $e_i$ is a strict Nash equilibrium.*

*Proof.* Inequality

$$p_j u_{ii} \geq p_j u_{ji}$$

implies

$$u_{ii} \geq p_1 u_{1i} + \cdots + p_n u_{ni}.$$

Thus $W(e_i, e_i) \geq W(p, e_i)$ and elementary strategy $e_i$ is a Nash equilibrium.

□

EXAMPLE 3 *For the Hawk-Dove game the mixed equilibrium $p = (V/C, 1 - V/C)$ is a NE. Elementary strategy $H$ ($e_1 = (1, 0)$) is a NE provided $V > C$. Elementary strategy $D$ ($e_2 = (0, 1)$) is not a NE because $W(e_2, e_2) < W(e_1, e_2)$.*

Let us consider a population of individuals. If every individual uses a strategy that corresponds to a strict NE, then any mutant strategy has a lower fitness and cannot increase in the population when rare. However, in a non-strict NE this is not so as there are mutant strategies that give the same fitness. Indeed, Let $p$ be a Nash equilibrium different from any elementary strategy. Then supp($p$) consists at least of two elements. and $W(e_i, p) = W(p, p)$, for every $i \in$ supp($p$). Let $q$ be any other strategy with the same support. Then

$$W(q, p) = \sum_{i=1}^n q_i W(e_i, p) = W(p, p).$$

Thus, at a mixed NE there are mutant strategies that get the same fitness as residents. If all elementary strategies are played at a NE, then any other strategy gets the same fitness. This means that a mixed Nash equilibrium is not protected against invasions by mutants that have the same payoff. The phenotype that corresponds to the Nash equilibrium has the highest possible fitness in the environment where other individuals play the same strategy, but there are infinitely many phenotypes with the same payoff. This motivated Maynard Smith and Price (1973) to select among all Nash equilibria those that resist invasions by mutants.

## 1.4 Evolutionarily stable strategies

Maynard Smith and Price (1973) introduced so called evolutionarily stable strategies (ESS) as those NE that are stable with respect to invasions by mutants. Thus, the ESS should correspond to an end point of evolution, as no other strategy (phenotype) can invade.

DEFINITION 7 *Strategy $p^* \in S_n$ is evolutionarily stable provided for every other strategy $p \neq p^*$ there exists $\overline{\varepsilon}(p) > 0$ such that*

$$W(p^*, \varepsilon p + (1 - \varepsilon)p^*) > W(p, \varepsilon p + (1 - \varepsilon)p^*)$$

*for every $0 < \varepsilon < \overline{\varepsilon}(p)$.*

If $W$ is linear in the second argument (which is the case of matrix games) the above inequality can be re-written as

$$(1 - \varepsilon)(W(p^*, p^*) - W(p, p^*)) + \varepsilon(W(p^*, p) - W(p, p)) > 0$$

for every $0 < \varepsilon < \overline{\varepsilon}(p)$. This implies that for pairwise matrix games $p^*$ is an ESS if and only if the following two conditions hold:

(1.) $W(p^*, p^*) \geq W(p, p^*)$ for every $p \in S_n$

(2.) If $p \neq p^*$ and $W(p^*, p^*) = W(p, p^*)$ then $W(p^*, p) > W(p, p)$.

The first condition is nothing else than condition on NE and the second condition is the so called stability condition. The latter condition shows that the ESS strategy is globally superior to other strategies.

The definition of ESS $p^*$ requires that for every other mutant strategy $p$ there exists an invasion barrier $\overline{\varepsilon}(p) > 0$ that depends on strategy $p$. The next proposition shows that for matrix games this invasion barrier is uniform, i. e., independent from the mutant strategy $p$.

PROPOSITION 5 (HOFBAUER AND SIGMUND (1998),WEIBULL (1995)) *For matrix games the invasion barrier can be chosen independently of the mutant strategy.*

*Proof.* For an ESS $p^*$ and $p \in S_n$ let us define

$$f(\varepsilon, p) = W(p^* - p, p^*) + \varepsilon W(p^* - p, p - p^*).$$

Function $f$ is linear in $\varepsilon$. As $p^*$ is an ESS it follows that either $f(0, p) > 0$, or $f(0, p) = 0$ in which case the slope $W(p^* - p, p - p^*) > 0$. Thus, there exists $1 > \overline{\varepsilon} > 0$ such that $f(\varepsilon, p) > 0$ for $\varepsilon < \overline{\varepsilon}$.

Let

$$C(p^*) = \{p \in S_n \mid p_i = 0 \text{ for some } i \in \text{supp}(p^*)\}. \tag{1.1}$$

be the union of all boundary faces of $S_n$ that do not contain $p^*$. Fix $q \in C(p^*)$ and consider function $f(\varepsilon, q)$. As $f$ is linear in $\varepsilon$, there exists at most one solution to $f(\varepsilon, q) = 0$. If such a solution exists, it is given by $\varepsilon_0 = \frac{W(p-p^*, p^*)}{W(p^*-p, p-p^*)}$. I define

$$\beta(q) = \begin{cases} \varepsilon_0 & \text{if } f(\varepsilon, p) \text{ has a solution } \varepsilon_0 \leq 1 \\ 1 & \text{otherwise.} \end{cases} \tag{1.2}$$

Function $\beta$ is continuous, positive and therefore it attains a positive minimum on the compact set $C(p^*)$. Thus, we proved that a global invasion barrier exists for all $q \in C(p^*)$.

Now, let us consider any strategy $p \in S_n$, $p \neq p^*$. Then here exists $q \in C(p^*)$ and $1 > \lambda > 0$ such that $p = \lambda q + (1 - \lambda)p^*$. Because $f(\varepsilon, p) = f(\varepsilon\lambda, q)$ it follows that $\beta(p) = \min\{\beta(q)/\lambda, 1\} \geq \beta(q)$.

$\square$

The next theorem shows that for a strategy to be an ESS it is enough if it is only locally superior (Hofbauer and Sigmund 1998; Weibull 1995).

PROPOSITION 6 *For matrix games strategy $p^* \in S_n$ is an ESS if and only if*

$$W(p^*, p) > W(p, p) \tag{1.3}$$

*for every $p \neq p^*$ in some neighborhood of $p^*$ in $S_n$.*

*Proof.* Let $p^*$ be an ESS and let $1 > \overline{\varepsilon} > 0$ be its the uniform invasion barrier that exists due to Proposition 5. Let $C(p)$ be defined by (1.1) and

$$V = \{p \in S_n \mid p = \varepsilon q + (1 - \varepsilon)p^* \text{ for some } q \in C(p^*), \ \varepsilon < \overline{\varepsilon}\}.$$

There exists a neighborhood $U$ of $p^*$ such that $U \subset V$. Let $p \in U$ and

$$W(q, p) < W(p^*, p).$$

Multiplying the inequality by $\varepsilon$ and adding $W((1 - \varepsilon)p^*, p)$ we get

$$W(p^*, p) > W(p, p).$$

Now I prove that local superiority condition (1.3) implies ESS. Let $q \in S_n$. Then there exists $\varepsilon > 0$ such that $p = \varepsilon q + (1 - \varepsilon)p^*$ belongs for every $\varepsilon < \overline{\varepsilon}$ to the neighborhood of $p^*$ for which inequality (1.3) holds. Then

$$W(p^*, p) > W(p, p) = \varepsilon W(q, p) + (1 - \varepsilon)W(p^*, p)$$

and

$$W(p^*, p) > W(q, p)$$

which implies that $p^*$ is an ESS.

$\square$

The local superiority of an ESS is used to define ESS for games where payoff is not a bilinear in strategies (ESS, Weibull 1995; Cressman and Hofbauer 2005).

The next proposition is important when searching for ESSs.

PROPOSITION 7 *If two different ESS $p^*$ and $q^*$ exist, then $supp(p^*)$ is not contained in $supp(p^*)$ and vice versa.*

*Proof.* Let $supp(p^*) \subset supp(q^*)$. Then for every elementary strategy $e_i$, $i \in supp(q^*)$, $W(e_i, q^*) = W(q^*, q^*)$. Therefore,

$$W(p^*, q^*) = \sum_{i=1}^{n} p_i^* W(e_i, q^*) = W(q^*, q^*).$$

It follows that $p^*$ is an alternative best response to $q^*$. Because $q^*$ is an ESS, the stability condition

$$W(p^*, p^*) < W(q^*, p^*)$$

contradicts with the assumption that $p^*$ is a NE.

$\square$

A consequence of this proposition is that there can be at most one interior ESS.

EXAMPLE 4 *The Hawk-Dove game has for $C > V$ one interior Nash equilibrium $p = (V/C, 1 - V/C)$. The stability condition holds because for $q \neq p$*

$$W(p - q, q) = \frac{1}{2} C \left( \frac{V}{C} - p \right)^2 > 0.$$

*Thus, $p$ is an ESS and because it is an interior ESS it is also unique.*

*If $C < V$, then elementary strategy $e_1 = (1, 0)$ (Hawk) is strict Nash equilibrium, thus an ESS.*

It is worthwhile to stress that an ESS is not resistant against simultaneous invasions of two or more mutant strategies. Let us consider the Hawk-Dove game with ESS $p^* = (3/4, 1/4)$. Let us consider simultaneous invasion by Hawks and Doves ($e_1 = (1, 0)$ and $e_2 = (0, 1)$). Both mutant strategies are at the same, low proportion $\frac{1}{2}\varepsilon$ where $\varepsilon$ is sufficiently small. This is formally equivalent with a fictious monomorphic mutant with strategy $q = (e_1 + e_2)/2 = (1/2, 1/2)$. The resulting population mix is $\omega = \varepsilon/2(e_1 + e_2) + (1 - \varepsilon)p^*$. Because $p^*$ is an ESS, it is true that the fictious

mutant does worse in the population mix $\omega$ than $p^*$. However, this does not mean that both invading phenotypes do worse. Indeed, since $\omega_1 < 3/4$ the Hawk strategy $e_1$ is the unique best reply against the fictious mutant with strategy $\omega$, i. e., $W(e_1, \omega) > W(p^*, \omega)$.

### 1.4.1 Analysis of two-player games with two strategies.

Let

$$U = \begin{pmatrix} a & b \\ c & d \end{pmatrix}$$

by the payoff matrix.

PROPOSITION 8 *Let either $a \neq c$ or $b \neq d$. Then every two-player game with two strategies has an ESS. There are the following possibilities:*

    *1. If $a \geq c$ and $d < b$ then $e_1$ is an ESS.*

    *2. If $a > c$ and $d > b$ then $e_1$ and $e_2$ are ESSs.*

    *3. If $a < c$ and $d \geq b$ then $e_2$ is an ESS.*

    *4. If $a \leq c$ and $d \leq b$ then $\left( \frac{b-d}{b-d+c-a}, \frac{c-a}{b-d+c-a} \right)$ is an ESS.*

Proof. If $a > c$ then elementary strategy $e_1$ is a strict NE, thus an ESS.

If $a = c$ then the stability condition from the definition of ESS requires that $W(e_2, e_2) < W(e_1, e_2)$, i. e., $d < b$. This shows that in the case 1., $e_1$ is an ESS.

Analogously we verify condition case 3. The case 2 is clear, because under these assumptions both elementary strategies are strict NE.

Let us consider case 4. There is no strict NE. The interior NE $p = (p_1, p_2)$ satisfies $W(e_1, p) = W(e_2, p)$ which gives

$$p_1 = \left( \frac{b-d}{b-d+c-a}, \frac{c-a}{b-d+c-a} \right).$$

Let us consider any other strategy $q = (q_1, q_2)$. Because

$$W(p, q) - W(q, q) = \frac{((b-d)(1-q_1) + (a-c)q_1)^2}{b-d+c-a} > 0,$$

we proved that strategy $p$ is an ESS.

<div align="right">□</div>

### 1.4.2 Rock-scissors-paper game

RSP game is an example of a game without an ESS. The three elementary strategies are $e_1 = (1, 0, 0)$ (rock), $e_2 = (0, 1, 0)$ (scissors), $e_3 = (0, 0, 1)$ (paper) and the payoff matrix is

$$U = \begin{pmatrix} 0 & 1 & -1 \\ -1 & 0 & 1 \\ 1 & -1 & 0 \end{pmatrix}$$

Let $p = (p_1, p_2, 1 - p_1 - p_2)$ and $q = (q_1, q_2, 1 - q_1 - q_2)$. Then

$$W(p, q) = \langle p, Uq \rangle = (q_1 - q_2) - (p_1 - p_2) + 3p_1 q_2 - 3p_2 q_1$$

and

$$W(p, p) = 0.$$

First, we observe that no elementary strategy is a Nash equilibrium (if strategy $e_i$ is a NE than $u_{ii} \geq u_{ij}$ for all $j = 1, 2, 3$).

Second, there does not exist any NE whose support has exactly two elementary strategies. For example, if a NE $q$ such that $\text{supp}(q) = \{1, 2\}$ exists then

$$W(e_1, q) = W(e_2, q)$$

which implies that $q_1 + q_2 = 2/3$. As $q_3 = 0$ this is impossible. Similarly, one can prove that no other NE with two elementary strategies in its support exists.

The interior NE satisfies $W(e_1, p) = W(e_2, p) = W(e_3, p) = W(p, p) = 0$ which gives $p = (1/3, 1/3, 1/3)$. However, this interior NE does not satisfy the stability condition $W(q, q) < W(p, q)$ because both sides are equal to 0. Thus, no ESS exists.

The fact that the RSP game has no interior ESS is a more general property of symmetric zero-sum games that satisfy $u_{ij} = -u_{ji}$ for every $i, j = 1, \cdots, n$.

PROPOSITION 9 *No mixed strategy can be an ESS of a symmetric zero-sum matrix game.*

Proof. For symmetric zero-sum games $W(p, p) = 0$ for every strategy $p \in S_n$. Let us assume that $p^*$ is a mixed ESS and let us take $p \neq p^*$ in a neighborhood of $p^*$ so that

$$W(p^*, p) > W(p, p) = 0 \tag{1.4}$$

and $\text{supp}(p) = \text{supp}(p^*)$. It follows that $W(p, p^*) = W(p^*, p^*) = 0$. However, from (1.4) it follows that $W(p, p^*) < 0$, a contradiction.

$\square$

Applications of RSP game can be found in Sinervo and Lively (1996) and Sinervo et al. (2000). These authors showed that males of the Common Side-blotched lizard occur in three phenotypes that differ in the level of aggressiveness. They also showed that the middle aggressive phenotype invades the non-aggressive phenotype, the non-aggressive phenotype invades the highly aggressive phenotype and the highly aggressive phenotype invades the middle aggressive phenotype which corresponds to the RSP game.

## 1.5 Habitat selection game

So far we have considered pairwise contest games where an individual plays against an opponent and the payoff depends just on what both individuals do. Such games are described by the payoff matrix, i. e., the fitness functions $W(u,v)$ is bilinear and can be written as $W(u,v) = \langle u, Uv \rangle$. On the contrary, in so called games against the field a focal animal does not play against any fixed opponent and its payoff depends on what everyone in the population is doing. Thus, the focal individual plays against the mean strategy in the population which is the distinctive feature of such games. In general, payoffs in these games can be non-linear in which case the game cannot be described as a matrix game. An example of such a game is the habitat selection game.

Fretwell and Lucas (1970) introduced the Ideal Free Distribution that aims to describe a distribution of animals in a heterogeneous environment consisting of discrete patches. The model assumes that animals are free to move between several patches, the travel time is negligible, each individual knows perfectly the quality of all patches and all individuals have the same competitive abilities. Assuming that these patches differ in their basic quality $B_i$ (i. e., their quality when unoccupied by any consumers), the IFD model predicts that the best patch will always be occupied. I will assume that $n$ patches are ordered so that the first patch has a higher basic quality than the second patch and so on $B_1 > \cdots > B_n > 0$, and fitness in each patch is $V_i(m_i)$ where $m_i$ is the animal density in patch $i$, $V_i(0) = B_i$ and $V_i$ is a decreasing function of animal density in that patch.

Let $p_i = m_i/(m_1 + \cdots + m_n)$ be the proportion of animals in patch $i$, i. e., $p = (p_1, \ldots, p_n)$ describes the spatial distribution of the population. I remark that for a monomorphic population, the distribution $p_i$ also specifies the individual strategy as the proportion of the lifetime an average animal spends in patch $i$. Then, fitness of a mutant with strategy $p' = (p'_1, \ldots, p'_n)$ in the resident monomorphic population with strategy (distribution) $p = (p_1, \ldots, p_n)$ is

$$W(p', p) = \langle p', V(pM) \rangle$$

where $V(pM) = (V_1(p_1 M), \cdots, V_n(p_n M))$ and $M$ is the overall population density. However, we do

not need to make the assumption that the population is monomorphic, because what really matters in calculating $W(p', p)$ above is the animal distribution $p \in S_n$. If the population is not monomorphic this distribution can be different from strategies animals use and we call it the population mean strategy. Thus, in the habitat selection game individuals do not enter pair-wise conflicts, but they play against the population mean strategy. This is why this game is an example of the game against the field.

DEFINITION 8 (FRETWELL AND LUCAS (1970)) *Distribution* $p = (p_1, \ldots, p_n)$ *is called the Ideal Free Distribution provided the following conditions hold:*

1. *There exists a number* $1 \leq k \leq n$ *such that* $p_1 > 0, \ldots, p_k > 0$ *and* $p_{k+1} = \cdots = p_n = 0$.

2. $V_1(m_1) = \cdots = V_k(m_k) = V^*$ *and* $V^* \geq V_i(m_i)$ *for* $i = k+1, \ldots, n$.

The IFD has been repeatedly given in the literature (e. g., Parker 1978; Parker 1984; Pulliam and Caraco 1984; Pulliam and Danielson 1991; Kennedy and Gray 1993; Morris 2003) as an example of the evolutionarily stable strategy. However, from the definition it is immediately clear that the IFD is a NE, but it is not clear that it satisfies the stability condition. This is proved in the next proposition.

PROPOSITION 10 (CRESSMAN AND KŘIVAN (2006)) *The IFD is an ESS.*

*Proof.* Let $p^*$ be the IFD at fixed population density $M = m_1 + \cdots + m_n$. First suppose that all patches are occupied (i. e., $k = n$ in Definition 8). Then

$$W(p, p') - W(p', p') =$$
$$\langle p, V(p'M) \rangle - \langle p', V(p'M) \rangle = \sum_{i=1}^n (p_i - p_i') V_i(p_i'M) = \sum_{i=1}^n (p_i - p_i') \left( V_i(p_i'M) - V_i(p_iM) \right).$$

Since $V_i(p_iM)$ is strictly decreasing, $p_i > p_i'$ if and only if $V_i(p_i'M) > V_i(p_iM)$. Thus $\langle p, V(p'M) \rangle > \langle p', V(p'M) \rangle$ unless $p = p'$. Thus, the local superiority condition holds.

Now suppose that not all patches are occupied ($k < n$) and define $V^* = V_1(p_1M) = \cdots = V_k(p_kM)$. Then

$$
\begin{aligned}
\langle p, V(p'M) \rangle - \langle p', V(p'M) \rangle &= \sum_{i=1}^n (p_i - p_i') V_i(p_i'M) \geq \sum_{i=1}^k (p_i - p_i') V_i(p_i'M) - \sum_{i=k+1}^n p_i' V^* \\
&= \sum_{i=1}^k (p_i - p_i') \left( V_i(p_i'M) - V^* \right) \geq 0
\end{aligned}
$$

by the same reasoning as above. The inequality is again strict unless $p = p'$.

$\square$

### 1.5.1 Patch payoff is a linear function

Following Křivan and Sirot (2002) I assume that the payoff in habitat $i$ is a linearly decreasing function of population density

$$V_i = r_i \left( 1 - \frac{m_i}{K_i} \right) \tag{1.5}$$

where $m_i$ is the population density in habitat $i$, $r_i$ is the intrinsic per capita growth rate in habitat $i$, and $K_i$ is its carrying capacity. The total population size in a two habitat environment is denoted by $M(= m_1 + m_2)$ and the proportion of the population in habitat $i$ is $p_i = m_i/M$.

Let us consider an individual which spends proportion $p'_1$ of its lifetime in habitat 1 and $p'_2$ in habitat 2. Provided population densities are fixed, then its payoff in the population with the population mean strategy $p = (p_1, p_2)$ is

$$W(p', p) = p'_1 V_1(p_1 M) + p'_2 V_2(p_2 M) = \langle p', Up \rangle,$$

where

$$U = \begin{pmatrix} r_1(1 - \frac{M}{K_1}) & r_1 \\ r_2 & r_2(1 - \frac{M}{K_2}) \end{pmatrix}.$$

This shows that the habitat selection game can be written as a matrix game. By definition, an IFD is a strategy for which all current choices of an individual as to how to partition its time between the two habitats have the same payoffs and no other possible choice has a higher payoff. In what follows I will assume that the per capita intrinsic population growth rate in habitat 1 is higher than that in habitat 2 $(r_1 > r_2)$. Then it is easy to derive the IFD (Křivan and Sirot 2002)

$$p_1 = \begin{cases} 1 & \text{if } M < K_1 \frac{r_1 - r_2}{r_1} \\ \frac{r_2 K_1}{r_2 K_1 + r_1 K_2} + \frac{K_1 K_2 (r_1 - r_2)}{(r_2 K_1 + r_1 K_2) M} & \text{otherwise.} \end{cases} \tag{1.6}$$

In the first case, payoff in habitat 1 is higher than is the payoff in habitat 2 for all possible population distributions because the competition in patch 1 is low due to low population densities. For higher population abundances, neither of the two habitats is always better than the other, and under the IFD animal payoff in both habitats must be the same $(V_1(p_1 M) = V_2(p_1 M))$. Once again, it is important to emphasize here that the IFD concept is very different from maximization of the mean animal fitness $\overline{W} = \langle p, V(p) \rangle$ which would lead to

$$p_1 = \begin{cases} 1 & \text{if } M < K_1 \frac{r_1 - r_2}{2r_1} \\ \frac{r_2 K_1}{r_1 K_2 + r_2 K_1} + \frac{K_1 K_2 (r_1 - r_2)}{2(r_1 K_2 + r_2 K_1) M} & \text{otherwise.} \end{cases} \tag{1.7}$$

The two expressions (1.6) and (1.7) are the same if and only if $r_1 = r_2$. Figure 1.1 shows that, while the latter strategy is never worse than the IFD, individuals using it obtain lower payoffs in one patch than in the other patch which makes this strategy vulnerable to invasions by individuals using a different strategy such as the IFD.
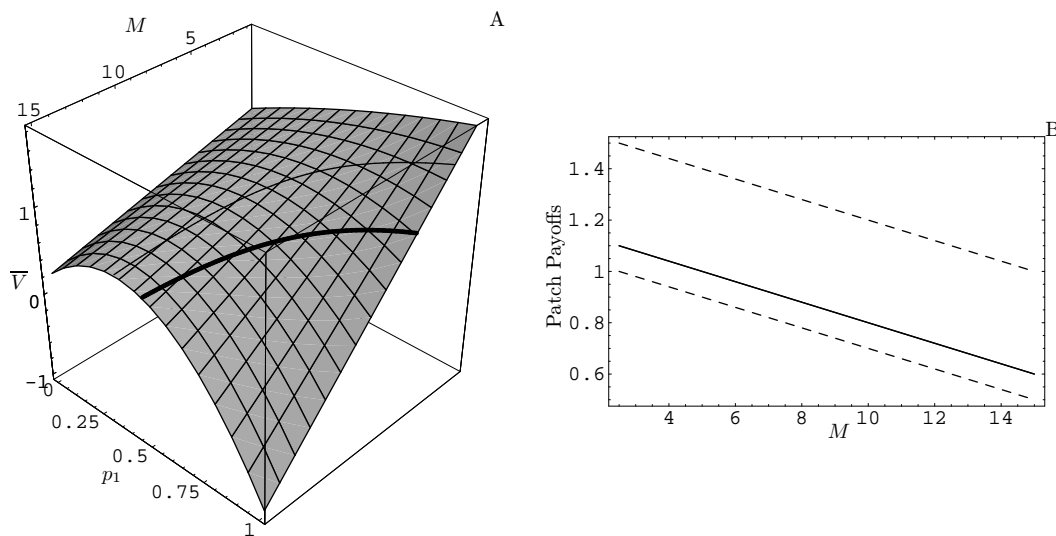
Figure 1.1: Panel A plots mean fitness $\overline{W}$ as a function of distribution $p_1$ and overall number of individuals $M$ for a two-patch model with linear payoff ($V_i = r_i(1 - \frac{p_i M}{K_i})$, $i = 1, 2$). The thick curve corresponds to the IFD, while the thin solid curve corresponds to the distribution along which the mean payoff maximizes. Panel B shows that along the IFD the fitness in both patches is the same (solid line) for all $M$ when both patches are occupied. On the other hand, for the strategy that maximizes the mean payoff, the patch specific payoffs are different (the two dashed lines correspond to payoffs in the two patches). Parameters used in simulations: $r_1 = 1$, $r_2 = 2$, $K_1 = 20$, $K_2 = 10$.

### 1.5.2   Parker's matching principle

Parker (1978) considered the case where resource input rates $r_i$, $i = 1, \ldots, n$ are constant and all resources in all patches are consumed immediately when they enter the system and so there is no standing crop. This leads to a particularly simple definition of animal payoff in a patch as the ratio of the resource input rate divided by the number of individuals there, i. e.,

$$V_i = \frac{r_i}{m_i} = \frac{r_i}{p_i M}. \tag{1.8}$$

The IFD for these payoff functions is called the matching principle and it states that animals distribute themselves so that their density in each patch is proportional to the rate with which resources arrive into the patch $p_i/p_j = r_i/r_j$. On the contrary to the case where patch payoff is a linear function of consumer strategy, all patches will be occupied now. Indeed, as the consumer density in a patch decreases, payoff $r_i/(p_i M)$ tends to infinity so there cannot be any unoccupied patch. This concept successfully predicts the distribution of house flies that arrive at a cow patch where they immediately mate (Parker 1978; Parker 1984; Blanckenhorn et al. 2000), or of fish that are fed at two feeders in a tank (Milinski 1979; Milinski 1988; Berec et al. 2006). For example, Berec et al. (2006) observed that distribution of two fish species (white cloud mountain minnow, *Tanichthys albonubes* and giant danio, *Danio aequipinnatus*) in a water tank closely matched the
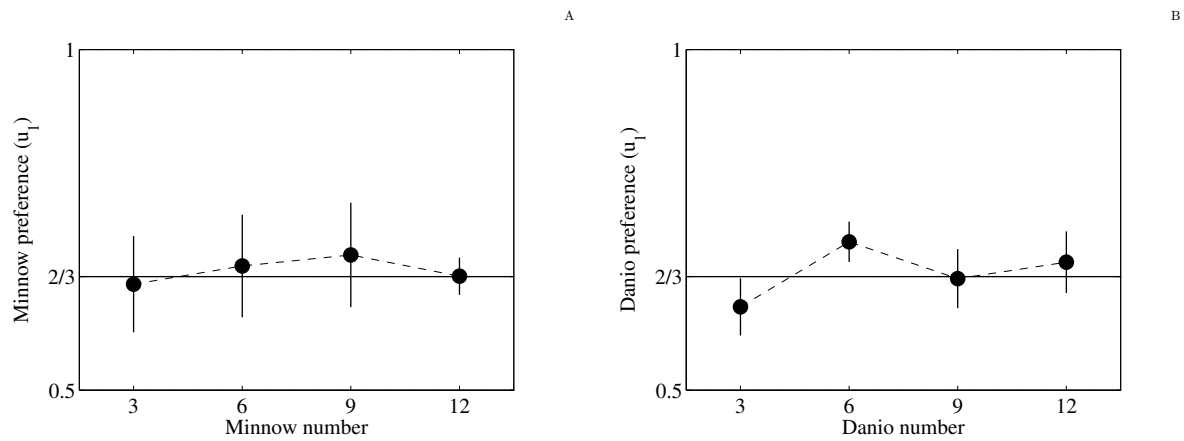
Figure 1.2: Panels show preferences for the more rewarding habitat 1 in minnow (A, mean $\pm$ SE) and danio (B) at different fish numbers. The solid line is the single-species IFD, corresponding to the distribution matching the ratio 2:1 of food supply rates. After Berec et al. (2006).

food input rate (2:1) at two feeders (Figure 1.2).

However, it has also been inappropriately applied to many other empirical systems where resources form a standing crop (for a review see Tregenza 1994). In Section 2.7.5 I extend this matching principle to situations where resources form a standing crop.

## 1.6   Replicator dynamics

So far I have considered monomorphic mutants that play against either monomorphic residents or against the population mean strategy. The ESS is then such a strategy that resist invasions by these mutants that use a different strategy. Now we will deal with polymorphic populations where each phenotype uses a different strategy. We say that a population is in state $p \in S_n$ if $p_i$ is the proportion of the population using strategy $e_i$. In this polymorphic interpretation the individual strategies and the mean strategy are different, because the mean strategy characterizes the population, not a single individual. A question arises how and if the ESS of the underlying game relates to the polymorphism.

EXAMPLE 5 *Let us consider the Hawk-Dove game. So far I have assumed that all individuals use the same strategy, so fitness of a mutant using strategy $\tilde{p} = (\tilde{p}_1, \tilde{p}_2)$ against a resident with strategy $p = (p_1, p_2)$ was $\langle \tilde{p}, Up \rangle$. The polymorphic setting assumes that proportion $p_1$ of individuals use Hawk strategy and proportion $p_2$ of individuals use Dove strategy. The average fitness in the population will be $\langle p, Up \rangle$ exactly as in the case of monomorphism, although no single individual uses the mixed strategy that corresponds to the mean strategy $p = (p_1, p_2)$. Nevertheless, we are interested in evolution of the proportion of Hawks and Doves in the population, and, in particular, we ask, if these proportions converge to the ESS of the Hawk-Dove game. In this setting, the Hawk-Dove game is also called the underlying game.*

To study the changes in proportions of different phenotypes in the population, we have to define some explicit dynamics. I will consider only continuous time dynamics, although discrete time dynamics can be used as well. Several such dynamics have been used in the game theoretical literature. In biological applications it seems that the most frequently used dynamics are those described by the so called replicator dynamics (e. g., Weibull 1995; Hofbauer and Sigmund 1998; Cressman 2003). In replicator dynamics phenotypes with fitness larger than is the average fitness in the population increase in frequency while those with lower than average fitness decrease. These relative changes in frequencies are due to the fact that the overall population numbers change too. Another class of dynamics are based on the so called best response dynamics (e. g., Weibull 1995; Hofbauer and Sigmund 1998; Cressman 2003). and they assume that a proportion of individuals

updates their strategy at each time and the update follows the best response with respect to the current strategy. In ecological context these dynamics are relevant description of animal dispersal that leads to the IFD.

Let us consider a polymorphic population where there are $n$ different phenotypes, each of them using its own strategy. I also assume that each of these phenotypes replicates in the sense that it produces offsprings of the same phenotype. Let $m_i$ be the abundance of the $i-$th phenotype and I will assume that the per capita population growth rate equals to fitness of the $i-$th phenotype $F_i$, i. e.,

$$\frac{dm_i(t)}{dt} = m_i(t)F_i(m_1, \cdots, m_n), \quad i = 1, \ldots, n.$$

Then the growth of the overall population $M = m_1 + \cdots + m_n$ is described by

$$\frac{dM}{dt} = M \sum_{i=1}^{n} x_i F_i = N\overline{F}$$

where $x_i = m_i/M$ is the frequency of the $i-$th phenotype. The replicator equation describes changes in relative frequencies of phenotypes in the population

$$\frac{dx_i}{dt} = x_i(F_i - \overline{F}). \tag{1.9}$$

This equation shows that the proportion of individuals using strategy $i$ increases in the population if these individuals have higher than average fitness.

Let us assume that the $n$ phenotypes are given by a matrix game with $m$ pure strategies and a payoff matrix $U$. If the phenotypes correspond to the pure strategies of the game then $m = n$. However, the phenotypes can be also correspond to mixed strategies in which case $m$ can differ from $n$. Each phenotype $p_i$, $i = 1, \cdots, n$ is characterized by a vector $(p_{i1}, \ldots, p_{im})$ which specifies frequency of elementary strategies used by this phenotype. Fitness of phenotype $i$ when played against phenotype $j$ is then $w_{ij} = \langle p_i, Up_j \rangle$. Fitness of phenotype $i$ in the population is $F_i(x) = \sum_{j=1}^{n} w_{ij}x_j$, the avarage fitness in the population is $\overline{F} = \langle x, Wx \rangle$, and the replicator equation has the following form

$$\frac{dx_i}{dt} = x_i(\langle e_i, Wx \rangle - \langle x, Wx \rangle).$$

It follows immediately from this form that every NE for the game with matrix $W$ is also the equilibrium of the replicator equation. Indeed, if a strategy $j$ is not contained in the support of the NE, then $x_j = 0$ and $dx_j/dt = 0$. If a strategy $j$ is in the support of the NE. At the NE all strategies that are played have the same fitness which equals to the average fitness in the population and so the expression in parentheses equals 0.

EXAMPLE 6 *Here I consider the replicator equation for Hawk-Dove game and I denote $F_H = F_1$ and $F_D = F_2$. Let $x$ be the frequency of Hawks in the population. Then*

$$F_H(x) = \frac{V-C}{2}x + V(1-x)$$

*and*

$$F_D(x) = (1-x)\frac{V}{2}.$$

*Then*

$$\overline{F}(x) = xF_H(x) + (1-x)F_D(x) = \frac{(V-Cx^2)}{2}$$

*and*

$$\frac{dx}{dt} = \frac{1}{2}x(1-x)(V-Cx)$$

*and the growth of the population is*

$$\frac{dM}{dt} = \frac{M}{2}(V-Cx^2).$$

*I remark that the interior distribution equilibrium of this equation corresponds to the mixed ESS for the underlying game.*

*In this example phenotypes correspond to elementary strategy of the game. We can consider another phenotype that corresponds to a mixed strategy $p = (p_1, p_2) \in S_2$. Then we have three phenotypes (Hawks, Doves and the mixed strategy phenotype; $n = 3$) while the underlying game has only two elementary strategy. The matrix $W$ is*

$$W = \begin{pmatrix} \frac{V-C}{2} & V & V - \frac{p_1}{2}(V+C) \\ 0 & \frac{V}{2} & (1-p_1)\frac{V}{2} \\ p_1\frac{V-C}{2} & \frac{V}{2}(1+p_1) & \frac{V-p_1^2 C}{2} \end{pmatrix}.$$

*It is easy to construct the replicator dynamics that corresponds to matrix $W$.*

The fact that for the Hawk-Dove game the ESS coincides with the asymptotically stable equilibrium of the replicator equation in the Hawk-Dove game holds for any two-strategy games as the next proposition shows.

PROPOSITION 11 *For any two-strategy matrix game, a strategy is an ESS if and only if the corresponding fixed point of the replicator dynamics is locally asymptotically stable.*

*Proof.* Let us consider two phenotypes corresponding to strategies $p$ and $q$. Let $x_p$ and $x_q$ be frequency of phenotype $p$ and $q$, respectively, in the population. Then

$$F_p(x_p, x_q) = \langle p, Up \rangle x_p + \langle p, Uq \rangle x_q$$

and

$$F_q(x_p, x_q) = \langle q, Up \rangle x_p + \langle q, Uq \rangle x_q$$

The replicator equation is

$$\frac{dx_p}{dt} = x_p(1 - x_p)(W_p - W_q)(x_p \langle p - q, Up \rangle - x_q \langle q - p, Uq \rangle.$$

If $p$ is an ESS then either $\langle p - q, Up \rangle > 0$ for any $p$, or $\langle q - p, Uq \rangle < 0$. In both cases we can find $\varepsilon > 0$ such that for $x_q < \varepsilon$ the right handside of the replicator equation will be positive. This implies that $x_p = 1$ is a stable equilibrium. Similarly, if $x_p = 1$ is stable, then for small perturbations the right hand side of the replicator equation must be positive which shows that $x_p = 1$ is also an ESS.

$\square$

PROPOSITION 12 (HOFBAUER AND SIGMUND (1998)) *Every ESS is an asymptotically stable equilibrium of the corresponding replicator equation.*

*Proof.* Let $x^* = (x_1^*, \cdots, x_n^*) \in S_n$. First we prove that function $P(x) = \Pi_{i=1}^n x_i^{x_i^*}$ attains its maximum at $x^*$, i. e., that

$$\Pi_{i=1}^n (x_i^*)^{x_i^*} \geq \Pi_{i=1}^n x_i^{x_i^*}$$

holds for every $x \in S_n$. This inequality can be written as

$$\sum_{i=1}^n x_i^* \ln \frac{x_i}{x_i^*} \leq 0.$$

Because logarithm is concave function

$$\sum_{i=1}^n x_i^* \ln \frac{x_i}{x_i^*} \leq \ln(\sum_{i=1}^n x_i) = \ln 1 = 0,$$

due to Jensen's inequality.

Second, I assume that $x^*$ is an ESS and I prove that $P$ is an increasing function along trajectories of the replicator equation. Indeed,

$$\frac{1}{P}\frac{dP(x(t))}{dt} = \frac{d \ln P(t)}{dt} = \sum_{i=1}^n \frac{x_i^*}{x_i}\frac{dx_i(t)}{dt} = \sum_{i=1}^n x_i^*(\langle e_i, Wx \rangle - \langle x, Wx \rangle) =$$

$$\langle x^*, Wx \rangle - \langle x, Wx \rangle > 0,$$

where the last inequality follows from the assumption that $x^*$ is an ESS. As $P$ is a Lyapunov function, trajectories of the replicator equation converge to $x^*$.

$\square$

One question remains. Is every locally asymptotically stable equilibrium of replicator dynamics also an ESS? One of the first examples that this is not so was given by Taylor and Jonker (1978).

EXAMPLE 7 *Taylor and Jonker (1978) considered a game with the payoff matrix*

$$W = \begin{pmatrix} 2 & 1 & 5 \\ 5 & \alpha & 0 \\ 1 & 4 & 3 \end{pmatrix}.$$

*The corresponding game has for* $-8 \le \alpha < \frac{17}{2}$ *one interior NE* $p^3 = (\frac{17-2\alpha}{36-\alpha}, \frac{11}{36-\alpha}, \frac{8+\alpha}{36-\alpha})$.

*Let us consider stability of this NE. Let* $q = (q_1, q_2, 1 - q_1 - q_2)$ *and*

$$f(q) = W(p^3, q) - W(q, q) = 4 - 4q_1 + q_1^2 - 18q_2 - 2q_1q_2 + q_2^2 - \alpha q_2^2 - \frac{11(-13 + 12q_1 + 60q_2)}{\alpha - 36}.$$

*The local superiority condition requires that* $f(q) > 0$ *for every* $q \neq p^3$. *For* $\alpha < 0$ $f$ *attains its maximum at* $p^3$. *Thus,* $p^3$ *is an ESS provided* $-8 \le \alpha < 0$. *Replicator dynamics for this game are*

$$\frac{dx_1}{dt} = 2 + x_1^2 - 2x_2 - x_1(3 + 2x_2) - x_2^2(\alpha - 1)$$
$$\frac{dx_2}{dt} = x_1^2 + x_1(5 - 2x_2) + (1 - x_2)(-3 + x_2(\alpha - 1))$$

*Equilibrium* $p^3$ *is locally asymptotically stable provided trace of the Jacobian matrix is negative and determinant is positive. The Jacobian matrix evaluated at* $p^3$ *is*

$$J = \begin{pmatrix} \frac{96+\alpha}{\alpha-36} & \frac{4(21+4\alpha)}{\alpha-36} \\ \frac{3(3\alpha-64)}{\alpha-36} & \frac{-60-16\alpha+\alpha^2}{\alpha-36} \end{pmatrix}.$$

*It is easy to see that these two conditions hold provided* $-8 < \alpha < 3$. *Thus, for* $0 < \alpha < 3$, $p^3$ *is asymptotically stable equilibrium of the replicator equation which is not an ESS.*

I remark that under the replicator equation a missing phenotype cannot enter the population. Thus, only the phenotypes that exist initially can replicate. This is because the replicator equation assumes exact replication of phenotypes, so that a phenotype produces exactly the same offspring. In the context of the habitat selection game replicator dynamics cannot describe animal dispersal as they do not assume that individuals move between patches. The next section shows a different dynamics that is more suitable for description of animal dispersal.

## 1.7 Dispersal dynamics

Here I consider habitat selection game again. We have already seen that the eventual outcome of a single species distribution in a heterogeneous environment (the IFD) is an ESS. This means, that

if such a distribution will be slightly perturbed, it will return back to the IFD. However, this does not tell us anything about the rules of animal dispersal that lead to the IFD.

To describe changes in population distribution due to dispersal, I define the dispersal matrix $D$. The entries of this matrix $(D_{ij})$ describe the transition probabilities that an individual currently in patch $j$ moves to patch $i$ in a unit time interval. The local changes in population numbers due to dispersal are described by (Cressman and Křivan 2006)

$$\frac{dm_i}{dt} = \sum_{j=1}^{n} \left( D_{ij}(m)m_j - D_{ji}(m)m_i \right) \text{ for } i = 1, \ldots, n \tag{1.10}$$

where $m = (m_1, \cdots, m_n)$ is the vector of population densities in $n$ patches. Thus, the first term in the above summation describes immigration to patch $i$ from other patches and the second term describes emigration from patch $i$ to other patches. Since the terms $D_{ii}(m)m_i$ describing movement from patch $i$ to itself cancel in (1.10), $D_{ii}(m)$ can be chosen in such a way that the sum of the entries in each column of the dispersal matrix equals 1. Furthermore, by taking the unit time interval short enough, all entries $D_{ij}(m)$ will be nonnegative. Dividing both sides of the above equation by total population size $M$ and writing the dispersal matrix as a function of the population distribution $(p = (p_1, \ldots, p_n))$ leads to the following vector dispersal dynamics

$$\frac{dp}{dt} = D(p)p - p. \tag{1.11}$$

The next proposition gives conditions under which trajectories of (1.11) converge to an equilibrium.

PROPOSITION 13 (CRESSMAN AND KŘIVAN (2006)) *Let us assume that dispersal matrix* $D : S_n \mapsto S_n$ *is continuous and* $D_{ij}(p)$ *does not decrease as the payoff in patch $i$ increases and does not increase as the payoff in patch $j$ increases. Then (1.11) has a unique globally asymptotically stable equilibrium distribution* $p^* \in S_n$.

*Proof.* Because $D(p)$ is continuous, the map $S_n \to S_n$ given by $p \to D(p)p$ is continuous. Since $S_n$ is a compact convex space, there exists at least one fixed point $p^*$ of this map by Brouwer's fixed point theorem (Binmore 1992). But any fixed point is an equilibrium of (1.11). Since $D(p^*)$ is a positive matrix (i. e., all its entries are positive), $\langle e_i, D(p^*)p^* \rangle = p_i^* > 0$ for all $1 \le i \le n$. That is, all patches are occupied at $p^*$.

To show asymptotic stability of $p^*$, linearize (1.11) about $p^*$ (see Hugie and Grand (1998) for the two-patch case)

$$\frac{dp_i}{dt} = \sum_j Q_{ij} \left( p_j - p_j^* \right)$$

where $Q$ is the Jacobian matrix of (1.11). From equation (1.10), $Q_{ij} = \frac{\partial D_{ij}(p^*)}{\partial p_j} p_j^* + D_{ij}(p^*) - \frac{\partial D_{ji}(p^*)}{\partial p_j} p_i^*$ for $i \neq j$. This is positive by our assumption. Because $\sum_{k=1}^{n} D_{ki} = 1$ for every $i = 1, \cdots, n$, each column sum of $Q$ is zero. Thus, $Q$ has an eigenvalue 0 corresponding to the left eigenvector given by the uniform distribution $p_i = \frac{1}{n}$. Furthermore, $Q_{ii} < 0$ and so $Q$ is diagonally dominant (Hofbauer and Sigmund 1998) in that

$$Q_{ii} + \sum_{j \neq i} \mid Q_{ji} \mid = 0$$

for all $i$. Gershgorin circle theorem implies that all other eigenvalues of $Q$ have negative real part (Hofbauer and Sigmund 1998) and so $p^*$ is asymptotically stable.

$\square$

The question now is under which conditions on dispersal the stable population distribution of dispersal model (1.11) will correspond to the IFD. Fretwell and Lucas (1970) assumed that animals are ideal in the sense that they know the quality of each patch. This implies that they should move directly to the best patch(es). It is interesting to note that under such assumption the dispersal matrix in (1.11) changes discontinuously near animal distributions where two (or more) habitats have the same (highest) payoff. Suppose there are two patches. The dispersal rates between these two patches are $D_{12}(p)$ and $D_{21}(p)$. If individuals disperse from patches with lower payoff to patches with a higher payoff only (which excludes random dispersal between patches), then they disperse from patch 2 to patch 1 ($D_{12}(p) > 0$ and $D_{21}(p) = 0$) when the payoff in patch 1 is higher than in patch 2 ($V_1 > V_2$) and conversely when the payoff in patch 2 is higher than that in patch 1 ($D_{12}(p) = 0$ and $D_{21}(p) > 0$). Thus, continuous dependence of the dispersal matrix $D(p)$ on the distribution $p$ immediately implies that, under the IFD (i. e., when $V_1(p_1 M) = V_2(p_2 M)$), there is no dispersal between the two patches ($D_{12} = D_{21} = 0$). However, if dispersal ceases under the IFD, then individuals cannot keep track of changes in other patch payoffs ( unless the migratory cues are obtained without moving such as through animals observing feeding rates as in Harper 1982). Out of the 5 empirical studies of fish and bird habitat distributions reviewed by Hugie and Grand (1998) that converged to the IFD, in only one instance was no movement between patches observed at equilibrium distribution and this was for a case where distance between patches was large. Thus, if we want animals to disperse between patches even under the IFD, then either the dispersal matrix must be a discontinuous function of population distribution $p$, or there must be some non-IFD (e. g., random) dispersal between patches (Hugie and Grand 1998) that prevents the IFD to be reached. If the dispersal matrix is discontinuous, trajectories if model (1.11) are defined in the Filippov sense.

The next proposition shows that trajectories of model (1.11) converge to the IFD under weaker assumptions than those originally imposed by Fretwell and Lucas (1970).

PROPOSITION 14 (CRESSMAN AND KŘIVAN (2006)) *Any solution of the dispersal dynamics (1.11) converges to the IFD under the following two conditions:*

**(a)** $D_{ij} = 0$ *if* $V_i < V_j$

**(b)** $D_{ij} > 0$ *for some* $i, j$ *with* $p_j > 0$ *and* $V_j < V_i = \max_{1 \leq k \leq n} V_k$.

*Proof.* I define $W(p) = \max_{1 \leq i \leq n} V_i(p_i M)$ and show that this function decreases along the trajectories of (1.11). This means that the function $W$ is a Lyapunov function (Filippov 1988) and all trajectories converge to the minimum value of $W$ which occurs only at the IFD. First, let us assume that dispersal dynamics are described by a model where the matrix $D(p)$ depends continuously on the distribution $p$. Unless all patches have the same payoff, assumption (b) implies that there exists a patch $i$ such that $W(p(t)) = V_i(p_i(t)M)$ and $D_{ij}(p(t)) > 0$ for some occupied patch $j$ with a lower payoff. Furthermore, $D_{ij} = 0$ if $V_i = V_j$ $(i \neq j)$ due to assumption (a) and the continuous dependence of $D(p)$ on $p$. I also have $D_{ii}(p) = 1$ since the sum of the entries in every column of the dispersal matrix equals 1 (i. e., it is a stochastic matrix). It follows that $\frac{dp_i}{dt} = (D(p)p - p)_i > 0$ and, consequently, $V_i$ and $W$ decrease along trajectories of model (1.11).

Second, I show that $W$ is a Lyapunov function even if the matrix $D(p)$ does not depend continuously on the distribution $p$. In this case, individuals can disperse between patches with the highest payoff and I cannot use the preceding argument. If there is a unique patch $i$ with highest payoff then $\frac{dp_i(t)}{dt} > 0$ and so $W(p(t))$ is strictly decreasing. Filippov (1988) showed that this condition is not enough to prove convergence of solutions to the minimum of the function $W$, because it is possible that $W$ can still increase along those trajectories of (1.11) that move along the intersection of equal payoff manifolds. I have to exclude such a case. Suppose a solution $p(t)$ moves along an intersection of equal payoff manifolds (i. e., $V_i(p_i(t)M) = W(p(t))$ for some finite set of indexes $i \in K$). It follows (Shevitz and Paden 1994) that $\frac{dW(p(t))}{dt} = \sum_{i \in K} \xi_i \frac{dV_i(p_i(t)M)}{dp_i} \frac{dp_i(t)}{dt}$ where $\sum_{i \in K} \xi_i = 1$. The derivative with respect to time of the equality $V_i(p_i(t)M) = V_j(p_j(t)M)$ for any $i, j \in K$ implies that $\frac{dV_i(p_i(t)M)}{dp_i} \frac{dp_i(t)}{dt} = \frac{dV_j(p_j(t)M)}{dp_j} \frac{dp_j(t)}{dt}$. In particular, all $\frac{dp_i(t)}{dt}$ $(i \in K)$ have the same sign (because all $\frac{dV_i}{dp_i}$ are negative). However, from (a) and (b), these derivatives must be positive (unless all patches provide the same payoff) and, consequently $\frac{dW(p(t))}{dt}$ is negative and $W$ decreases along trajectories of (1.11).

□

It is important to emphasize that these conditions do not require "ideal animals" that know their environment perfectly in the sense that they always move directly to the best patch as originally

assumed by Fretwell and Lucas (1970). Instead, an individual only needs to be able to compare the payoff in one other patch that it samples (perhaps at random) with its payoff in its current patch, a much weaker assumption. This is one explanation for the prevalence that the IFD is observed in the experimental literature despite the fact that clearly the species in many of these experiments were non-ideal.

Below I illustrate these results using some explicit dispersal dynamics. Most of these dispersal dynamics satisfy the above two assumptions but I am also interested in situations where some individuals disperse between patches at random, in which case our first condition does not hold.

### 1.7.1  Ideal animals and the best response dynamics

I start with dispersal dynamics that assume ideal animals, exactly as Fretwell and Lucas (1970) did. Thus, if these animals are in a suboptimal patch, they always disperse directly to the patch(es) with the highest payoff. If, for a given distribution $p = (p_1, \cdots, p_n)$, the payoff $V_i$ in patch $i$ is larger than in any other patch, then the corresponding dispersal matrix has 1's in the $i$-th row (because the probability that an animal disperses from any other patch to patch $i$ equals 1) and 0's everywhere else.

I will document this for the case with 3 patches ($n = 3$, Figure 1.3A) where I set $V_i(p_i M) = r_i(1 - p_i M / K_i)$. The inequalities

$$V_1(p_1 M) > \max\{V_2(p_2 M), V_3(p_3 M)\},$$

$$V_2(p_2 M) > \max\{V_1(p_1 M), V_3(p_3 M)\},$$

and

$$V_3(p_3 M) > \max\{V_1(p_1 M), V_2(p_2 M)\}$$

split the distribution phase space (shown as the dotted triangle in Figure 1.3A, left panel) into three parts. In each of these three parts the best patch is uniquely given and the dispersal matrix $D(p)$ is constant and equal to one of the following three matrices

$$D^1 = \begin{pmatrix} 1 & 1 & 1 \\ 0 & 0 & 0 \\ 0 & 0 & 0 \end{pmatrix}, \quad D^2 = \begin{pmatrix} 0 & 0 & 0 \\ 1 & 1 & 1 \\ 0 & 0 & 0 \end{pmatrix}, \quad D^3 = \begin{pmatrix} 0 & 0 & 0 \\ 0 & 0 & 0 \\ 1 & 1 & 1 \end{pmatrix}.$$

I stress here that although the matrices $D^1$, $D^2$, and $D^3$ are frequency independent, the dispersal matrix $D(p)$ is frequency dependent because its entries depend on the distribution $p$. Specifically, dispersal matrix $D(p)$ is piece-wise constant and changes its value when the distribution crosses one of the three equal payoff lines $V_1(p_1 M) = V_2(p_2 M) > V_3(p_3 M)$, $V_2(p_2 M) = V_3(p_3 M) > V_1(p_1 M)$,
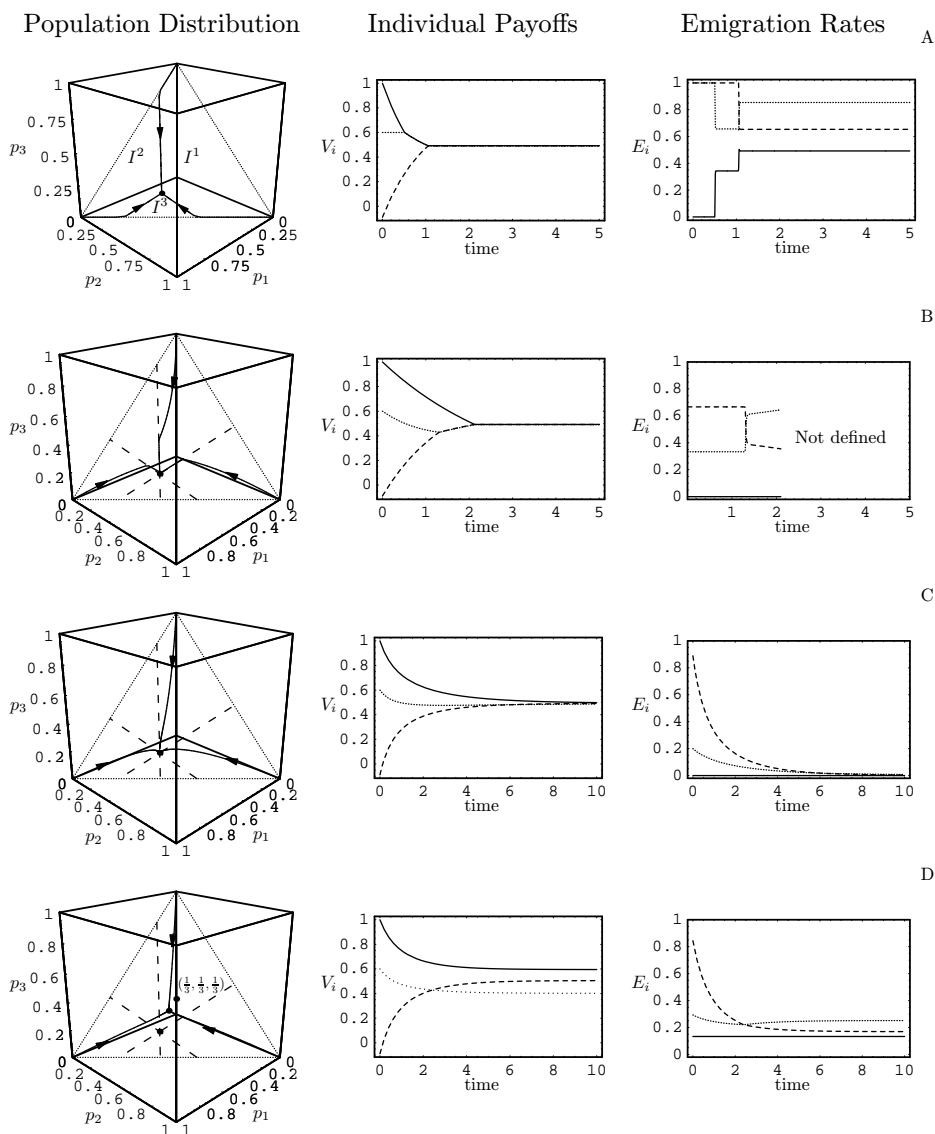
Figure 1.3: The left panel shows three trajectories for dispersal dynamics (1.11) when individuals are ideal (A), individuals are myopic (B), when dispersal is proportional to difference in patch payoffs (C, $\mu = 0.5$ in formula (1.15)), and when dispersal is suboptimal with some random dispersal (D, $\mu = 0.5$ and $\varepsilon = 0.2$ in formulas (1.15) and (1.18) respectively). The trajectories are shown in a probability simplex phase space $(p_1, p_2, p_3)$ where $0 \le p_i \le 1$ and $p_1 + p_2 + p_3 = 1$. The vertices of the triangle correspond to distributions where all individuals occupy one patch only. The IFD is shown as the solid dot at the intersection of dashed lines. The middle panel shows changes in individual payoffs along the trajectory that starts at the initial distribution $(0, 1, 0)$. The solid line is the payoff in the first patch, the dashed line is the payoff in the second patch and the dotted line is the payoff in the third patch, respectively. The right panel shows emigration rates from these respective patches along the same trajectory. Parameters: $r_1 = 1$, $r_2 = 0.8$, $r_3 = 0.6$, $K_1 = 10$, $K_2 = 9$, $K_3 = 8$, $M = 10$.

$V_1(p_1M) = V_3(p_3M) > V_2(p_2M)$ (which are the three lines that meet at the interior point in Figure 1.3, left panel). If population size $(M)$ is large enough so that all habitats are occupied at the IFD, these three equal payoff lines intersect at the IFD (the solid dot in Figure 1.3A)

$$
\begin{aligned}
p_1^* &= \frac{K_1(K_3r_2(r_1-r_3)+(Mr_2+K_2(r_1-r_2))r_3)}{M(K_3r_1r_2+K_2r_1r_3+K_1r_2r_3)} \\
p_2^* &= \frac{K_2(K_3r_1(r_2-r_3)+(Mr_1+K_1(r_2-r_1))r_3)}{M(K_3r_1r_2+K_2r_1r_3+K_1r_2r_3)} \\
p_3^* &= \frac{K_3(K_1r_2(r_3-r_1)+(Mr_2+K_2(r_3-r_2))r_1)}{M(K_3r_1r_2+K_2r_1r_3+K_1r_2r_3)}.
\end{aligned}
\tag{1.12}
$$

As the right hand side of (1.11) is discontinuous along the equal payoff lines, the solutions of (1.11) are defined along these discontinuity manifolds in the sense of Filippov (1988). Let us consider ideal individuals whose dispersal matrix for the case where $V_1(p_1M) > \max\{V_2(p_2M), V_3(p_3M)\}$ is $D^1$ and $D^2$ when $V_2(p_2M) > \max\{V_1(p_1M), V_3(p_3M)\}$. Thus, the dispersal matrix $D(p)$ is discontinuous when the distribution crosses the equal payoff curve $V_1(p_1M) = V_2(p_2M) > V_3(p_3M)$. The Filippov solution then consists of defining the dispersal matrix $D^{12}$ along this curve as

$$
D^{12} = uD^1 + (1-u)D^2 = \begin{pmatrix} u & u & u \\ v & v & v \\ 0 & 0 & 0 \end{pmatrix},
\tag{1.13}
$$

where $u$ is any number between 0 and 1 and $v = 1-u$. Such a definition is biologically very realistic because it says that, if two patches both have the highest fitness (in our case these are patch 1 and patch 2), then the probability of moving to these two patches from the remaining patches (in our case from patch 3) is anywhere between 0 and 1. That is, the probability of moving from patch 3 to patch 1 is $u$ while the probability of moving from patch 3 to patch 2 is $1-u$. The dispersal matrix $D^{12}$ is a convex combination of dispersal matrices in the two adjacent regions of the phase space (i. e., a convex combination of $D^1$ and $D^2$). The dispersal dynamics along the equal payoff line $V_1(p_1M) = V_2(p_2M) > V_3(p_3M)$ are

$$
\begin{aligned}
\frac{dp_1}{dt} &= u - p_1 \\
\frac{dp_2}{dt} &= 1 - u - p_2 \\
\frac{dp_3}{dt} &= -p_3.
\end{aligned}
\tag{1.14}
$$

Similarly, at the IFD $p^*$ the dispersal matrix $D^*$ is given as a convex combination $u_1D^1 + u_2D^2 + u_3D^3$ of the three adjacent dispersal matrices (i. e., $u_i \geq 0$ satisfy $u_1+u_2+u_3 = 1$). Since $D^*p^* = p^*$ at the IFD, it follows that $u_i = p_i^*$ and so

$$
D^* = \begin{pmatrix} p_1^* & p_1^* & p_1^* \\ p_2^* & p_2^* & p_2^* \\ p_3^* & p_3^* & p_3^* \end{pmatrix}.
$$

Three trajectories of (1.11) are shown in Figure 1.3A (left panel) as solid lines. The IFD is reached in finite time as is clearly documented in Figure 1.3A (middle panel) where patch payoffs equalize in a finite time when the IFD is achieved.

For example, let us consider an initial distribution where all individuals occupy patch 2 only, corresponding to the lower right corner of the triangle in Figure 1.3A (left panel). For the particular parameters used in this figure, the "best" patch is then the first patch and so individuals initially disperse there. Thus, initially, payoff in patch one decreases, payoff in patch two increases and payoff in patch three does not change (Figure 1.3A, middle panel). Once the population reaches the equal payoff line where the payoff in patch 1 equals the payoff in patch 3, individuals then start to disperse to patch 3 as well because both patch 1 and patch 3 are the "best" patches. The animal distribution must stay on this equal payoff line. Indeed, if slightly more individuals moved to patch 1 (so that the corresponding trajectory shifted slightly off and below the equal payoff line), the payoff in this patch would decrease below the payoff in patch 3 and, immediately, patch 3 would become the best patch. This forces the trajectory to move back to the equal payoff line.

The above specific example can be extended to any number of patches. The dynamics given by (1.11) are also called the best response dynamics (Hofbauer and Sigmund 1998) because they can be used to model individuals who choose the best strategy with respect to the present state of the system. Under our assumptions, the IFD is globally asymptotically stable regardless of the number of patches. That is, every trajectory of (1.11) will converge to the IFD when the dispersal matrix corresponds to ideal animals. Furthermore, dispersal does not cease at the IFD. In fact, at the IFD (1.12), the dispersal rates are equal to the population distribution, i. e., $D_{ij} = p_i^*$, $i, j = 1, 2, 3$. That is, the probability of migrating from any other patch to patch $i$, or to stay in patch $i$ and not to disperse is positive (and equal to $p_i^*$). If the total population density $M = K_1 + K_2 + K_3$ corresponds to the population equilibrium (i. e., $V_1(p_1 M) = V_2(p_2 M) = V_3(p_3 M) = 0$), then the IFD (1.12) simplifies to $p_i^* = K_i/(K_1 + K_2 + K_3)$ and corresponds exactly to balanced dispersal (Holt and Barfield 2001). This agrees with the theoretical prediction given by McPeek and Holt (1992) that the dispersal rate from patch $j$ to patch $i$ (which is $D_{ij} = p_i^*$) is inversely related to the carrying capacity $K_j$ of patch $j$. Furthermore, the emigration rate from patch $j$ ($E_j$, defined as the sum of the dispersal rates from patch $j$ to other patches, e. g., $E_3 = p_1^* + p_2^* = (K_1 + K_2)/(K_1 + K_2 + K_3)$ for $j = 3$) at the IFD is also inversely related to $K_j$ in agreement with experimental results such as Osawa (2000) and Diffendorfer (1998). In fact, for our models, a comparison of patch payoffs and emigration rates (the middle and right panels of Figure 1.3A respectively) shows these are also inversely related along trajectories of (1.11) that have not yet reached the IFD. Indeed, for every time instant, if the payoff in patch $i$ is higher than that in patch $j$ (i. e., $V_i > V_j$) then the emigration rate from patch $i$ is lower than from patch $j$. Along this trajectory the emigration rates

are piece-wise constant and it is clear that they do not cease when the IFD is reached.

## 1.7.2 Myopic animals and better response dynamics

The assumption that animals are ideal in the sense they immediately move to the best patch is in many cases unrealistic because it means that animals know their environment perfectly. Other, more realistic dispersal rules that are based on local knowledge can be considered. For example, I can assume that individuals sample patches at random and switch to a new habitat only if it has a higher payoff. If the sampled patch has a lower payoff, then the individual moves back to the patch it started from. This type of behavior was observed in the sticklebacks of Milinski (1988) where it continued after the IFD was reached as some fish checked the resource level in each patch. It is also a common assumption in simulations of real ecosystems (e. g., Mooij et al. (2002) used this behavior to simulate the movement of snail kites in their Florida wetlands habitat). In our model, the probability that an individual switches from a patch $j$ with a lower payoff ($V_j$) to a patch $i$ with a higher payoff ($V_i$) is $1/n$ due to random sampling of the $n$ patches (here I assume that with probability $1/n$ an individual "samples" its own patch). The probability that an individual switches in the opposite direction (i. e., from patch $i$ to patch $j$) is zero. If all patches have different payoffs, the probability that an individual returns to the same patch it started from is $k/n$ where $k$ is the number of patches with a lower payoff. I will call individuals that follow such dispersal rules "myopic", because their behavior depends only on a local knowledge of their environment.

I illustrate this dispersal rule in the case of three patches. Once again, the dispersal matrix $D(p)$ is piece-wise constant. Migration rates change when the population distribution crosses one of the equal payoff lines (dashed lines in Figure 1.3B), which leads to six different values of the dispersal matrix. For example, in the region of the distribution space where $V_1 > V_2 > V_3$, the dispersal matrix is

$$D(p) = D^{123} = \begin{pmatrix} 1 & 1/3 & 1/3 \\ 0 & 2/3 & 1/3 \\ 0 & 0 & 1/3 \end{pmatrix}.$$

Indeed, because the payoff in the first patch is highest, all individuals from patch 1 that sampled any other patch will return which gives dispersal probability $D_{11}^{123} = 1$. On the other hand, $1/3$ of individuals from patch 2 and patch 3 sample patch 1 and stay there. This gives the first row in the dispersal matrix $D^{123}$. Likewise, all individuals that sampled patch 2 from patch 1 will move back to patch 1 leading to $D_{21}^{123} = 0$. Furthermore, $1/3$ of individuals from patch 2 sample patch 3 and return to patch 2, which together with $1/3$ of individuals from patch 2 that did not sample any other patch gives $D_{22}^{123} = 2/3$. Also, $1/3$ of individuals from patch 3 sampled patch 2 and stay there. This gives the second row of the dispersal matrix. For the third row, all individuals from

patch 1 and patch 2 that sampled patch 3 return, and only 1/3 of individuals from patch 3 (i. e., those that did not sample any other patch) stay in patch 3. The dispersal matrices in any of the other remaining parts of the distribution phase space can be constructed similarly.

The dispersal dynamics are shown in Figure 1.3B. As predicted, they converge to the IFD which is the same as the one for ideal animals. In contrast to the ideal case (Figure 1.3A), trajectories in Figure 1.3B do not evolve immediately in the direction of the current best patch. This is because individuals from the worst patch can disperse to either of the two other patches that have a higher payoff. There is another important difference when compared with ideal animals; namely, it is no longer possible to compute dispersal rates at the IFD, because these rates are not defined uniquely (Figure 1.3B, right panel). This is because at the IFD, the dispersal matrix is a convex combination of 6 matrices that correspond to six regions of the phase space adjacent to the IFD (see Figure 1.3B, left panel). That is, at the equilibrium, the Filippov regularization is $D^* = u_1 D^{123} + u_2 D^{132} + u_3 D^{312} + u_4 D^{213} + u_5 D^{231} + u_6 D^{321}$ where $u_i \geq 0$ satisfy $u_1 + \cdots + u_6 = 1$. Since the IFD condition $D^* p^* = p^*$ has only three equations, it is impossible to compute uniquely the six values $u_i$, $i = 1, \ldots, 6$. In other words, it is in principle impossible to predict the dispersal rates at the IFD when animals are myopic. However, as with ideal animals, the distribution dynamics continue to be uniquely defined for myopic animals and there will still be dispersal at the IFD.

### 1.7.3   Preferences for patches are proportional to differences in payoffs

The two dispersal dynamics studied above assumed that individuals disperse even if their distribution is at the IFD. Migration dynamics can also be developed in which dispersal matrices $I(p)$ depend continuously on the population distribution $p$ (e. g., Hugie and Grand 2003). In other words, a small change in the distribution causes small changes in individual strategies. However, as I already discussed, under the assumption that individuals never disperse to patches with a lower payoff, continuity immediately implies there can be no dispersal among patches with the same payoff. Although this assumption is therefore unrealistic in many situations, there are circumstances where continuous dependence makes sense. For instance, if individuals can perceive their environment by some sensory stimuli that do not require them to visit the other patches, they do not need to disperse when patch payoffs are the same (i. e., when the distribution corresponds to the IFD).

One of the simplest examples of such a dispersal matrix is given by

$$D_{ij}(p) = \begin{cases} \mu(V_i - V_j) & \text{if } V_i > V_j, \quad i \neq j \\ 0 & \text{if } V_i \leq V_j, \quad i \neq j \\ 1 - \sum_{V_i < V_\ell} \mu(V_\ell - V_i) & \text{if } i = j, \end{cases} \tag{1.15}$$

where $\mu > 0$ is so small that $D_{ii}$ is positive. The above matrix describes dispersal which increases as the difference between the payoffs increases. That is, the higher the benefit to moving to a new patch, the more willing individuals are to do so. As our two general conditions are satisfied (i. e., individuals do not disperse to patches with a lower payoff and some disperse to a patch with the highest payoff), the trajectories of these dispersal dynamics converge to the IFD. In this example, dispersal ceases at the IFD ($D_{ij} = 0$ for $i \neq j$). Furthermore, convergence to the IFD can no longer occur in finite time since the resulting dynamical system has a continuous vector field near the IFD. The case with three patches is shown in Figure 1.3C.

It is interesting to note that when dispersal rates are given by

$$D_{ij}(p) = \begin{cases} \mu p_i(V_i - V_j) & \text{if } V_i > V_j, \quad i \neq j \\ 0 & \text{if } V_i \leq V_j, \quad i \neq j \\ 1 - \mu \sum_{V_i < V_\ell} p_\ell(V_\ell - V_i) & \text{if } i = j. \end{cases} \tag{1.16}$$

model (1.11) becomes the replicator equation

$$\frac{dp_i}{dt} = \mu p_i \left( V_i(p_i M) - \overline{V}(p, M) \right), \quad i = 1, \ldots, n. \tag{1.17}$$

Here individuals disperse to patches that provide them with a higher payoff, but only provided these better patches are already occupied which is an unrealistic assumption for animal dispersal.

### 1.7.4 Suboptimal dispersal

In this section, I assume that there are some individuals that will move from patches with higher payoffs to patches with lower payoffs but the probability of such maladaptive movement will be small when compared with the probability of moving from a worse patch to a better patch. This section can then be interpreted as a dispersal model that combines both IFD and non-IFD dispersal (sensu Hugie and Grand 1998). One interpretation of adding random dispersal is that it allows an individual to make a mistake in assessing the payoff of a sampled patch. When the component of dispersal that leads to the IFD varies continuously with payoff differences as in the previous section, we show that undermatching occurs. It is interesting observation that for ideal or myopic animals the resulting population distribution can still correspond to the IFD even if individuals make errors in their decisions where to move.

Assume that the dispersal matrix has the form

$$D_{ij}(p) = \frac{\varepsilon}{n} + (1 - \varepsilon)J_{ij}(p) \tag{1.18}$$

where parameter $\varepsilon$ ($0 \leq \varepsilon \leq 1$) measures the degree of random versus frequency-dependent dispersal in the population. For example, matrix $J$ can be any of the dispersal matrices considered previously that describe frequency-dependent dispersal. When $\varepsilon = 1$, dispersal matrix (1.18) describes

unconditional random dispersal since every individual has the same probability to move to any one of the other $n - 1$ patches or to stay in the current patch. The corresponding random dispersal dynamics then has the globally asymptotically stable uniform equilibrium distribution $p_i^* = 1/n$.

Suppose that matrix $D$ depends continuously on distribution $p$ and satisfies assumptions of Proposition 13. There exists an asymptotically stable equilibrium $p^*$ and due to random dispersal all patches are occupied at this equilibrium distribution. If dispersal under $J$ converges to the IFD, this equilibrium distribution ranges from the uniform distribution when $\varepsilon = 1$ (shown as $(1/3, 1/3, 1/3)$ in Figure 1.3D) to the IFD when $\varepsilon = 0$. For positive $\varepsilon$ (such as in Figure 1.3D), there is undermatching since fewer individuals are in the better patch than predicted by the IFD. The extent of undermatching increases as the component of IFD movement in the population decreases (i. e., as $\varepsilon$ approaches one).

Somewhat counter intuitively, if the dispersal matrix can change abruptly with population distribution, then the IFD can still be reached even if individuals make errors in their decisions (i. e., when $\varepsilon > 0$) and dispersal under $J$ corresponds to ideal (or myopic) individuals. This is clearly documented in Figure 1.4, where the stable distribution is shown as a function of the degree of randomness ($\varepsilon$) in individual behavior. This figure assumes that, when $\varepsilon = 0$, individuals are ideal and their dispersal is described by the best response dynamics. We observe that, even with some random dispersal (here $\varepsilon$ can be any value up to 0.2), the stable population distribution still corresponds exactly with the IFD and, despite the randomness in individual movement, there is no undermatching. For this phenomenon to occur, the dispersal matrix $J$ corresponding to IFD movement cannot depend continuously on the population distribution since it is crucial that the IFD movement under $J$ continue even when the IFD is reached in order to offset the random (i. e., non-IFD) dispersal component.

Suboptimal dispersal patterns can also emerge when individual movement depends on other factors besides resource abundance. For instance, animals may exhibit exploratory behavior based in part on the memory of patch payoffs received in the past (our models all assume dispersal rates depend only on current payoffs). The two-patch simulation study of Regelmann (1984) shows that combining this effect with some tendency to move to better patches again leads to the IFD. Furthermore, in a variety of taxa, it has been shown (e. g. Weisser 2001) that animals select patches with lower predation risk. Thus, risky patches can be occupied by disproportionately fewer consumers than would be the case without predation risk, while safe patches can be occupied disproportionately more often. Similarly, animals may prefer to move to already occupied patches where they can find mates to patches with no or low occupancy. Qualitatively, dispersal then combines two mechanisms: an increase in immigration rates to patches occupied by conspecifics because of increased mating probability or decreased predation risk and; an increase in emigration
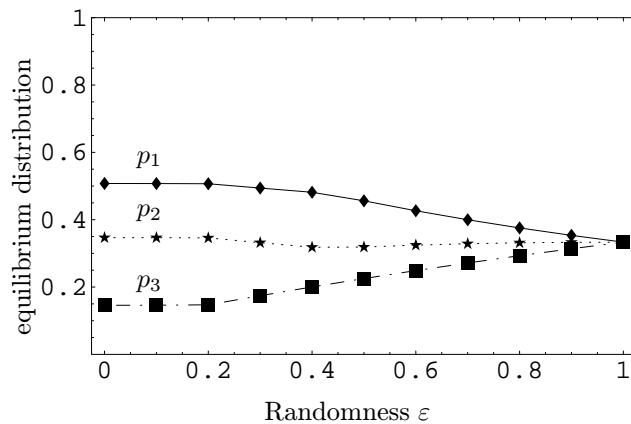
Figure 1.4: Dependence of the equilibrium distribution on the degree of randomness $\varepsilon$ for migration dynamics given by migration matrix (1.18) when matrix $J$ is given by the best response dynamics. For $\varepsilon$ smaller than approximately 0.2, the distribution corresponds exactly to the IFD $(p_1^*, p_2^*, p_3^*) = (0.51, 0.35, 0.14)$. As $\varepsilon$ tends to 1, the distribution converges to the uniform distribution $(1/3, 1/3, 1/3)$. Parameters as in Figure 1.3.

rate from a patch as the number of individuals increase there. For instance, these two tendencies are captured by the dispersal matrix

$$D_{ij}(p) = p_i \frac{1}{n}(1 - \mu V_j) \text{ for } i \neq j \tag{1.19}$$

where the factors $p_i$ and $\frac{1}{n}(1 - \mu V_j)$ model the first and second mechanisms respectively. The second factor can also be interpreted as an individual's dissatisfaction with a low payoff in its current patch together with a random component $\frac{1}{n}$ whereby these individuals have not chosen the destination patch. What is interesting for us is that the IFD again emerges for dispersal matrix (1.19) that includes some random dispersal and also varies continuously with frequency. The reason for this is that (1.11) again leads to the replicator equation (1.17) of the previous section since the maladaptive movement of some individuals is more than offset by net dispersal to better patches and the aggregate population behavior results in balanced dispersal at the IFD. That is, the overall population distribution moves towards the IFD even though individuals do not behave optimally, a phenomenon that has been noted many times in habitat selection models (e. g. Houston and McNamara 1988; Hugie and Grand 1998; Stamps 2001).

In summary, while suboptimal dispersal may lead to undermatching as in Hugie and Grand (1998), it can often result in the IFD outcome along with continued movement between patches at this equilibrium.

## 1.8   Distribution of lady beetles

In this section I will study dispersal modes for lady beetles. In particular, using some data from the field on distribution of lady beetles I will search for the best model (within a given set of models) of dispersal dynamics. Several authors observed (e. g. Turchin and Kareiva 1989; Hodek and Honěk 1996; Elliott and Kieckhefer 2000; Osawa 2000; Evans and Toler 2007) that density of adult lady beetles is positively correlated with aphid density. There is empirical evidence that the time coccinellids remain in experimental plots is positively correlated with patch quality. Banks (1957) and Osawa (2000) observed that lady beetles spend more of their time searching where prey are dense than where prey are sparse. Ives et al. (1993) observed positive correlation between the time females of lady beetle stayed on a fireweed (*Epilobium angustifolium* L.) stem and aphid density. These authors also observed a similar relationship on a larger spatial scale where scattered individuals of fireweed were manipulated experimentally to harbor varying numbers of aphids. Van der Werf et al. (2000) observed increased residence time and 10-20 times higher abundance of lady beetles in sugar sprayed plots when compared with control plots. As the emigration rate is inversely proportional to the staying time, these works (reviewed in Evans 2003) provide solid evidence that emigration rate decreases with increasing number of prey. Cardinale et al. (2006) observed a linear negative relationship between the emigration rate of lady beetles and the logarithm of aphid density. However, even when aphids are abundant at a given habitat a significant proportion of coccinellid adults disperses every day (Ives 1981; Frazer 1988). Interference between conspecifics can be one of the reasons for dispersal. For example, Růžička and Zemek (2007) observed that coccinellid larvae avoid staying on substrates with tracks of other larvae. These observations suggest that emigration rate may depend on both aphid and conspecifics density.

With respect to immigration the situation is less clear. Honěk (1980) (see also Hodek and Honěk 1996) estimated that the minimum aphid abundance capable of retaining predators is about 10 aphids per square meter of the crop area. Tracking individual lady beetles Osawa (2000) showed that short range movement of a lady beetle within plants of the same species or genus led to a better habitat only in approx. 44% of observed cases. However, movement between different subpopulations (i. e., plants of different genus) led to a better habitat in 75% of observations. Cardinale et al. (2006) observed no correlation between immigration rates and aphid density.

An idealized model describing spatial distribution of consumers in a patchy environment is the Ideal Free Distribution (IFD; Fretwell and Lucas 1970). At the IFD, consumer payoff in all occupied patches is the same and the number of immigrants to a given patch must equal the number of emigrants from the patch. Such a pattern of equalized immigration and emigration is called "balanced dispersal" (McPeek and Holt 1992; Doncaster et al. 1997; Holt and Barfield 2001).

Under balanced dispersal, there is an inverse relation between local population size and its dispersal rate. In other words, individuals at good sites are less likely to disperse then those from poor sites. Unbalanced dispersal caused by e. g., random animal movements between patches leads to a higher consumer density in the poor patch and a lower density in the good patch when compared with the IFD. This phenomenon is known as "undermatching" (Milinski 1988; Kennedy and Gray 1993; Houston et al. 1995; Jackson et al. 2004). It was shown that unconditional (i. e., random) dispersal should be selected against in spatially heterogeneous environments (Hastings 1983; Holt 1985; McPeek and Holt 1992). The Fretwell and Lucas concept is static in the sense that it does not address the question how a population distribution achieves the IFD. Cressman and Křivan (2006) studied various dispersal dynamics that lead to the IFD. They proved that if individuals never move to patches with a lower payoff and they do not ignore the best patch then the resulting distribution will correspond to the IFD.

I construct models that describe predator dispersal in a heterogeneous environment consisting of $n$ patches. consumer distribution dynamics are described by (1.10). I will assume that $D_{ij}$ is product of an immigration rate $b_j(m_j)$ and an emigration rate $a_i(m_i)$ that depend continuously on the consumer density. This means that emigration from a patch and immigration to a patch are independent processes. These assumptions lead to the following form of dispersal dynamics

$$\frac{dm_i}{dt} = a_i(m_i) \sum_{j=1}^{n} b_j(m_j)m_j - b_i(m_i)m_i \sum_{j=1}^{n} a_j(m_j) \quad \text{for } i = 1, \ldots, n. \tag{1.20}$$

The first term on the right hand side describes immigration to patch $i$ and the second term emigration from patch $i$. The equilibrium distribution $m^* = (m_1^*, \cdots, m_n^*)$ of model (1.20) satisfies the following equation

$$\frac{a_i(m_i^*)}{b_i(m_i^*)m_i^*} = C \quad \text{for } i = 1, \cdots, n \tag{1.21}$$

where constant $C$ is given by

$$C = \frac{\sum_{j=1}^{n} a_j(m_j^*)}{\sum_{j=1}^{n} b_j(m_j^*)m_j^*}.$$

Proposition 13 shows that provided dispersal matrix changes continuously with changing distribution and that immigration to a patch does not decrease as a payoff in that patch increases and emigration from a patch does not increase as the payoff in that patch increases then the equilibrium distribution is locally asymptotically stable. These assumptions hold for all dispersal models I will consider below.

### 1.8.1 Patch payoff

I will assume that each patch is characterized by its payoff $V_i$ and I will consider two patch payoffs. The first payoff is given by patch quality (measured as aphid abundance $K_i$ in the patch) per an individual lady beetle

$$V_i = \frac{K_i}{m_i} \tag{1.22}$$

which leads to Parker's input matching principle (Section 1.5.2)

$$\frac{m_i}{m_j} = \frac{K_i}{K_j} \quad \text{for } i, j = 1, \dots, n$$

(e. g. Parker 1978; Parker and Stuart 1976; Milinski and Parker 1991; Sutherland 1996).

As an alternative, I will also consider the case where patch payoff does not depend on the number of conspecifics, i. e.,

$$V_i = K_i. \tag{1.23}$$

In this case, under the IFD only the patch(es) with the highest $K_i$ will be occupied.

### 1.8.2 Emigration

Ives et al. (1993) and Osawa (2000) observed that the patch staying time of a lady beetle increases with aphid density. Here, I will generalize this observation by assuming that the staying time increases linearly with patch payoff (the proportionality constant cancels out in subsequent calculations and I set it arbitrarily equal to 1) . As the emigration rate from the $i$-th patch is inversely proportional to patch payoff (i. e., $b_i = \frac{1}{V_i}$) I get

$$b_i = \frac{m_i}{K_i} \tag{1.24}$$

when $V_i$ is given by equation (1.22) and

$$b_i = \frac{1}{K_i} \tag{1.25}$$

when $V_i$ is given by (1.23). In both cases, emigration rates from patch $i$ always decrease with increasing number of aphids in that patch.

### 1.8.3 Immigration is unconditional

Here I assume that the probability of immigrating to any of the $n$ patches is the same and equal to $a_i = 1/n$ (assuming that animals can return to the patch they departed from). From (1.21) it follows that for emigration rates given by (1.24) the equilibrium distribution satisfies

$$m_i = c\sqrt{K_i} \quad \text{for every } i = 1, \dots, n, \tag{1.26}$$

where $c$ is a constant. Thus, $m_i/m_j = \sqrt{K_i}/\sqrt{K_j}$ which is not the IFD. Unconditional immigration leads to "undermatching" where better patches get lower animal numbers when compared with the IFD.

For emigration rates (1.25) that depend on the aphid density only the equilibrium distribution is

$$m_i = cK_i \quad \text{for every } i = 1, \ldots, n. \tag{1.27}$$

It is interesting to note that despite the fact that immigration is random and emigration rates depend on the patch quality only, the resulting lady beetle distribution corresponds to the Parker's matching principle, thus to the IFD.

### 1.8.4  Immigration is proportional to patch quality

Here I assume that immigration is directly proportional to patch quality $K_i$. This means that individuals can sense prey abundance, but their decision where to immigrate is not influenced by the number of conspecifics already present in the patch. The immigration rates are $a_i = \frac{K_i}{K_1+\cdots+K_n}$. When substituted to (1.21) the equilibrium distribution for emigration rates (1.24) is given by (1.27). Once again we get the Parker's matching principle.

For alternative emigration rates (1.25) the corresponding equilibrium is

$$m_i = cK_i^2 \quad \text{for every } i = 1, \ldots, n. \tag{1.28}$$

Thus $m_i/m_j = K_i^2/K_j^2$ which corresponds to the "overmatching" because good patches contain a higher proportion of lady beetles than would correspond to the IFD.

### 1.8.5  Immigration is proportional to patch payoff

Another possibility is to consider the case where immigration rate is proportional to patch payoff $V_i$. In this case the dispersing individuals must be able not only to sense the number of aphids in a patch but also the number of conspecifics in that patch. The corresponding immigration rates are

$$a_i = \frac{K_i/m_i}{K_1/m_1 + \cdots + K_n/m_n}.$$

When substituted to (1.21) the equilibrium distribution for emigration rates given by (1.24) is

$$m_i = cK_i^{\frac{2}{3}} \quad \text{for} \quad i = 1, \ldots, n. \tag{1.29}$$

Thus, $m_i/m_j = (K_i/K_j)^{\frac{2}{3}}$ which corresponds to undermatching.

For alternative emigration rates (1.25) the predicted distribution is given by the Parker's matching principle (1.27).

| Model | Parameter estimate | Asymptotic SE | Confidence Interval | Mean Sum of Squares |
|---|---|---|---|---|
| $c\sqrt{K}$ | $c = 2.138$ | 0.174 | $(1.78, 2.49)$ | 1800 |
| $cK$ | $c = 0.016$ | 0.003 | $(0.01, 0.02)$ | 4845 |
| $cK^{2/3}$ | $c = 0.452$ | 0.051 | $(0.35, 0.55)$ | 2903 |
| $cK^2$ | $c = 6.7 * 10^{-7}$ | $2.1 \times 10^{-7}$ | $(2.5 \times 10^{-7}, 1.1 \times 10^{-6})$ | 7266 |
| $cK^d$ | $c = 11.509$ | 3.445 | $(4.51, 18.50)$ | 1120 |
| | $d = 0.300$ | 0.037 | $(0.22, 0.37)$ | |

Table 1.1: Best fit parameter(s) for models (1.26), (1.27), (1.29), (1.28) and a general power law using data on coccinellids distribution taken from Honěk (1982).

.

## 1.8.6  Which model fits data best?

Honěk (1982) (reprinted in Hodek and Honěk 1996) published data that relate density of *Coccinella septempunctata* to aphid density (Figure 1.5). For these data I estimated the unknown parameter $c$ in models (1.26), (1.27), (1.28), (1.29) using regression function `Regress` of Mathematica 6. Function `Regress` finds a least-squares fit to a list of data for a given linear combination of functions. For example, to estimate parameter $c$ for (1.26) I used command `Regress[data,{`$\sqrt{x}$`},`$x$`,IncludeConstant->False]`. Without setting the optional argument `IncludeConstant` to `False` value, Mathematica would automatically estimate parameters $k$ and $c$ for model $k + c\sqrt{x}$. With this optional argument, the absolute term $k$ is not included. The results are given in Table 1.1 and Figure 1.5. Because Figure 1.5 plots the data in the log-log scale, line slopes correspond to exponents of corresponding models. As least-squares minimize the sum of squared errors the predicted values must fit observed data for high lady beetle densities quite well. Thus, most of the data are above the estimated lines in Figure 1.5.

First, I will consider results for emigration rates given by (1.24). The corresponding distributions are then given by models (1.26), (1.27) and (1.29). Among these models, model (1.26) that corresponds to unconditional immigration (solid line in Figure 1.5) fits the data best (in the sense of mean sum of squares, Table 1.1) while model (1.27) that corresponds to the IFD provides the worst fit (dotted line in Figure 1.5).

Second, when emigration rates are given by (1.25), the corresponding distributions are given by models (1.27) and (1.28) because the model with unconditional immigration and the model with immigration proportional to patch payoff lead to the same distribution (1.27). Model (1.28) gives even worse fit (long-dashed line) than model (1.27).
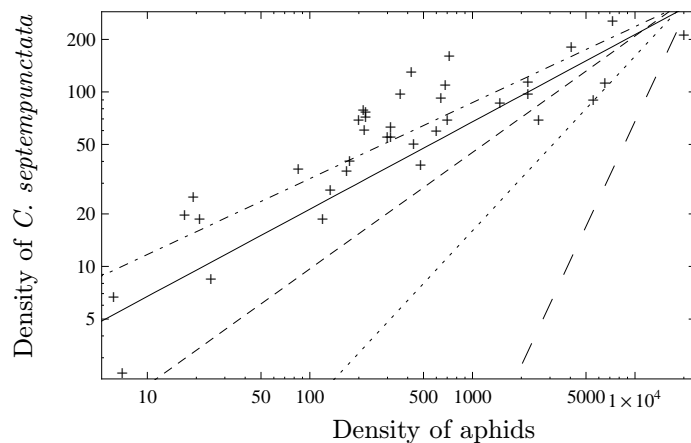
Figure 1.5: This figure shows the relation between abundance of *C. septempunctata* adults and aphids (*Acyrthosiphon pisum*). Data (crosses) were taken from Honěk (1982). The solid line is for model (1.26), the short-dashed line for model (1.29), the dotted line for model (1.27), the long-dashed line for model (1.28) and the dash-dotted line for a general power law function.

In addition, I also estimated parameters for a general power function $m_i = cK_i^d$. Not surprisingly, the general power law with two estimated parameters $c = 4.3$ and $d = 0.435$ gives the best least-squares fit (dot-dashed line in Figure 1.5, mean sum of squares=1580).

## 1.9  Asymmetric games

So far I have considered games between individuals of the same species. A question arises how one can extend these game theoretical concepts to two or multiple species. Such games are called asymmetric as the opponents are of different species.

Let us consider two species. Elementary strategies of the first species are $e_1, \ldots, e_n$ and elementary strategies of the second species are $f_1, \ldots, f_m$, respectively. By $p = (p_1, \ldots, p_n)$ and $q = (q_1, \ldots, q_m)$ I denote mixed strategies for the first and second species, respectivelly. For the games in the normal form I also assume there are four matrices $A$, $B$, $C$, $D$ that define payoffs $V_i(p, q) = \langle e_i, Ap + Bq \rangle$ and $W_j(p, q) = \langle f_j, Cp + Dq \rangle$ for elementary strategies against (mixed) strategy $(p, q)$. Concept of the Nash equilibrium readily generalizes for two (or more) species.

DEFINITION 9 *Strategy* $(p^*, q^*) \in S_n \times S_m$ *is called the Nash equilibrium, if*

$$\langle p^*, V(p^*, q^*) \rangle \geq \langle p, V(p^*, q^*) \rangle$$

*and*

$$\langle q^*, W(p^*, q^*)\rangle \geq \langle q, W(p^*, q^*)\rangle$$

*for any $p \in S_n$ and $q \in S_m$.*

The question is how to extend the notion of evolutionarily stability for asymmetric games. There have been several attempts in the literature to extend the single-species ESS concept to non symmetric games that model multiple species interactions. An early attempt by Taylor (1979) (see also Thomas (1986)) took the sum of payoff functions for each species and searched for a single-species ESS with respect to this lumped payoff function. From the evolution point of view this suggestion is not acceptable because it assumes the two species "share" their payoff.

Another attempt has developed over the past twenty years through the work of J. S. Brown and T. L. Vincent (surveyed in Vincent and Brown 2005). This approach was originally based on what is now called their "Darwinian dynamics" that couples population dynamics with a strategy dynamics when the set of pure strategies for a given species is a continuum. When applied to a game that has linear payoffs, no ESS candidate that involves a mixed strategy qualifies as an ESS for them (p. 293 in Vincent and Brown 2005) (see also p. 152 in Brown and Vincent 1987). For the habitat selection game this approach excludes the possibility that a single population can occupy several patches.

Here I follow Cressman (1992) (see also Cressman 1996; Cressman 2003) who defined a two-species ESS $(p^*, q^*)$ as a NE such that, if the population distributions of the two species are shifted slightly to $(p, q)$, then an individual in at least one species does better by playing its ESS strategy than by playing the slightly perturbed strategy of this species.

DEFINITION 10 (CRESSMAN (1992)) *A strategy $(p^*, q^*) \in S_n \times S_m$ is caled an ESS if at least one of the inequalities*

$$\langle p^*, V(p, q)\rangle > \langle p, V(p, q)\rangle \ \ \text{or} \ \ \langle q^*, W(p, q)\rangle > \langle q, W(p, q)\rangle \tag{1.30}$$

*is true for each perturbed pair of distributions $(p, q) \in S_n \times S_m$ sufficiently close (but not equal) to $(p^*, q^*)$.*

*A strategy $(p^*, q^*)$ is called a weak ESS if at least one of the conditions is true for each perturbed pair of distributions $(p, q)$ such that $p \neq p^*$, $q \neq q^*$ and $(p, q)$ is close to $(p^*, q^*)$.*

PROPOSITION 15 *Every two-species ESS is a Nash equilibrium.*

*Proof.* Let $(p^*, q^*)$ be an ESS and let us consider a point $(p, q^*)$ in a neighborhood of $(p^*, q^*)$. Then the first of the two conditions (1.30) holds, i. e.,

$$\langle p^*, V(p, q^*)\rangle > \langle p, V(p, q^*)\rangle$$

and continuity of payoff function $V$ implies

$$\langle p^*, V(p^*, q^*)\rangle \geq \langle p, V(p^*, q^*)\rangle.$$

The other inequality is proved analogously.

□

The two-species ESS definition can be rephrased that at least one of the two strategies is locally superior.

The following characterization of the interior two-species ESS was given in Cressman (1996), Cressman (1996).

PROPOSITION 16 *A strategy* $(p^*, q^*)$ *in the interior of* $S_n \times S_m$ *is an ESS if and only if it is the unique NE and there is an* $r > 0$ *such that*

$$\langle p - p^*, A(p - p^*) + B(q - q^*)\rangle + r\langle q - q^*, C(p - p^*) + D(q - q^*)\rangle < 0 \qquad (1.31)$$

*for all* $(p, q) \neq (p^*, q^*)$.

A special case of two-species games are bi-matrix games where the payoffs are given as

$$V_i(p, q) = \langle e_i, Aq\rangle, \quad W_j(q, p) = \langle f_j, Bp\rangle. \qquad (1.32)$$

Thus, the distinctive feature of bi-matrix games is that payoff of species one depends on strategies of species two only, and vice versa. An important consequence of the ESS definition is non-existence of an interior ESS for bi-matrix games (Selten 1980; Hofbauer and Sigmund 1998).

PROPOSITION 17 *If* $(p^*, q^*)$ *is an ESS of a bi-matrix game then* $p^*$ *and* $q^*$ *are pure strategies.*

*Proof.* Let us take $(p, q) = (p^*, q)$ sufficiently close but not equal to $(p^*, q^*)$. Then, necessarily,

$$\langle q^*, Bp^*\rangle > \langle q, Bp^*\rangle.$$

Similarly, taking $(p, q) = (p, q^*)$ sufficiently close but not equal to $(p^*, q^*)$ we get

$$\langle p^*, Aq^*\rangle > \langle p, Aq^*\rangle.$$

This shows that the ESS must be a strict NE.

□

For two-species assymetric games we can extend single-species dynamics. For example, the replicator dynamics extended for two-species are

$$\begin{aligned}
\frac{dp_i}{dt} &= p_i(V_i(p,q) - \overline{V}(p,q)) \\
\frac{dq_j}{dt} &= q_j(W_j(p,q) - \overline{W}(p,q)).
\end{aligned} \tag{1.33}$$

Similarly, the two-species dispersal dynamics are

$$\begin{aligned}
\frac{dp}{dt} &= \nu(I(p,q)p - p) \\
\frac{dq}{dt} &= \xi(J(p,q)q - q)
\end{aligned} \tag{1.34}$$

where $(p,q) \in S_n \times S_m$ and $I$ and $J$ are dispersal matrices. Parameters $\nu$ and $\xi$ reflect different time scales for the two species (and without the loss of generality $\nu$ can be set equal to 1). Thus, dispersal dynamics are defined by some specific dispersal rules given by transition matrices $I$ and $J$ and by time scales $\nu$ and $\xi$.

Similarly to the single-species case it is important to to know how the two-species ESS relates to equilibrium of replicator and dispersal dynamics.

PROPOSITION 18 (CRESSMAN (2003), KŘIVAN ET AL. (2008)) *The two-species interior ESS is globally asymptotically stable equilibrium of replicator (1.33) and best response dynamics (1.34).*

To show the interior ESS $(p^*, q^*)$ is globally asymptotically stable for the replicator dynamics we consider Lyapunov function (Cressman 2003)

$$F(p,q) = \Pi_{i=1}^{n} p_i^{p_i^*} (\Pi_{j=1}^{m} q_i^{q_i^*})^r,$$

where $r$ is that from Proposition 16. Derivative of this function along trajectories of (1.33) is negative because

$$\frac{dF}{dt} = F(p,q)\left( \langle p - p^*, A(p-p^*) + B(q-q^*) \rangle + r\langle q - q^*, C(p-p^*) + D(q-q^*) \rangle < 0 \right).$$

To show the interior ESS $(p^*, q^*)$ is globally asymptotically stable for the class of best response dynamics, we follow Křivan et al. (2008). Specifically, for a fixed $\nu$ and $\xi$, define

$$F(p,q) = \max_i (Ap + Bq)_i - \langle p, Ap + Bq \rangle + \frac{r\xi}{\nu}(\max_i (Cp + Dq)_i - \langle q, Cp + Dq \rangle).$$

Then $F(p,q) \geq 0$ for all $(p,q)$ with equality if and only if $(p,q) = (p^*, q^*)$. When $(p,q)$ has a unique best response $b_1$ and $b_2$ for species one and two respectively, then $\frac{dp}{dt} = \nu(b_1 - p)$ and $\frac{dq}{dt} = \xi(b_2 - q)$

(see (1.34)). Thus

$$
\begin{aligned}
\frac{dF}{dt} \;=\;& -\nu\langle b_1 - p, Ap + Bq\rangle + \langle b_1 - p, [\nu A(b_1 - p) + \xi B(b_2 - q)]\rangle \\
& -\frac{r\xi^2}{\nu}(b_2 - q)\cdot(Cp + Dq) + \frac{r\xi}{\nu}(b_2 - q)\cdot[\nu C(b_1 - p) + \xi D(b_2 - q)] \\
\;\le\;& \nu\left[(b_1 - p)\cdot\left(A(b_1 - p) + \frac{\xi}{\nu}B(b_2 - q)\right) + \frac{r\xi}{\nu}(b_2 - q)\cdot\left(C(b_1 - p) + D\frac{\xi}{\nu}(b_2 - q)\right)\right] \\
\;\le\;& 0
\end{aligned}
$$

by (1.31) where $b_1 - p$ is a nonnegative scalar multiple of some $\hat{p} - p^*$ and $\frac{\xi}{\nu}(b_2 - q)$ is a nonnegative scalar multiple of some $\hat{q} - q^*$. In fact, $\dfrac{dF}{dt} = 0$ if and only if $(p, q)$ is a NE (and so equal to $(p^*, q^*)$).

The above argument also holds when $(p, q)$ does not have a unique best response by simply taking $b_1$ and $b_2$ as the directions of the vector field in (1.34) whenever the trajectory of the best response dynamics has a tangent line (which occurs for almost all positive times $t$). Then $\dfrac{dF}{dt} \le 0$ at all such points and so $F$ is decreasing. This shows that $(p^*, q^*)$ is globally asymptotically stable.

$\square$

### 1.9.1 The habitat selection game for competing species

In this section I extend the single species Ideal Free Distribution for two competing species in heterogeneous environment consisting of two habitat patches. The Lotka–Volterra payoff functions for two competing species (see also Section 2.7.1) in patch $i$ (Křivan and Sirot 2002; Cressman et al. 2004) are

$$
\begin{aligned}
V_i(p_i, q_i) &= r_i\left(1 - \frac{p_i M}{K_i} - \frac{\alpha_i q_i N}{K_i}\right) \\
W_i(p_i, q_i) &= s_i\left(1 - \frac{q_i N}{L_i} - \frac{\beta_i p_i M}{L_i}\right).
\end{aligned}
\tag{1.35}
$$

Here, the overall fixed densities of species one and two are $M$ and $N$, respectively, and $p_i$ and $q_i$, respectively, are their distributions in patch $i = (1, 2)$. Positive parameters $\alpha_i$ (respectively, $\beta_i$), are interspecific competition coefficients, $r_i$ (respectively, $s_i$) are the intrinsic per capita population growth rates and $K_i$ (respectively $L_i$) are the environmental carrying capacities. All these parameters are assumed to be patch specific.

The payoff functions of the habitat selection game can be based on pairwise interactions and written in the form $V_i(p, q) = (Ap + Bq)_i$, $W_i(p, q) = (Cp + Dq)_i$ where $A, B, C, D$ are:

$$
A = \begin{pmatrix} r_1(1 - M/K_1) & r_1 \\ r_2 & r_2(1 - M/K_2) \end{pmatrix}
$$

,

$$
B = \begin{pmatrix} -\alpha_1 r_1 N/K_1 & 0 \\ 0 & -\alpha_2 r_2 N/K_2 \end{pmatrix}
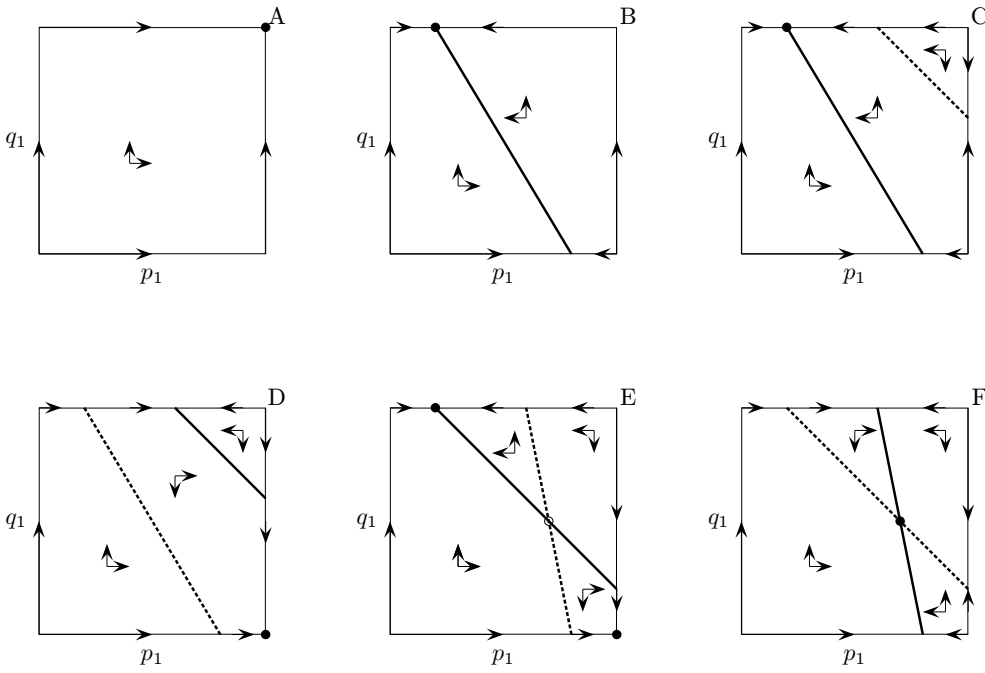$$

Figure 1.6: ESS (solid dots) for two competing species. In panel F is the interior NE an ESS. In panel E the interior NE (circle) is not an ESS and there are two other boundary NE that are both ESSs. The dashed and dotted lines are the equal-payoff lines for species 1 and species 2, respectively.

,

$$C = \begin{pmatrix} -\beta_1 s_1 M/L_1 & 0 \\ 0 & -\beta_2 s_2 M/L_2 \end{pmatrix}$$

,

$$D = \begin{pmatrix} s_1(1 - N/L_1) & s_1 \\ s_2 & s_2(1 - N/L_2) \end{pmatrix}.$$

The NE structure of the two-patch habitat selection game relies heavily on the analysis of the two equal payoff lines, one for each species. The equal payoff line for species one is defined to be those $(p, q) \in S_2 \times S_2$ for which $V_1(p_1, q_1) = V_2(p_2, q_2)$. Similarly, the equal payoff line for species two satisfies $W_1(p_1, q_1) = W_2(p_2, q_2)$. Since payoffs are linear functions and since $p_2 = 1 - p_1$ and $q_2 = 1 - q_1$, these are lines in the coordinates $p_1$ and $q_1$ as indicated in Figure 1.6. The equal-payoff line for species one (solid line in Figure 1.6) is

$$q_1 = \frac{K_1(K_2(r_1 - r_2) + r_2(M + N\alpha_2))}{N(K_2 r_1 \alpha_1 + K_1 r_2 \alpha_2)} - \frac{M(K_2 r_1 + K_1 r_2)}{N(K_2 r_1 \alpha_1 + K_1 r_2 \alpha_2)} p_1$$

and for species two (dotted line in Figure 1.6)

$$q_1 = \frac{L_1(L_2(s_1 - s_2) + s_2(N + M\beta_2))}{N(L_2 s_1 + L_1 s_2)} - \frac{M(L_2 s_1 \beta_1 + L_1 s_2 \beta_2)}{N(L_2 s_1 + L_1 s_2)} p_1.$$

Clearly, both of these lines have negative slope. If the two equal payoff lines do not intersect in the unit square, the two species cannot coexist in both patches at a NE. This means that at least one species will reside in a single habitat only. If only one species is entirely in its higher payoff patch, then the other species will distribute itself according to the single-species IFD conditional on species one being in its single patch. That is, there is then exactly one NE, which must automatically be on the boundary of the unit square (Figure 1.6).

An ESS (shown as the solid dots in Figure 1.6) on the boundary of the unit square can then be found by following the arrows in Figure 1.6 which indicate directions in which the payoff for species 1 increases (horizontal arrows) and similarly for species 2 (vertical arrows). A boundary ESS is then any point where all nearby boundary arrows point towards it as well as all nearby interior arrows perpendicular to this boundary. In particular, a vertex is an ESS if and only if both adjacent boundary arrows point in that direction. That is, if the two equal-payoff lines do not intersect in the unit square (Figure 1.6A-D), then there exists a unique ESS such that at least one population occupies one habitat only. To determine whether an interior intersection of the two equal-payoff lines is a two-species ESS requires more care. The analysis of Figure 1.6E shows the the interior intersection (shown as an empty circle) is not a two-species ESS. However, if the two equal-fitness lines are interchanged (Figure 1.6F), the interior intersection is the only two-species ESS.

To summarize, for the two-species two-habitat competition model, there is exactly one ESS for all possible parameter values except as in Figure 1.6E where the two equal-payoff lines intersect

in the interior of the unit square and the equal-payoff line for species 2 is steeper than is the equal-fitness line for species 1 which happens when

$$\frac{r_1 K_2 + r_2 K_1}{\alpha_1 r_1 K_2 + \alpha_2 r_2 K_1} > \frac{\beta_1 s_1 L_2 + \beta_2 s_2 L_1}{s_1 L_2 + s_2 L_1}.$$

In this case there are two ESSs and, without some additional information (for example about the order of colonization), it is impossible to predict which of the two corresponding species spatial distributions will be attained for the two species. This inequality can be rewritten as

$$r_1 s_1 K_2 L_2 (1-\alpha_1\beta_1) + r_1 s_2 K_2 L_1 (1-\alpha_1\beta_2) + r_2 s_1 K_1 L_2 (1-\alpha_2\beta_1) + r_2 s_2 K_1 L_1 (1-\alpha_2\beta_2) < 0. \quad (1.36)$$

It is obvious from this latter inequality that if interspecific competition is weak ($\alpha_i$ and $\beta_j$ are sufficiently small so that $\alpha_i\beta_j < 1$) a unique ESS exists. The same holds if one species is dominant over the other species in both habitats (e. g., $\alpha$'s are much smaller than $\beta$'s, or vice versa).

### 1.9.2 Two-Patch Predator-Prey Systems

Now I study the IFD for predators ($C$) and their prey ($R$) in a two patch environment. Again I assume that fitness is measured by the per capita population growth in each patch and the payoff functions of the prey and predator species in patch $i$ are given by the Lotka–Volterra model (see also Section 2.2)

$$V_i = r_i - \lambda_i q_i C \text{ and } W_i = e_i \lambda_i p_i R - m_i, \quad (1.37)$$

respectively. Since the $V_i$ and $W_i$ exhibit no intraspecific effects on individual payoff, the equal payoff line for the prey (species one) is (see the dashed horizontal line in Figure 1.7A)

$$q_1^* = \frac{r_1 - r_2 + \lambda_2 C}{C(\lambda_1 + \lambda_2)} \quad (1.38)$$

and the equal payoff line for the predator (species two) is (see the dotted vertical line in Figure 1.7A)

$$p_1^* = \frac{m_1 - m_2 + e_2 R \lambda_2}{R(e_1 \lambda_1 + e_2 \lambda_2)}, \quad (1.39)$$

respectively. If one of these lines (say the vertical line for the predator) does not intersect the unit square, then any NE has all of the predators in one patch.

The above payoffs can be represented through the bi-matrix game (1.32) where

$$A = \begin{pmatrix} r_1 - \lambda_1 C & r_1 \\ r_2 & r_2 - \lambda_2 C \end{pmatrix}$$

and

$$B = \begin{pmatrix} e_1 \lambda_1 R - m_1 & -m_1 \\ -m_2 & e_2 \lambda_2 R - m_2 \end{pmatrix}$$

In what follows I will assume that patch 1 is better for prey when compared with patch 2 ($r_1 > r_2$). Let us assume that $m_1 \geq m_2$ and

$$R^* = \frac{m_1 - m_2}{e_1 \lambda_1}, \quad C^* = \frac{r_1 - r_2}{\lambda_1}.$$

Then for low prey densities ($R < R^*$) the NE predicts that all prey will occupy patch 1 and all predators patch 2. This is because prey density is low and it does not compensate for a higher predator mortality rate in patch 1. As all predators are in patch 2, all prey will stay in patch 1. Thus, the two populations spatially segregate. If prey density is high ($R > R^*$) while consumer density is low ($C < C^*$) the NE predicts that both population will occupy patch 1 only. This is because overcritical prey density makes patch 1 more profitable fro predators. As predator density is low, patch 1 continues to be more profitable for prey as well. For high densities of both populations ($R > R^*$, $C > C^*$) the NE predicts that both populations occupy both patches and population distribution is given by ($p_1^*, q_1^*$). If $R = R^*$ or $C = C^*$ there are infinitely many NEs. If $R = R^*$ and $C \leq C^*$ the set of NE consists of all couples ($p_1, q_1$) = ($p_1, 1$) where $0 \leq p_1 \leq 1$. Similarly, when $R = R^*$ and $C > C^*$ then the set of NE is as in the latter case but with $0 \leq p_1 \leq p_1^*$. When $R > R^*$ and $C = C^*$ then ($p_1, q_1$) = ($1, q_1$) where $q_1^* \leq q_1 \leq 1$.

Similarly, one can get the NE for the case where $m_1 < m_2$.

Let us consider the interior NE ($p^*, q^*$). The horizontal and vertical arrows in Figure 1.7A indicate the direction in which fitness increases. These directions satisfy our definition for the weak ESS. I remark that the interior NE is never an ESS because at distributions that lie on these lines neither prey nor predator fitness increases in the direction toward ($p^*, q^*$). This result also follows from Proposition 17. Moreover, this equilibrium is globally asymptotically stable for the continuous-time best response dynamics (Figure 1.7A; Křivan et al. 2008). A strict NE, which corresponds to a situation where all predators are in one patch and the prey are either all in the same patch or all in the other patch, is automatically asymptotically stable for evolutionary dynamics such as better response dynamics by one part of the Folk Theorem of Evolutionary Game Theory (p. 11, Cressman 2003) applied to two-player bimatrix games.

## 1.10    Optimal diet selection model

The classical model of diet selection is based on the assumption that resources are distributed uniformly randomly within a foraging patch. In such a scenario, consumers must decide, upon each encounter with a food item, whether or not it should attack that item or ignore it and search for another, possibly more profitable food item. There is some experimental evidence that some animals can make decisions with respect to composition of their diet (Stephens and Krebs 1986; Hanson
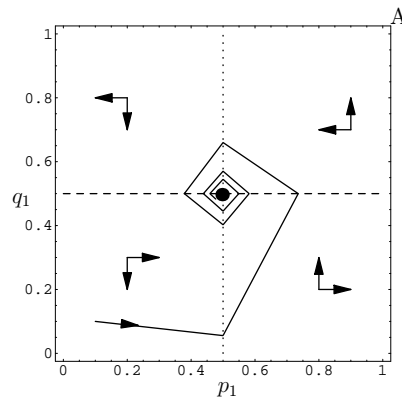
Figure 1.7: Two-patch Lotka–Volterra predator-prey system with a weak interior ESS. The vertical (horizontal) line through the weak ESS is the predator (prey) equal payoff line. These lines are given by given by (1.38) and (1.39). The horizontal and vertical arrows indicate the directions under best response dynamics. Trajectories of the best response dynamics evolve counterclockwise around the weak ESS. Other parameters: $M = N = 10$, $r_1 = r_2 = 1$, $s_1 = s_2 = 1$, $\alpha_1 = \alpha_2 = 0.1$, $\beta_1 = \beta_2 = 0.9$, $\xi = \nu = 1$.

and Green 1989; Belovsky and Schmitz 1994; Bulmer 1994). The standard model describing this foraging process is based on the assumption that consumers attempt to maximize their net rate of energy intake while foraging, which leads to the maximization of

$$\frac{E}{T_s + T_h},\tag{1.40}$$

(Charnov and Orians 1971; Charnov 1976; Stephens and Krebs 1986). Here $T_s$ represents the total time spent searching for resources, $T_h$ denotes the total time spent by handling resources and $E$ is the net amount of energy gained in the total time $T_s + T_h$.

In the $n-$resource species case, where the abundance of resource $i$ is denoted as $R_i$

$$T_h = T_s \sum_{i=1}^{n} \lambda_i h_i u_i R_i,$$

where $u_i$ denotes the probability that a consumer will attack resource $i$ upon an encounter, $\lambda_i$ represents the cropping rate of consumers for resource $i$, if alone, and $h_i$ is the handling time a consumer needs to process one food item of resource $i$.

The total net amount of energy obtained in time $T_s + T_h$ is

$$E = T_s \sum_{i=1}^{n} e_i u_i \lambda_i R_i,$$

where $e_i$ is the expected net energy gained from the $i-$th resource item. Thus, the surrogate for a fitness function (1.40) becomes

$$W = \frac{\sum_{i=1}^{n} e_i u_i \lambda_i R_i}{1 + \sum_{i=1}^{n} h_i u_i \lambda_i R_i},\tag{1.41}$$

(Charnov 1976; Stephens and Krebs 1986). The question that optimal foraging theory solves is to predict composition of consumer diet choice. To maximize $W$ we calculate partial derivative

$$\frac{\partial W}{\partial u_i} = \lambda_i R_i \frac{e_i(1 + \sum_{j \neq i, j=1}^n h_j u_j \lambda_j R_j) - h_i \sum_{j \neq i, j=1}^n e_j u_j \lambda_j R_j}{(1 + \sum_{j \neq i, j=1}^n h_j u_j \lambda_j R_j)^2}.$$

As this formula is independent of $u_i$, optimization of $W$ with respect to $u_i$ is independent of this variable. Thus, $W$ is maximized with respect to this variable either for $u_i = 0$ or $u_i = 1$. This is called zero-one rule in the literature on optimal foraging. If

$$\frac{e_i}{h_i} < \frac{\sum_{j \neq i, j=1}^n e_j u_j \lambda_j R_j}{1 + \sum_{j \neq i, j=1}^n h_j u_j \lambda_j R_j}$$

then the optimal value is $u_i = 0$, if the opposite inequality holds then $u_i = 1$.

To determine the optimal diet selection it is useful to rank resource species according to the profitability ratios $e_i/h_i$ in a decreasing order. The main result, derived from the maximization of fitness function (1.41) is that the most profitable resource 1 will be always included in the consumer diet ($u_1 = 1$). Resource $j$ will only be included provided

$$\frac{e_j}{h_j} > \frac{\sum_{i=1}^{j-1} e_i \lambda_i R_i}{1 + \sum_{i=1}^{j-1} h_i \lambda_i R_i},$$

(Stephens and Krebs 1986). This shows that inclusion of resource $j$ depends on density of resources that are already included in the diet. For two resources, this then leads to a critical density for resource 1

$$R_1^* = \frac{e_2}{\lambda_1(e_1 h_2 - e_2 h_1)} \tag{1.42}$$

such that if resource 1's density is below this threshold, resource 2 will be included in the optimal diet, i. e., $u_2 = 1$. If, however, the density of resource 1 is larger than the threshold, the optimal diet will consist only of resource 1. If the density of prey type 1 equals $R_1^*$ then consumer preference for the alternative resource ($u_2$) cannot be determined directly and it may be anywhere between 0 and 1. These conditions cause $u_2$ to be a step-like function of the density of the more profitable resource species

$$u_2(R_1) \in \begin{cases} \{0\} & \text{if } R_1 > R_1^* \\ \{u \mid 0 \leq u \leq 1\} & \text{if } R_1 = R_1^* \\ \{1\} & \text{if } R_1 < R_1^*. \end{cases} \tag{1.43}$$

The diet selection model assumes that consumers are omniscient and they are perfect optimizers. This then leads to instantaneous resource switching. More gradual switching (called also partial preferences) may also be observed (see also review in Stephens and Krebs 1986). Various mechanisms have been proposed to explain this discrepancy within the energy rate maximization models.
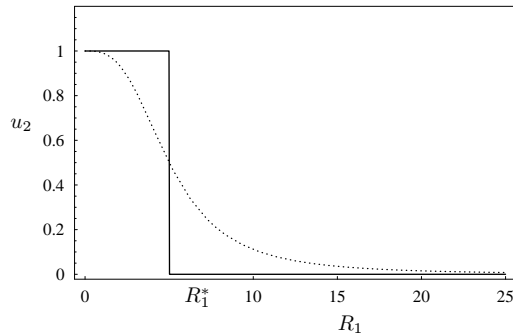
Figure 1.8: Optimal foraging strategies for diet selection model (solid line). The less profitable resource type is included in consumer diet when the density of the preferred resource is below the switching density $R_1^*$. Otherwise consumers specialize on the more profitable resource type. A more gradual switching described by function (1.44) (with $\mu = 5$) is shown as dotted line.

They range from incorrect classification of prey types by predators (Krebs et al. 1977; Rechten et al. 1983), uncertainty about the actual resource densities (McNamara and Houston 1987), a limited memory capacity of predators (Bélisle and Cresswell 1997), limited spatial omniscience (Berec and Křivan 2000) and individual differences in physiological state (Mangel and Clark 1988; Houston and McNamara 1999; Křivan and Vrkoč 2000). These departures from the assumptions made in optimal foraging models all lead to a more gradual switching which can be modeled as

$$u_2(R_1) = \frac{R_1^{*\mu}}{R_1^\mu + R_1^{*\mu}} \tag{1.44}$$

where parameter $\mu$ determines the width of the predators' switching interval (van Baalen et al. 2001). The higher $\mu$, the more closely gradual switching function $u_2(R_1)$ approximates the stepwise optimum switch (Figure 1.8, dotted line).

# Chapter 2

# The effects of adaptive behavior on population dynamics

The classical models of behavioral ecology, e. g., patch and diet choice models, introduced in Chapter 1, do not consider population dynamics. On the contrary, classical models of population dynamics do not consider animal adaptive behaviors. One argument that led to separation of behavioral and population ecology is based on time separation argument. As the two processes run on different time scales, they do not interfere one with another. In this chapter I show that this is not so. Combining these two types of models leads to a behavioral-population feedback. Individual behavior influences population dynamics which, in turn, influences animal behavior. I will show that such a feedback can have important consequences both for population dynamics and animal behavior.

## 2.1 Habitat selection game for growing populations

In Section 1.5 I showed that for a fixed population size the IFD is an ESS provided patch payoffs decrease with increasing number of individuals. Mechanism that can lead to such dependency can be related to increased competition for available space, to interference between animals etc. Such a negative effect of individuals of one species on its own population growth is called intraspecific competition. Assuming that patch payoff is proportional to the per capita population growth rate this assumption leads to the following population dynamics of the overall population abundance $M = m_1 + \cdots + m_n$ in $n$ patches

$$\frac{dM(t)}{dt} = M(t)F(M(t)) \tag{2.1}$$

where

$$F(M) \quad = \quad p_1(M)V_1(p_1(M)M) + \cdots + p_n(M)V_n(p_n(M)M)$$

is the expected fitness of the population mean strategy. Because animal distribution depends on the population abundance $M$, I make this dependence explicit by writing $p(M) = (p_1(M), \cdots, p_n(M))$. I first show that, at the population equilibrium, all patches will be completely occupied. This is a non-trivial prediction, because outside of the population equilibrium, consumers, when at low densities, will occupy the best patch(es) only (see (1.6) on page 19). Suppose $M^*$ is a positive population equilibrium of (2.1). Then all strategies that are present in the IFD (i. e., those strategies for which $p_i(M^*) > 0$) must satisfy $V_i(p_i(M^*)M^*) = 0$ because all these $V_i(p_i(M^*)M^*)$ are equal at the IFD (animal fitness is equalized over all occupied patches under the IFD) and the equilibrium population growth rate is zero ($F(M^*) = 0$). Moreover, in population equilibrium all habitats will be occupied, because if some habitat were empty (i. e., $p_i(M^*) = 0$) then $V_i(p_i(M^*)M^*) > 0$ and so individuals moving to that habitat would obtain a higher payoff then those staying in other habitats. Thus, at the population equilibrium $M^*$, all habitats will be occupied and individual fitness will be the same (and equal to zero) in all habitats. When patch payoff $V_i = r_i(1 - \frac{p_i(M)M}{K_i})$ is derived from the logistic population growth This immediately implies that at the population equilibrium, the density in each habitat is given by its carrying capacity (i. e., $m_i^* = K_i$ for all $i$) and so the overall population abundance is $M^* = K_1 + \cdots + K_n$. The IFD in a two patch environment where $r_1 > r_2$ is given by (1.6) on page 19. Population dynamics are described by a piecewise logistic equation

$$\frac{dM}{dt} = \begin{cases} r_1 M \left(1 - \dfrac{M}{K_1}\right) & \text{if } M < K_1 \frac{r_1 - r_2}{r_1} \\[3mm] \dfrac{r_1 r_2 M}{K_2 r_1 + K_1 r_2}(K_1 + K_2 - M) & \text{if } M \geq K_1 \frac{r_1 - r_2}{r_1}. \end{cases} \tag{2.2}$$

For any given initial population density, the total population reaches equilibrium abundance $K_1 + K_2$, at which the population density in either habitat equals the carrying capacity of that habitat (Figure 2.1, bottom panel). At the population equilibrium population distribution "matches" carrying capacities

$$\frac{p_1^*}{p_2^*} = \frac{K_1}{K_2}.$$

I compare the case where animals distribute at each population abundance according to the IFD with the case where animals disperse between patches with fixed preferences that are independent from population densities (e. g., at random in which case $p_1 = 0.5$). This corresponds to the case where

$$\frac{dM}{dt} = p_1 M r_1 \left(1 - \frac{p_1 M}{K_1}\right) + p_2 M r_2 \left(1 - \frac{p_2 M}{K_2}\right)$$
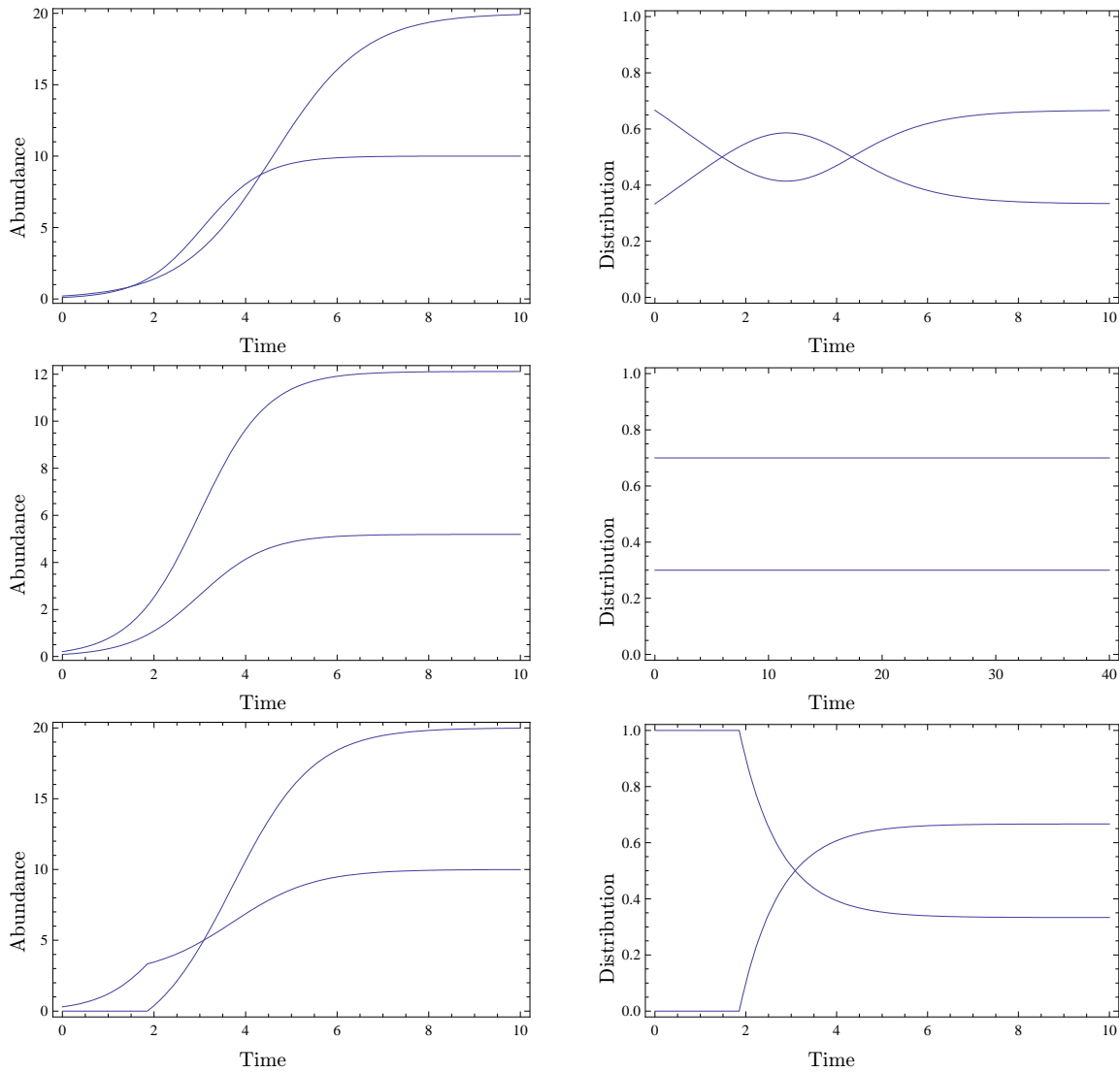
Figure 2.1: Solutions of the logistic model in a two patch environment. Top panel assumes no dispersal at all (see model (2.3)), the middle panel assumes fixed dispersal independent of population density ($p_1 = 0.7$), and the bottom panel assumes that animals follow the IFD and population dynamics are given by model (2.2). The left panel shows population dynamics while the right panel shows population distributions. Parameters: $r_1 = 1.5$, $r_2 = 1$, $K_1 = 10$, $K_2 = 20$.

where $p = (p_1, p_2)$ is fixed (i. e., independent of the population size $M$). The corresponding equilibrium is

$$M^* = \frac{K_1 K_2 (p_1 r_1 + p_2 r_2)}{K_2 r_1 p_1^2 + K_1 p_2^2 r_2}.$$

We observe that $m_i^* = p_i M^* = K_i$ if $p_1 = K_1/(K_1 + K_2)$, which corresponds to the so called balanced dispersal (Holt and Barfield 2001). One trajectory of model with fixed preferences is shown in Figure 2.1 (middle panel, $p_1 = 0.7$, $K_1 = 10$, $K_2 = 20$). The corresponding population equilibrium is $M^* \approx 17.31$, far below $K_1 + K_2 = 30$. This is because disproportionally many individuals move to patch 1 when compared with balanced dispersal.

It is interesting to point out that the same qualitative result as in the case where animal distribution tracks the IFD emerges from the model without dispersal (e. g., sessile organisms). This leads to two independent logistic equations

$$\frac{dm_i}{dt} = m_i \left(1 - \frac{m_i}{K_i}\right), \quad i = 1, 2. \tag{2.3}$$

Contrary to the case where animal distribution tracks instantaneously the IFD, now the time scale for the dynamics of animal distribution (given by $p_i = m_i/(m_1 + m_2)$) is of the same order as the population dynamics. Clearly, $m_i$ converges to $K_i$ and $M^* = K_1 + K_2$ (Figure 2.1, top panel). That is, from a population point of view that does not observe whether individuals change habitats or not, the two stable limiting distributions look identical; namely, the proportion of individuals in a given habitat is exactly equal to its carrying capacity. Thus, one can wonder if this is a general property, or if this is limited to the special case of (single species) habitat selection models. In fact, we will see in Section 2.7.2 that individual behavior is important for two-species IFD (i. e., qualitative predictions when animals can move are different than those when they cannot).

## 2.2 The Lotka-Volterra predator-prey model

Why a complete closure of fishery during the First World War caused an increase in predatory fish and a decrease in prey fish in the Adriatic See? This was the question that led Vito Volterra (Volterra 1926) to formulate a mathematical conceptualization of prey–predator population dynamics. In his endeavor to explain mechanisms by which predators regulate their prey, he constructed a mathematical model that describes temporal changes in prey and predator abundances. The model makes several simplifying assumptions such as: (i) the populations are large enough so it makes sense to treat their abundances as continuous rather than discrete variables; (ii) the populations are well mixed in the environment (which is the reason why this type of models is sometimes called mass action models in an analogy with chemical kinetics); (iii) the populations are closed in the sense

that there is no immigration or emigration; (iv) the population dynamics are completely determin-istic, i. e., no random events are considered; (v) in absence of predators, prey grow exponentially; (vi) the per predator rate of prey consumption is a linear function of prey abundance; (vii) preda-tors are specialists and without the prey their population will decline exponentially; (viii) the rate with which consumed prey are converted to new predators is a linear function of prey abundance; (ix) both populations are unstructured (e. g., by sex, age, size etc.); (x) reproduction immediately follows feeding etc.

If $R(t)$ and $C(t)$ are the prey and predator abundance, respectively, then under the above assumptions the population dynamics are described by two differential equations

$$
\begin{aligned}
\frac{dR}{dt} &= (r - \lambda C)R, \\[2mm]
\frac{dC}{dt} &= (e\lambda R - m)C,
\end{aligned}
\tag{2.4}
$$

where $r$ is the per capita prey growth rate, $\lambda$ is the rate of search and capture (hereafter search rate) of a single predator for an individual prey item so that $\lambda R$ is the per predator rate of prey consumption (i. e., the functional response), $e$ is the rate with which consumed prey are converted into predator births, and $m$ is the per capita predator mortality rate. Model (2.4), which was independently formulated by Alfred Lotka (Lotka 1926), is today known as the Lotka–Volterra prey-predator model. For initial population abundances $R(0)$ and $C(0)$, this model predicts future abundance of prey $R(t)$ and predators $C(t)$ (Figure 2.2A).

From the ecological point of view, the important information such a model can provide is whether or not population abundances tend to an equilibrium at which both species will coexists. At the equilibrium, predator and prey abundances do not change (i. e., $\frac{dR}{dt} = \frac{dC}{dt} = 0$), which gives

$$
R^* = \frac{m}{e\lambda} \quad \text{and} \quad C^* = \frac{r}{\lambda}.
$$

This equilibrium (shown as the solid dot in Figure 2.2B) is at the intersection of the prey and predator isoclines, which are the lines in the phase space along which $\frac{dR}{dt} = 0$ and $\frac{dC}{dt} = 0$ (shown as the dashed lines in Figure 2.2B). Interestingly, the prey equilibrium depends only on parameters that describe population growth of predators whereas the predator equilibrium depends on the prey per capita growth rate $r$. Thus, increasing the prey growth rate $r$ (which is sometimes called enrichment in the ecological literature) does not change the prey equilibrium density, but it increases the predator equilibrium abundance.

The Lotka–Volterra model (2.4) is an example of a conservative system with the first integral

$$
V(R, C) = m\left(\frac{R}{R^*} - 1 - \ln\frac{R}{R^*}\right) + r\left(\frac{C}{C^*} - 1 - \ln\frac{C}{C^*}\right),
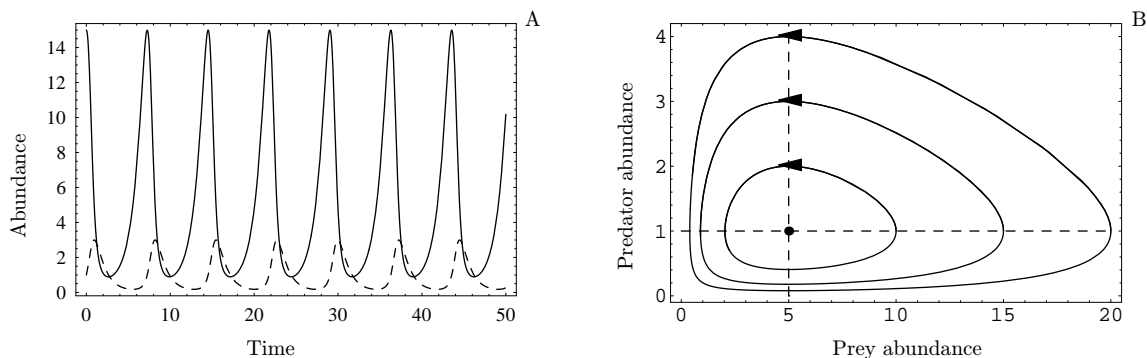\tag{2.5}
$$

Figure 2.2: Solutions of the Lotka–Volterra model (2.4) in time domain (A, solid line shows prey abundance, dashed line predator abundance) and in the prey-predator abundance phase space (B). Dashed lines in panel B are the isoclines. Parameters: $r = 1$, $\lambda = 1$, $e = 0.2$, $m = 1$.

which is constant along the trajectories of the model, since

$$\frac{dV(R(t), C(t))}{dt} = \frac{\partial V}{\partial R} R(r - \lambda C) + \frac{\partial V}{\partial C} C(e\lambda R - m) = 0.$$

As function $V$ is positive for positive population abundances (because the inequality $x - \ln x \geq 1$ holds for every $x > 0$) and it minimizes at the equilibrium point $(R^*, C^*)$, it is a Lyapunov function. Thus, solutions of the equation $V(R, C) = const$, which are closed curves in the prey–predator phase space (Figure 2.2B), correspond to solutions of model (2.4). This analysis shows that both prey and predator numbers will oscillate periodically around the equilibrium with the amplitude and frequency that depend on the initial prey and predator densities. Moreover, the average values of prey and predator densities over one period coincide with their equilibrium densities $R^*$ and $C^*$. Indeed, the equation for prey can be rewritten as

$$\frac{d\ln(R)}{dt} = r - \lambda C.$$

Integration of this equation over one population cycle of length $T$ time units gives

$$\ln(R(T)) - \ln(R(0)) = rT - \lambda \int_0^T C(t)dt.$$

Since $T$ is the period, the left hand side of the above equality is zero (because $R(0) = R(T)$) and

$$\overline{C} = \frac{1}{T} \int_0^T C(t)dt = \frac{r}{\lambda} = C^*,$$

where $\overline{C}$ denotes the average predator density. Similarly, the average prey density over each cycle equals the prey equilibrium density.

The above analysis shows that the prey-predator equilibrium is Lyapunov stable (i. e., after a small perturbation the animal abundances stay close to the equilibrium, Figure 2.2B), but it is not

asymptotically stable because the population abundances do not return to the equilibrium. This particular type of equilibrium stability is sometimes called the neutral stability. The eigenvalues of the Lotka–Volterra model evaluated at the equilibrium are purely imaginary ($\pm i\sqrt{rm}$) which implies that the period of prey-predator cycles with a small amplitude is approximately $2\pi/\sqrt{rm}$.

The mechanism that makes prey–predator coexistence possible in this particular model is the time lag between prey and predator abundances, with the predator population lagging behind the prey population (Figure 2.2A). The Lotka–Volterra model shows that (i) predators can control exponentially growing prey populations (this type of regulation is called the top-down regulation), (ii) both prey and predators can coexist indefinitely, (iii) the indefinite coexistence does not occur at equilibrium population densities, but along a population cycle. Can this model explain the question about the observed changes in predator and prey fish abundances during the First World War? Volterra hypothesized that fishery reduces the prey per capita growth rate $r$ and increases the predator mortality rate $m$, while the interaction rates $e$ and $\lambda$ do not change. Thus, ceased fishery during the First World War should lead to a decrease in average prey fish population $R^*$ and to an increase in the average predator fish population $C^*$, exactly as observed (Volterra 1926).

## 2.3 The Lotka–Volterra model with foraging-predation risk trade-offs

Animals are under constantly acting foraging-predation trade-off: to obtain food they have to be active, but activity increases predation risk. It is well known that individuals change their behavior under predation risk by reducing their activity level, or escaping to a safer areas (e. g., Murdoch 1969; Werner and Gilliam 1984; Fraser and Huntingford 1986; Holbrook and Schmitt 1988; Brown and Alkon 1990; Kotler et al. 1992; Brown 1998; Lima 1998a; Lima 1998b; Sih 1998; Brown et al. 2001; Dall et al. 2001; Peacor and Werner 2001; Werner and Peacor 2003; Brown and Kotler 2004; Kotler et al. 2004; Preisser et al. 2005). It is even more fascinating that rapid morphological and physiological adaptations were recently observed (e. g., Wikelski and Thom 2000; Yalden 2000; Relyea and Auld 2004; Losos et al. 2006). For example, the latter authors showed that within a single generation *Anolis sagrei*, a common Bahamian lizard can change the length of its hindlimbs as a result of habitat shift (from terrestrial to aboreal habitat) in response to increased predation risk in the terrestrial habitat.

Following Křivan (2007), I extend the classical Lotka–Volterra predator-prey model (2.4) by considering such a trade-off. I consider prey ($u$) and predator ($v$) activity levels that are numbers between 0 and 1. I will assume that parameters of the Lotka–Volterra model are linear functions

of these activity levels and I obtain the following model

$$\frac{dR}{dt} = (r_1 u + r_2 - (\lambda_1 u + \lambda_2 v)P)\,R$$

$$\frac{dP}{dt} = (e(\lambda_1 u + \lambda_2 v)R - (m_1 + m_2 v))\,P.$$

(2.6)

Increased prey activity ($u$) increases prey growth rate ($r_1 u + r_2$) but it also increases the encounter rate with predators ($\lambda_1 u + \lambda_2 v$). Similarly, increasing predator activity ($v$) increases both predator growth rate ($e(\lambda_1 u + \lambda_2 v)R$) and mortality rate ($m_1 + m_2 v$). Here $r_2$ and $m_1$ are the prey background growth rate and predator mortality rate, respectively, that are independent of activity level. Positive (negative) $r_2$ models the case where prey population grows (declines) if prey are completely inactive ($u = 0$). In what follows I will assume that $r_1 + r_2 > 0$ which means that active prey always reach a positive population growth rate. All other parameters in model (2.6) are positive and they have the same meaning as in the classical Lotka–Volterra model (2.4).

### 2.3.1 Predators only behave adaptively

To model predators that adjust their activity to current prey density I fix prey activity level at some arbitrary value (here $u = 1$) and I assume that predators behave so that their per capita population growth rate maximizes. Thus, predators should be maximally active provided their population growth rate exceeds the mortality rate associated with predator activity (i. e., $v = 1$ if $R > R_s = m_2/(e\lambda_2)$) and they should be inactive otherwise (i. e., $v = 0$ if $R < R_s$).

For prey densities above the switching threshold ($R > R_s$) predators are active ($v = 1$) and population dynamics are

$$\frac{dR}{dt} = (r_1 + r_2 - (\lambda_1 + \lambda_2)P)R$$

$$\frac{dP}{dt} = (e(\lambda_1 + \lambda_2)R - (m_1 + m_2))P.$$

(2.7)

These are the classical Lotka–Volterra equations with equilibrium

$$E_1 = \left( \frac{m_1 + m_2}{e(\lambda_1 + \lambda_2)}, \frac{r_1 + r_2}{\lambda_1 + \lambda_2} \right).$$

The resource equilibrium is higher than the switching threshold $R_s$ if

$$\frac{\lambda_2}{m_2} > \frac{\lambda_1}{m_1}.$$

(2.8)

Similarly, when prey density is below the threshold ($R < R_s$), predators are inactive ($v = 0$) and

population dynamics are

$$\frac{dR}{dt} = (r_1 + r_2 - \lambda_1 P)R$$

$$\frac{dP}{dt} = (e\lambda_1 R - m_1)P$$

(2.9)

with equilibrium

$$E_2 = \left( \frac{m_1}{e\lambda_1}, \frac{r_1 + r_2}{\lambda_1} \right).$$

This resource equilibrium density is lower than the threshold resource level $R_s$ if the inequality in (2.8) is reversed. I remark that for $R = R_s$, predator activity $v$ is not uniquely defined by maximizing predator fitness. I define a set-valued map $S : R \times R \rightsquigarrow [0, 1]$ that associates to every prey and predator density $(R, P)$ the corresponding optimal predator strategy $v$. This is a set-valued map because $S(R_s, P) = \{u \mid 0 \le u \le 1\}$. For this reason, model (2.6) when predators behave adaptively is not a differential equation, but a differential inclusion (for more details see Appendix).

First, I study behavior of model (2.6) using isoclines. The switch at $R = R_s$ causes the prey isocline to be Z-shaped (see the horizontal dotted line in Figure 2.3). The isocline consists of three parts: two horizontal lines and the vertical line segment joining them. The vertical segment is located at the prey density ($R = R_s$) where predators switch between active and inactive state. In the vicinity and to the right of the vertical part of the isocline prey population decreases while to the left it increases (see the arrows in Figure 2.3). It is clear that trajectories are "pushed" from both sides to the vertical part of the prey isocline and they cannot cross it. Thus, by definition (Rosenzweig and MacArthur 1963), the vertical segment is indeed a part of the prey isocline. This is clearly shown in Figure 2.3 where upon reaching the vertical part of the prey isocline trajectories cannot cross it and they move along it (downward in panel A and upward in panel B) before they settle on a Lotka–Volterra cycle (Křivan 1997; van Baalen et al. 2001).

The predator isocline is a vertical line (vertical dotted line in Figure 2.3) exactly as in the classical Lotka–Volterra case. The position of this isocline depends on the benefit/cost ratio ($\lambda_2/m_2$) which is due to predator activity. This ratio relates the added benefit expressed as the increased predator cropping rate ($\lambda_2$) to the added cost expressed as the increased predator mortality rate ($m_2$). If the predator benefit/cost ratio is high so that

$$\frac{\lambda_2}{m_2} > \frac{\lambda_1}{m_1}$$

(2.10)

then the predator isocline is to the right of the switching threshold $R_s$ (Figure 2.3A) and it is to the left if the opposite inequality holds (Figure 2.3B). In the first case the population equilibrium is in the part of the prey-predator density phase space where predator activity is at its maximum ($v = 1$), while in the second case predators are inactive at the equilibrium ($v = 0$). Using a
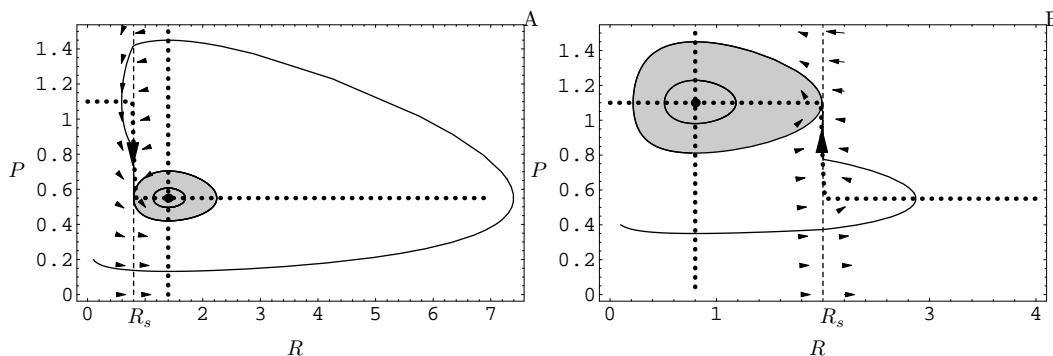
Figure 2.3: Solutions of model (2.6) where only predator behavior is adaptive. The dotted lines are isoclines, the dashed line shows the critical prey density $R_s = m_2/(e\lambda_2)$ below (above) which predators are inactive (active). The global attractor is shown in gray. The arrows along the switching line show direction of trajectories. In panel A the predator benefit/cost ratio ($\lambda_2/m_2$) is high, inequality (2.10) holds, and the population equilibrium is in the region of the prey-predator density phase space where predator activity is at its maximum ($v = 1$, $m_1 = 0.2$, $m_2 = 0.08$). Panel B considers the opposite case where inequality (2.10) does not hold and predators are inactive at the population equilibrium ($v = 0$, $m_1 = 0.08$, $m_2 = 0.2$). Other parameters: $r_1 = 1$, $r_2 = 0.1$, $\lambda_1 = 1$, $\lambda_2 = 1$, $e = 0.1$.

Lyapunov function it can be proved that trajectories converge to a global attractor shown in Figure 2.3 as the gray area. Let us consider the case where (2.10) holds (the other case follows the same path). Then

$$V(R,P) = \frac{1}{\lambda_1 + \lambda_2}(R - R^* - R^* \ln \frac{R}{R^*}) + \frac{1}{e(\lambda_1 + \lambda_2)}(P - P^* - P^* \ln \frac{P}{P^*})$$

is the classical Lyapunov function for model (2.7), i. e., for $R > R_s$. For $R \le R_s$ I get

$$\frac{dV}{dt} = \frac{(r_1 + r_2)(e\lambda_2 R - m_2) + P(\lambda_1 m_2 - \lambda_2 m_1)}{e(\lambda_1 + \lambda_2)^2} < 0$$

due to (2.10). Thus, to the left of the switching threshold $R = R_s$ $V$ decreases along trajectories of (2.9). Due to LaSalle theorem (Hofbauer and Sigmund 1998; Boukal and Křivan 1999), the attractor is bounded by the largest Lotka–Volterra cycle that is to the right of the line $R = R_s$ (Figure 2.3A). The attractor is formed of the Lotka–Volterra cycles of model (2.7). Contrary to the classical case where the amplitude of oscillations depends on the initial population densities, this attractor is bounded, i. e., the amplitude of maximum prey and predator oscillations is bounded. The bound is proportional to the distance of the equilibrium from the switching line ($R = R_s$). When $\frac{\lambda_2}{m_2} < \frac{\lambda_1}{m_1}$ the attractor is to the left of the switching line (Figure 2.3B) and the analysis is similar.

## 2.3.2 Adaptive prey

Here I consider the case where only prey behave adaptively. I set predator activity level to some fixed value (here to the maximum value $v = 1$). In this case the optimal prey strategy that

maximizes the per capita prey population growth rate is to be inactive when predator density is above a critical threshold given by $P_s = r_1/\lambda_1$ and to be active if the opposite inequality holds. This switching leads to a step like predator isocline (the dotted vertical line in Figure 2.4). According to its definition, trajectories cannot cross predator isocline in the vertical direction which is clearly documented in Figure 2.4A where a trajectory slides along the horizontal part of the predator isocline before it settles on a Lotka–Volterra cycle.

For predator densities that are lower than the switching threshold $(P < P_s = \frac{r_1}{\lambda_1})$ prey are active $(u = 1)$ and population dynamics are given by (2.7). The corresponding equilibrium $E_1$ is in the region of the predator-prey density phase space where $P < P_s$ if

$$\frac{r_2}{\lambda_2} < \frac{r_1}{\lambda_1}. \tag{2.11}$$

For predator densities that are higher than the switching threshold $(P > P_s)$ prey are inactive $(u = 0)$ and population dynamics are

$$
\begin{aligned}
\frac{dR}{dt} &= (r_2 - \lambda_2 P)R \\
\frac{dP}{dt} &= (e\lambda_2 R - (m_1 + m_2))P.
\end{aligned}
\tag{2.12}
$$

These population dynamics have equilibrium

$$E_3 = \left( \frac{m_1 + m_2}{e\lambda_2}, \frac{r_2}{\lambda_2} \right)$$

which is in the region where $P > P_s$ when inequality in (2.11) is reversed.

The prey isocline is the horizontal dotted line in Figure 2.4. Its position depends on the component of the benefit/cost ratio $(r_1/\lambda_1)$ which is due to prey activity. This ratio relates the added benefit expressed as the increased intrinsic per capita prey population growth rate to the added cost expressed as the increased prey mortality rate due to increased predation. If the prey benefit/cost ratio is high so that

$$\frac{r_1}{\lambda_1} > \frac{r_2}{\lambda_2} \tag{2.13}$$

then the prey isocline is below the switching line (Figure 2.4A) while if the opposite inequality holds then it is above the switching line (Figure 2.4B). If the background prey population growth rate is negative $(r_2 < 0)$, inequality (2.13) always holds. To maximize population growth rate at low predator density prey must be active. This leads to a high encounter rate between prey and predators (which is given by $\lambda_1 + \lambda_2$). The corresponding part of the predator isocline is the vertical segment at the point $R_1 = (m_1 + m_2)/(e(\lambda_1 + \lambda_2))$. When predator density is higher than the switching density, prey are inactive which shifts the predator isocline to the point $R_2 = (m_1 + m_2)/(e\lambda_2)$ that is to the right of $R_1$ (Figure 2.4). All trajectories converge to a global

attractor (shown as the gray area) that is formed by closed Lotka-Volterra cycles. Once again, prey and predator amplitude is bounded which prevents predator and prey densities become too low. When population densities settle on the attractor, the short term prey behavior effects attenuate: prey are either completely active (Figure 2.4A), or completely inactive (Figure 2.4B) and no changes in their activities should be observed.

### 2.3.3  Both species are adaptive

Finally, I consider the case where both prey and predators adjust their activity levels adaptively. This results in a predator-prey game because prey activity level depends on predator activity and vice versa. I assume that the activity levels reach the Ideal Free Distribution (Fretwell and Lucas 1970), i. e., neither prey, nor predators can increase their fitness by changing their strategy. The corresponding activity levels combine the activity level for adaptive prey with those for adaptive predators.

In what follows I will consider two possibilities: either prey population can increase when prey are completely inactive ($r_2 > 0$), or not ($r_2 < 0$). First I consider the case where prey can increase when inactive ($r_2 > 0$). The two switching thresholds ($R_s$ and $P_s$) split the prey–predator population density phase space in four parts (dashed lines in Figure 2.5). The short term predictions at the behavioral time scale for fixed prey and predator densities suggest that when prey density is lower (higher) than the threshold ($R_s$), predators are inactive (active). Similarly, when predator density is higher (lower) then the threshold ($P_s$), prey are inactive (active) due to high (low) predation risk. To obtain predictions at the population time scale I study population dynamics (2.6) where I substitute the optimal prey and predator activity levels. The graphical analysis shown in Figure 2.5 is based on the position of isoclines (dotted lines). The prey isocline is either L-shaped (when $r_2 > 0$, Figure 2.5A-D), or Z-shaped (when $r_2 < 0$, Figure 2.5E-F). This is because to the left of the predator switching line (the vertical dashed line in Figure 2.5) and above the prey switching line (the horizontal dashed line), i. e., in the upper left corner in Figure 2.5, both predators and prey are inactive, they do not interact, and prey population growth is always positive (if $r_2 > 0$), or negative (if $r_2 < 0$). Thus, prey isocline cannot intersect this region of the prey–predator phase space. Similarly, in the lower left corner of Figure 2.5A, prey are active ($u = 1$) and predators are inactive ($v = 0$). Substituting these activity values in model (2.6) I observe that the corresponding prey isocline is the horizontal line given by $P = (r_1 + r_2)/\lambda_1$. However, this line is in the lower left region of the prey–predator phase space only provided $r_2 < 0$ (and $r_1 + r_2 > 0$; Figure 2.5E and F) which then leads to Z-shaped prey isocline. For positive $r_2$ this segment of line is not in the lower left corner of the phase space and the prey isocline is L-shaped.

For positive $r_2$, depending on other parameters, there are four qualitative possibilities for position of predator and prey isoclines (Figure 2.5A-D). First, I consider the case where prey benefit/cost ratio is high ($r_1/\lambda_1 > r_2/\lambda_2$, Panels A and B).

If predator benefit/cost ratio is high ($\lambda_2/m_2 > \lambda_1/m_1$, Figure 2.5A) the population equilibrium is located in the part of the population density phase space where both predators and prey are active ($u = v = 1$) because prey density is high and predator density is low. This equilibrium is neutrally stable and trajectories converge to a bounded attractor (Figure 2.5A).

If predator benefit/cost ratio is low ($\lambda_2/m_2 < \lambda_1/m_1$, Figure 2.5B), the intersection of the two isoclines coincides with the intersection of the two switching lines ($R_s = m_2/(e\lambda_2)$ and $P_s = r_1/\lambda_1$) and population dynamics converge to this equilibrium. It is interesting to note that predator and prey activities at this equilibrium are intermediate and can be calculated explicitly. Indeed, at this equilibrium the right handside of model (2.6) must be zero by definition. Substituting the prey and predator equilibrium values allows me to calculate the activity levels at the population equilibrium

$$u^* = \frac{m_1\lambda_2}{m_2\lambda_1}; \quad v^* = \frac{r_2\lambda_1}{r_1\lambda_2}. \tag{2.14}$$

The stability of this equilibrium can also be proved by constructing Lyapunov function

$$V = \frac{m_2}{e_2\lambda_2}\left(\frac{R}{R_s} - 1 - \ln(\frac{R}{R_s})\right) + \frac{r_1}{\lambda_1}\left(\frac{P}{P_s} - 1 - \ln(\frac{P}{P_s})\right).$$

Indeed, in the region where $R > R_s$ and $P > P_s$, $u = 0$ and $v = 1$ and

$$\frac{dV}{dt} = \frac{(r_1\lambda_2 - r_2\lambda_1)(m_2 - \lambda_2 eR) + \lambda_2 m_1(r_1 - \lambda_1 P)}{e\lambda_1\lambda_2} < 0.$$

In the region where $R < R_s$ and $P > P_s$, $u = 0$ and $v = 0$ and

$$\frac{dV}{dt} = \frac{\lambda_1 r_2(\lambda_2 eR - m_2) + \lambda_2 m_1(r_1 - \lambda_1 P)}{e\lambda_1\lambda_2} < 0.$$

In the region where $R < R_s$ and $P < P_s$, $u = 1$ and $v = 0$ and

$$\frac{dV}{dt} = \frac{(m_1\lambda_2 - m_2\lambda_1)(r_1 - \lambda_1 P) + r_2\lambda_1(e\lambda_2 R - m_2)}{e\lambda_1\lambda_2} < 0.$$

In the region where $R > R_s$ and $P < P_s$, $u = 1$ and $v = 1$ and

$$\frac{dV}{dt} = \frac{(m_1\lambda_2 - m_2\lambda_1)(r_1 - \lambda_1 P) + (r_2\lambda_1 - r_1\lambda_2)(e\lambda_2 R - m_2)}{e\lambda_1\lambda_2} < 0.$$

Because along the lines $R = R_s$ and $P = P_s$ trajectories cannot diverge from the equilibrium, it follows that the equilibrium is globally asymptotically stable.

Second, I consider the case where prey benefit/cost ratio is low ($r_1/\lambda_1 < r_2/\lambda_2$). The two cases (Panel C assumes $\lambda_2/m_2 < \lambda_1/m_1$ and Panel D assumes $\lambda_2/m_2 > \lambda_1/m_1$) are qualitatively similar because when population dynamics reach the attractor, predators are active ($v = 1$) and
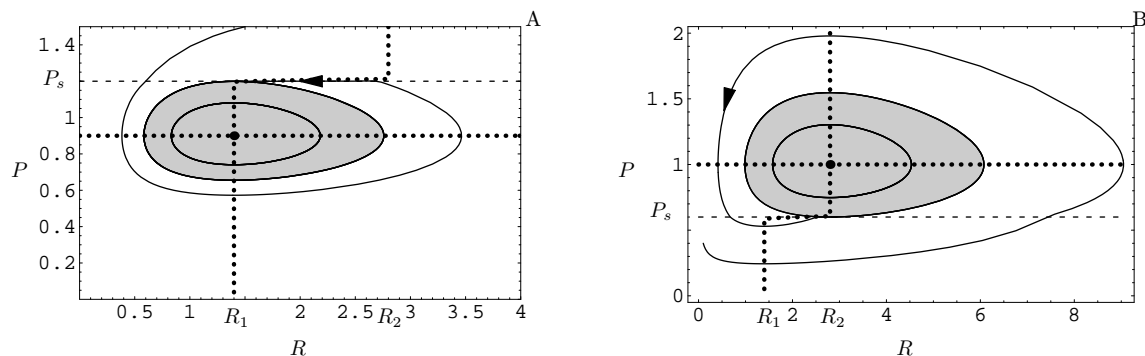
Figure 2.4: Solutions of model (2.6) when prey are adaptive. The dotted lines are isoclines, the dashed line is the predator critical density $P_s = r_1/\lambda_1$ above (below) which prey are inactive (active). The global attractor is shown in gray. Panel A shows the case where prey benefit/cost ratio ($r_1/\lambda_1$) is high and inequality (2.13) holds ($r_1 = 1.2$, $r_2 = 0.6$), panel B shows the opposite case ($r_1 = 0.6$, $r_2 = 1.2$). Other parameters: $\lambda_1 = 1$, $\lambda_2 = 1$, $m_1 = 0.08$, $m_2 = 0.2$, $e = 0.1$.

prey inactive ($u = 0$). In both cases the equilibrium is neutrally stable and all trajectories converge to the bounded attractor.

If $r_2 < 0$ there are two possibilities shown in Figure 2.5, panels E ($\lambda_2/m_2 > \lambda_1/m_1$) and F ($\lambda_2/m_2 < \lambda_1/m_1$). In both cases the equilibrium predator density is in the region of the prey–predator phase space where prey are active ($u = 1$). Predators can be either active (Panel E), or inactive (Panel F) at the population equilibrium.

## 2.4   The functional response

The Lotka–Volterra model (2.4) on page 60 assumes that the prey consumption rate by a predator is directly proportional to the prey abundance, i. e., $\lambda R$. This means that predator feeding is limited only by the amount of prey in the environment. While this may be realistic at low prey densities, it is certainly an unrealistic assumption at high prey densities where predators are limited e. g., by time and digestive constraints. The need for a more realistic description of predator feeding came from the experimental work of G. F. Gause (Gause 1934; Gause et al. 1936) on protist prey-predator interactions. He observed that to explain his experimental observations, the linear functional dependencies of the Lotka–Volterra model must be replaced by nonlinear functions.

To understand the nature of prey–predator interactions, M. E. Solomon (Solomon 1949) introduced concept of functional and numerical responses. The functional response describes prey consumption rate by a single predator as a function of prey abundance, while the numerical response describes the effect of prey consumption on the predator recruitment. Most simple prey–predator models such as the Lotka–Volterra model assume that production of new predators is directly pro-
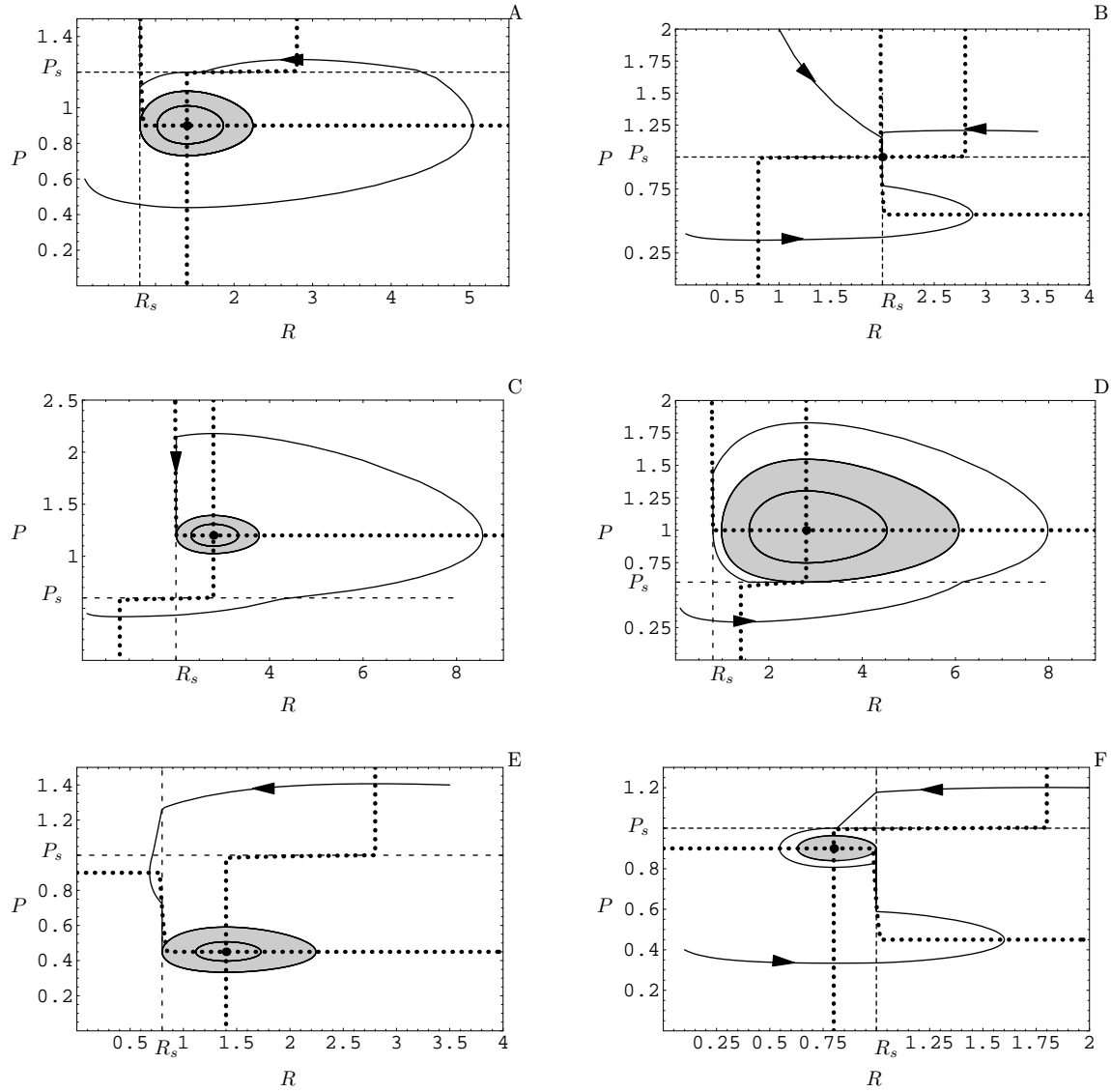
Figure 2.5: Solutions of model (2.6) when both prey and predators are adaptive. The dotted lines are isoclines, the dashed lines correspond to prey ($R_s = m_2/(e\lambda_2)$) and predator ($P_s = r_1/\lambda_1$) switching densities. The gray area denotes the attractor. Parameter $r_2$ is positive in Panels A-D and negative in panels E and F. Parameters used in simulations: $A: r_1 = 1, r_2 = 0.6, m_1 = 0.2, m_2 = 0.08$, $B: r_1 = 1, r_2 = 0.6, m_1 = 0.08, m_2 = 0.2$, $C: r_1 = 0.6, r_2 = 1, m_1 = 0.08, m_2 = 0.2$, $D: r_1 = 0.6, r_2 = 1, m_1 = 0.2, m_2 = 0.08$, $E: r_1 = 1, r_2 = -0.1, m_1 = 0.2, m_2 = 0.08$, $F: r_1 = 1, r_2 = -0.1, m_1 = 0.08, m_2 = 0.1$. Parameters $\lambda_1 = 1, \lambda_2 = 1, e = 0.1$ were the same in all simulations.

portional to the food consumption. In this case, the numerical response is directly proportional to the functional response. The constant of proportionality, $e$ in model (2.4), is the efficiency with which prey are converted to newborn predators.

Finally, C. S. Holling (1966) introduced three types of functional responses (Figure 2.6). The Type I functional response is the most similar to the Lotka–Volterra linear functional response, but it assumes a ceiling on prey consumption rate

$$f_I(R) = \min\{\lambda R, const\}$$

where $const$ is the prey consumption rate when prey abundance is high (Figure 2.6A). This functional response is found in passive predators that do not hunt actively (e. g., web-building spiders and filter feeders).

The Type II functional response assumes that predators are limited by total available time $T$. During this time predators are assumed either to search for prey (for $T_s$ time units), or to handle prey (for $T_h$ units). If the predator search rate is $\lambda$ and $R$ is the current prey density then the encounter rate of a searching predator with prey is $\lambda R$. If handling of a single prey item takes $h$ time units then $T_h = h \lambda R T_s$. Thus, $T = T_s + T_h = T_s(1 + h \lambda R)$ and the number of consumed prey by a predator during time $T$ is $\lambda R T_s$. The average consumption rate over time interval $T$ is then

$$f_{II}(R) = \frac{\lambda R T_s}{T} = \frac{\lambda R}{1 + h \lambda R},$$

which is the Holling Type II functional response (Figure 2.6B). This functional response is concave and for large prey abundances it converges to $1/h$, which is the upper limit on consumption. The form of the Holling type II functional response is equivalent with the Michaelis-Menten rate of substrate uptake as a function of the substrate concentration.

The Holling Type II functional response assumes that the predator search rate $\lambda$ is independent of the prey density. However, there are several ecological processes that can make this parameter itself a function of prey abundance i. e., $\lambda(R)$. These processes include e. g., predator inability to effectively capture prey when at low densities, predator learning, searching images, predator switching between several prey types, optimal predator foraging etc. When substituted to the Holling Type II functional response, this added complexity can change the concave shape of the functional response to a sigmoid shape (Figure 2.6C). Sigmoid functional responses are called the Holling type III functional responses. A prototype of such a functional response is obtained when $\lambda$ is replaced by $\lambda R^{\mu-1}$ in the Holling type II functional response, which then leads to a particular form of the Holling type III functional response

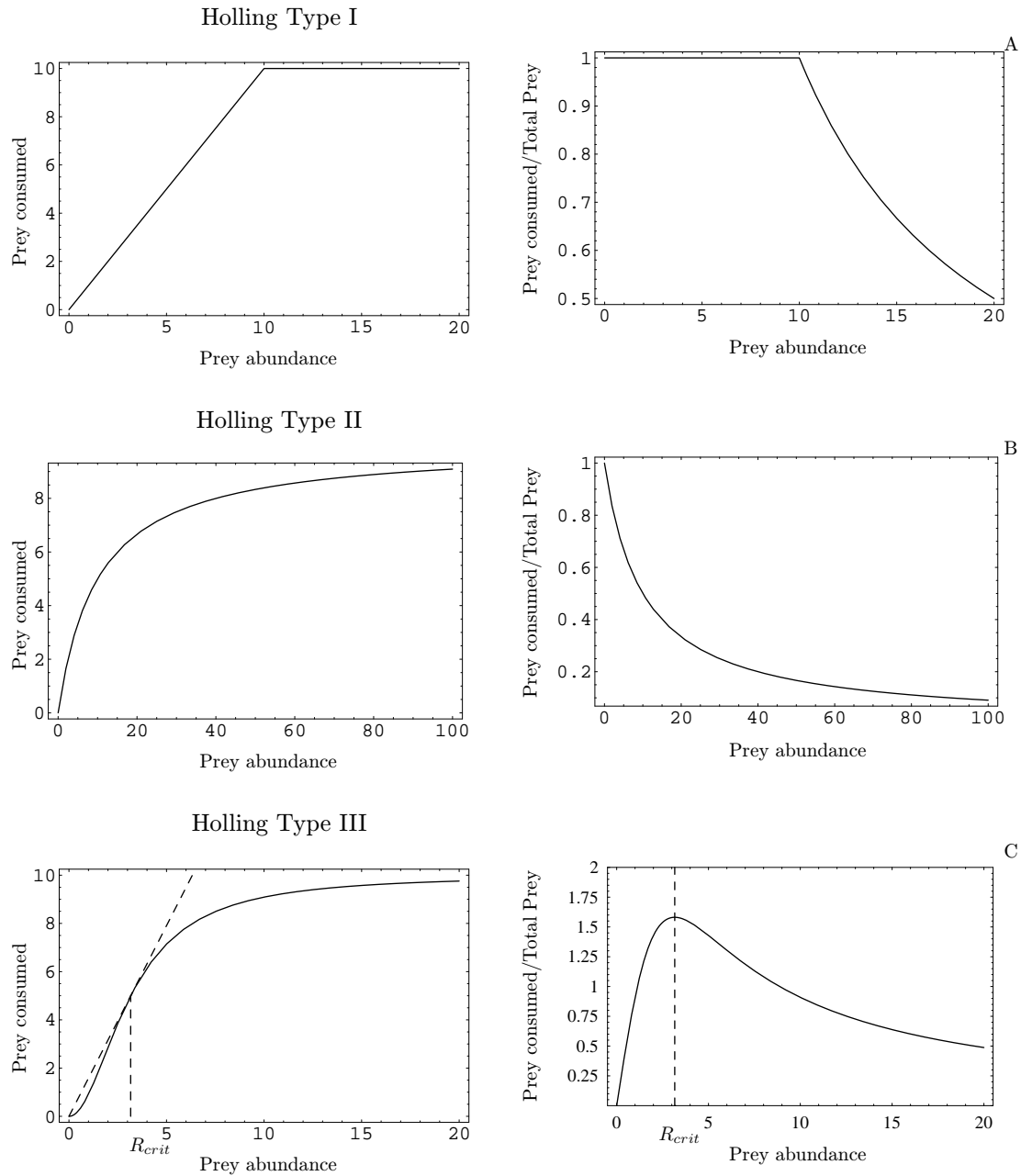$$f_{III}(R) = \frac{\lambda R^\mu}{1 + \lambda h R^\mu},$$

Figure 2.6: The three Holling type functional responses (left panel A- Type I, B-Type II, C-Type III). $R_{crit}$ in panel C is the critical prey density below which the functional response is stabilizing. The right panel shows the effect of the functional response on the equilibrium stability. Stability condition (2.20) requires that the ratio of consumed prey to total prey abundance is an increasing function of prey abundance. Parameters: $\lambda = 1$, $h = 0.1$.
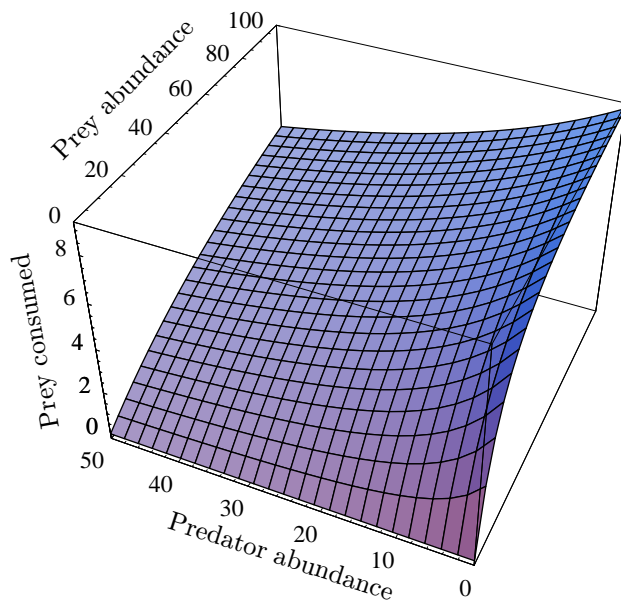
Figure 2.7: The Beddington-DeAngelis functional response (2.15). Parameters: $\lambda = 1$, $h = 0.1$, $z = 0.2$.

with parameter $\mu \geq 1$ ($\mu = 2$ in Figure 2.6C). For $\mu = 1$ the above functional response coincides with the Holling type II functional response, while for $\mu > 1$ the predator search rate increases with increasing prey density. This functional response is also called the Hill function. In enzymatic reaction kinetics the Hill function often describes a cooperative binding of several substrate molecules with an allosteric enzyme that has several binding sites.

The Holling functional responses consider a single predator and are thus functions of prey abundance only. If many predators are present, the per predator prey consumption rate can be influenced by predator interference that makes the functional response also dependent on predator density. A prototype of such a functional response is the Beddington–DeAngelis functional response

$$f(R, C) = \frac{\lambda R}{1 + \lambda h R + z C},\tag{2.15}$$

where $z$ is a positive parameter that models predator interference (Figure 2.7).

The functional responses considered so far can be extended to multiple resources. In a homogeneous environment where a searching consumer encounters resources sequentially, multiple resource Holling type II functional response for resource $i$ is

$$f_i = \frac{e_i u_i \lambda_i R_i}{1 + \sum_{i=1}^{n} u_i h_i \lambda_i R_i}, \quad i = 1, \dots, n.$$

Here $0 \leq u_i \leq 1$ is the consumer preference for resource $i$ and other parameters have the same meaning as for a single resource.
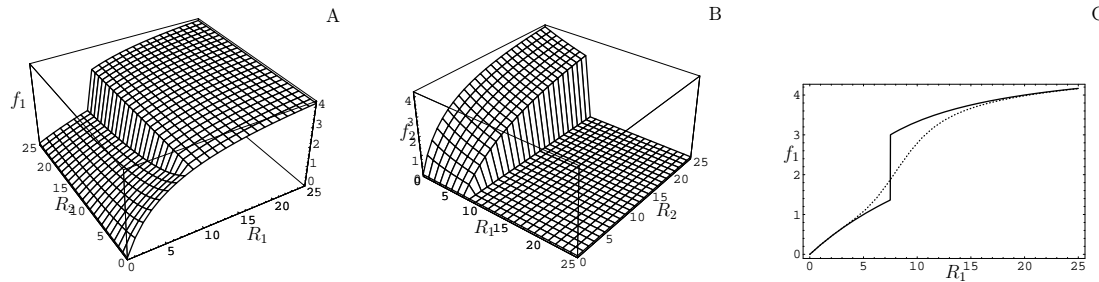
Figure 2.8: Functional responses (2.16) (panel A) and (2.17) (panel B) for optimally foraging predators on two resources in a homogeneous environment. Panel C shows the case where resource two abundance is fixed at $R_2 = 15$. Parameters: $e_1 = 1.$, $e_2 = 0.6$, $h_1 = 0.2$, $h_2 = 0.2$, $\lambda_1 = 1.$, $\lambda_2 = 1$.

Here I assume that consumers follow optimal diet selection described in Section 1.10. For two resources, with resource 1 being more profitable than resource 2 ($e_1/h_1 > e_2/h_2$) the switch in consumer diet choice $u_2(R_1)$ described by (1.43) on page 54 leads to the following functional response with respect to the more profitable resource 1

$$f_1 = \frac{\lambda_1 R_1}{1 + h_1 \lambda_1 R_1 + u_2(R_1) h_2 \lambda_2 R_2} \tag{2.16}$$

(Figure 2.8A) and to the functional response with respect to the less preferred resource 2

$$f_2 = \frac{u_2(R_1)\lambda_2 R_2}{1 + h_1 \lambda_1 R_1 + u_2(R_1) h_2 \lambda_2 R_2}, \tag{2.17}$$

(Figure 2.8B). At the switching density of the preferred resource type these functional responses are multivalued functions.

Assuming that the density of the less profitable resource species ($R_2$) is constant, I obtain a preferred resource functional response by taking a cross-section of the multiple resource functional response (the 3-dimensional surface in Figure 2.8A) parallel to the axis representing the primary resource. The cross section is saturating with a discontinuity at the preferred resource switching density (Figure 2.8C, solid curve).

Substituting a more gradual switching described by (1.44) on page 55 into a Holling type II functional response for two resources , I get a Holling type III sigmoidal functional response with respect to the first resource (Figure 2.8C, dotted line). Thus, adaptive foraging in multiple resource environment is another mechanism that can lead to the Holling type III functional response.

## 2.5 Effects of functional and numerical responses on prey-predator stability

How does the shape of functional and numerical responses influence prey-predator stability? To study this question I replace the linear functional and numerical responses in the Lotka–Volterra

predator prey model (2.4) by general functions $f$ and $g$. In addition, I will also assume that the per capita prey growth rate is density dependent. A general representation of a prey-predator model is then

$$\frac{dR}{dt} = r(R)R - f(R, C)C,$$

$$\frac{dC}{dt} = (g(R, C) - m)C.$$

For $r(R) = r$, $f(R, C) = \lambda R$ and $g(R, C) = e\lambda R$, the above model coincides with the Lotka–Volterra model (2.4).

In what follows I will assume that model (2.18) has a single positive equilibrium $R^*$ and $C^*$. Then the question is, what is the long term behavior of prey and predator abundances. Do they converge to this equilibrium? The usual starting point to answer this question is to study conditions under which the equilibrium is locally asymptotically stable. Conditions that guarantee local asymptotic stability of the equilibrium are given in terms of the Jacobian matrix evaluated at the equilibrium of model (2.18):

$$\begin{pmatrix} \frac{dr(R^*)}{dR}R^* + r(R^*) - \frac{\partial f(R^*, C^*)}{\partial R}C^* & , & -f(R^*, C^*) - \frac{\partial f(R^*, C^*)}{\partial C}C^* \\ \frac{\partial g(R^*, C^*)}{\partial R}C^* & , & \frac{\partial g(R^*, C^*)}{\partial C}C^* \end{pmatrix}.$$

To derive the above matrix I used the fact that at the equilibrium, $g(R^*, C^*) = m$. If the sum of the two diagonal elements (i. e., the trace) of the Jacobian matrix is negative and the determinant is positive then the equilibrium is locally asymptotically stable. This leads to the following two general conditions:

$$\frac{dr(R^*)}{dR}R^* + r(R^*) - \frac{\partial f(R^*, C^*)}{\partial R}C^* + \frac{\partial g(R^*, C^*)}{\partial C}C^* < 0 \tag{2.18}$$

$$\left(\frac{dr(R^*)}{dR}R^* + r(R^*) - \frac{\partial f(R^*, C^*)}{\partial R}C^*\right)\frac{\partial g(R^*, C^*)}{\partial C} + \left(f(R^*, C^*) + \frac{\partial f(R^*, C^*)}{\partial C^*}C^*\right)\frac{\partial g(R^*, C^*)}{\partial R} > 0. \tag{2.19}$$

Although these two conditions look quite formidable, they will substantially simplify for particular cases of functional and numerical responses considered in the next section.

## 2.5.1 Prey growth is density independent

Here I assume that the per capita prey growth rate is density independent ($r(R) = r$), which implies that in stability conditions (2.18) and (2.19), $\frac{dr(R^*)}{dR} = 0$. This case corresponds to the original Lotka–Volterra model in the sense that the only mechanism that regulates the exponential prey growth is predation (i. e., top-down regulation).

First, I will consider the effect of replacing the linear functional response by a non-linear functional response in the Lotka–Volterra model. Prey-predator population dynamics are described by

$$\frac{dR}{dt} = rR - f(R)C,$$

$$\frac{dC}{dt} = (g(R) - m)C.$$

For these dynamics the stability conditions (2.18) and (2.19) substantially simplify because functional and numerical responses are independent of the predator density (i. e., $\partial f/\partial C = \partial g/\partial C = 0$). Substituting the predator equilibrium abundance $C^* = rR^*/f(R^*)$, in stability conditions (2.18) and (2.19) gives

$$\frac{df(R^*)}{dR} > \frac{f(R^*)}{R^*} \tag{2.20}$$

and

$$\frac{dg(R^*)}{dR} > 0.$$

The latter condition states that the numerical response should be an increasing function of prey abundance. This condition will be satisfied for any reasonable numerical response and I will focus on the first condition. This stability condition can be interpreted graphically. The equilibrium is locally asymptotically stable provided the slope of the tangent line to the graph of the functional response at the point $(R^*, f(R^*))$ is higher than is the slope of the line that passes through the origin and the point $(R^*, f(R^*))$. For example, in Figure 2.6C this happens if the prey equilibrium density is to the left of the critical value $R_{crit}$ at which both slopes are the same (i. e., the tangent to the graph, shown as the dashed line, passes through the origin). Alternatively, stability condition (2.20) states that for a prey-predator equilibrium to be locally asymptotically stable it is sufficient that the ratio of consumed prey to total prey (i. e., $f(R)/R$, Figure 2.6, right panel) is an increasing function of prey density at the equilibrium. Indeed, condition (2.20) is nothing else then expression of the fact that derivative of function $f(R)/R$ with respect to prey density is positive. This is equivalent with saying that the prey zero isocline ($C = rR/f(R)$, shown as the horizontal dashed curve in Figures 2.2B, 2.9) has a negative slope at the equilibrium (Rosenzweig and MacArthur 1963). Clearly, a linear functional response used in the Lotka–Volterra model, the type I functional response and the type II functional response do not satisfy stability condition (2.20) because $f_{II}(R)/R$ is a decreasing function over the entire range of prey densities (Figure 2.6A,B, right panel). This means that the interior equilibrium is not asymptotically stable and I can ask what happens if populations are shifted of the equilibrium. In the case of the Lotka–Volterra model with the linear functional response I already know that after a perturbation trajectories oscillate around the equilibrium (Figure 2.2).

Now I consider the effect of the Holling Type II functional response on the prey-predator equilibrium stability. For small handling times the Holling type II functional response causes trajectories to spiral outward from the equilibrium (Figure 2.9B)

$$R^* = \frac{m}{(e - hm)\lambda}, \quad C^* = \frac{er}{(e - hm)\lambda}.$$

When prey density is high, the Holling type II functional response is saturated and equal approximately to $1/h$. Substituting this value in (2.20) and integrating the model, it was proved (Svirezhev and Logofet 1983) that for large handling times that satisfy $h > e\lambda/(r + m)$ there are trajectories along which both prey and predator populations grow to infinity (one such trajectory is shown in Figure 2.9C). In this latter case the prey population escapes completely the predator regulation. This happens, e. g., when predators are inefficient when handling prey (i. e., when the handling time is large), or the intrinsic per capita prey growth rate is high. This analysis validates the statement that the Holling type II functional response is destabilizing, which means that when handling times are positive, the neutrally stable equilibrium of the Lotka-Volterra model becomes unstable.

The Holling type I functional response combines the effects of the linear functional response with the Holling type II functional response for large handling times. Thus, when the prey-predator equilibrium is in the part of the prey-predator phase space where the functional response increases linearly (Figure 2.9A), small perturbations lead to periodic oscillations around the equilibrium while large perturbations lead to trajectories that diverge from the equilibrium.

Prey-predator coexistence can occur only either at the equilibrium, or along a limit cycle. However, in the case of the prey-predator model (2.20) with the Holling type II functional response it can be proved that no limit cycle exists. Indeed, because for the Holling type II functional response
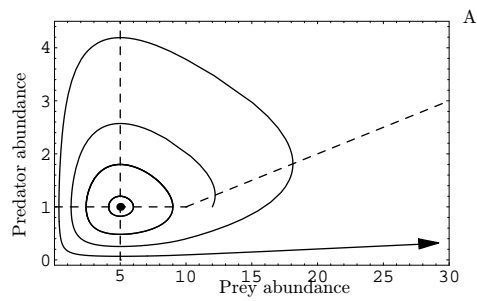
$$\frac{\partial}{\partial R}\left(\frac{1}{RC}(rR - f(R)C)\right) + \frac{\partial}{\partial C}\left(\frac{1}{RC}(g(R)C - mC)\right) = \frac{1}{R}\left(\frac{f(R)}{R} - \frac{df(R)}{dR}\right) > 0, \qquad (2.21)$$

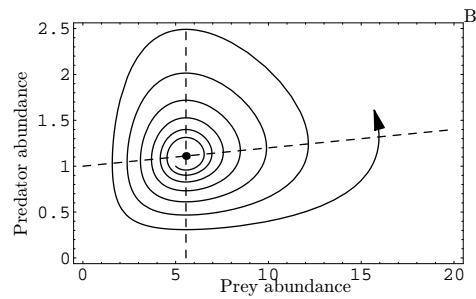the Dulac criterion excludes prey-predator limit cycles.

The functional response that meets the local stability condition (2.20) is the Holling type III response. But, the stabilizing effects of predators will occur only at low to medium prey equilibrium densities (those that are to the left of $R_{crit}$ in Figure 2.6C). This is the case shown in Figure 2.9D. At a higher prey equilibrium density, the functional response saturates and predators cannot regulate their prey (Figure 2.9E).

Second, I consider the case where functional and numerical responses depend on the predator density too. A prototype of such functions is the Beddington–DeAngelis functional response (2.15). To simplify analysis, I assume that the handling time in the Beddington–DeAngelis functional
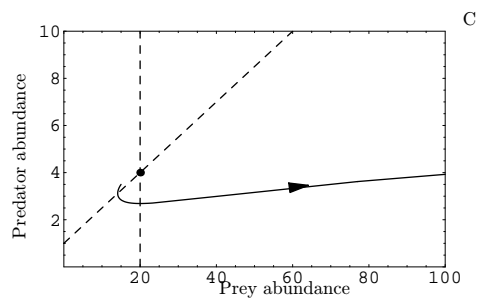
Figure 2.9: Dependence of prey–predator population dynamics on the functional response. Panel A shows solutions of the Lotka–Volterra model with the Holling type I functional response, Panels B (small handling time) and C (large handling time) show destabilizing effect of the Holling type II functional response, panel D and E shows the stabilizing and destabilizing effect of the Holling type III functional response, panel F shows the stabilizing effect of the Beddington-deAngelis functional response (2.15) when handling time is neglected ($h = 0$). Dashed lines are isoclines. Parameters: $r = 1$, $\lambda = 1$, $e = 0.2$, $h = 0.02$, $m = 1$ (except panel E where $m = 5.5$). The upper ceiling for the Holling type I functinal response was set to 10.

response is zero ($h = 0$). Thus, prey-predator population dynamics are described by

$$\frac{dR}{dt} = rR - \frac{\lambda R}{1 + zC}C,$$

$$\frac{dC}{dt} = (g(R, C) - m)C.$$

At the population equilibrium the first stability condition (2.18) simplifies to $\frac{\partial g(R^*, C^*)}{\partial C} < 0$ which means that the predator growth must be negatively density dependent. The second stability condition (2.19) simplifies to $\frac{\partial g(R^*, C^*)}{\partial R} > 0$, which holds provided the numerical response increases with increasing prey density. This analysis implies that density dependent predator growth stabilizes prey-predator population dynamics when handling times are neglected (Figure 2.9F). Depending on the parameters, positive handling times can surpass the stabilizing effect of predator interference leading to an unstable equilibrium.

## 2.5.2 Prey growth is density dependent

Now I consider the case where the per capita prey growth rate is density dependent and decreases with increasing prey density ($\frac{dr(R)}{dR} < 0$). The simplest prototype of such dependence is a linear decrease in the per capita prey growth rate ($r(R) = r(1 - \frac{R}{K})$), which is then the logistic equation with the carrying capacity $K$. Limitation of prey growth by resources (here modeled as the environmental carrying capacity $K$) is also called the bottom-up regulation. Clearly, the negative density dependent prey growth promotes prey–predator coexistence because the prey growth is now controlled by two independent mechanisms: top-down and bottom-up regulation. This is reflected in stability condition (2.18) where the left hand side of the inequality is smaller for the negative density dependent prey growth rate when compared with exponentially growing prey.

The Lotka–Volterra model with the logistic prey growth rate is

$$\begin{aligned} \frac{dR}{dt} &= rR\left(1 - \frac{R}{K}\right) - \lambda RC, \\ \frac{dC}{dt} &= (e\lambda R - m)C. \end{aligned}$$

(2.22)

Provided $K > \frac{m}{e\lambda}$, the interior equilibrium of this system is

$$R^* = \frac{m}{e\lambda} \quad \text{and} \quad C^* = \frac{(eK\lambda - m)r}{eK\lambda^2}$$

and local stability conditions (2.18) and (2.19) hold for all parameter values. Using the first integral $V$ given by formula (2.5) as a Lyapunov function it is easy to see that this equilibrium is globally asymptotically stable (i. e., all trajectories of model (2.22) with initially both populations present converge to this equilibrium). Indeed, function $V$ decreases along the trajectories of model (2.22)

because

$$\frac{dV(R(t), C(t))}{dt} = -\frac{r}{K}(R(t) - R^*)^2 \leq 0.$$

Replacing the linear functional response in model (2.22) by the Holling type II functional response leads to the Rosenzweig–MacArthur prey–predator model (Rosenzweig and MacArthur 1963)

$$
\begin{aligned}
\frac{dR}{dt} &= rR\left(1 - \frac{R}{K}\right) - \frac{\lambda R}{1 + \lambda h R}C, \\
\frac{dC}{dt} &= \left(\frac{e\lambda R}{1 + \lambda h R} - m\right)C.
\end{aligned}
\tag{2.23}
$$

Provided the following two conditions are met

$$m < \frac{e}{h} \quad \text{and} \quad K > \frac{m}{\lambda(e - mh)}$$

the prey–predator equilibrium is

$$R^* = \frac{m}{(e - hm)\lambda} \quad \text{and} \quad C^* = \frac{er(\lambda K(e - mh) - m)}{K(e - hm)^2 \lambda^2}.$$

Local stability condition (2.18) holds for carrying capacities that meet the following constraint

$$K < \frac{e + hm}{\lambda h(e - hm)} := K_{crit}.$$

Stability condition (2.19) holds for all parameter values. Using the Dulac criterion it can be proved that no limit cycles exist and the equilibrium is globally asymptotically stable (Figure 2.10A). At the critical carrying capacity $K_{crit}$ the equilibrium undergoes the Hopf bifurcation and for higher carrying capacities a unique globally stable limit cycle exists (Figure 2.10B). This model shows that prey–predator coexistence is not limited to an equilibrium. In fact, as the environmental carrying capacity ($K$) increases, the stable interior equilibrium is destabilized and a globally stable limit cycle appears (Hofbauer and Sigmund 1998). This phenomenon was termed the paradox of enrichment because, contrary to the intuition, enriched environments (i. e., environments with a higher $K$) do not promote species coexistence at an equilibrium (Rosenzweig 1971). This paradox is easy to understand, because an increase in the environmental carrying capacity means a weaker bottom-up regulation, thus a less stable prey–predator population dynamics due to the destabilizing Holling type II functional response.

### 2.5.3 Effects of the optimal diet choice on predator-prey dynamics

The previous section assumed a single prey or resource. Here I consider a system consisting of two resource types denoted by a preferred resource $R_1$, and an alternative resource $R_2$, respectively, and consumers $C$. Following van Baalen et al. (2001) I assume that the abundance of the alternative
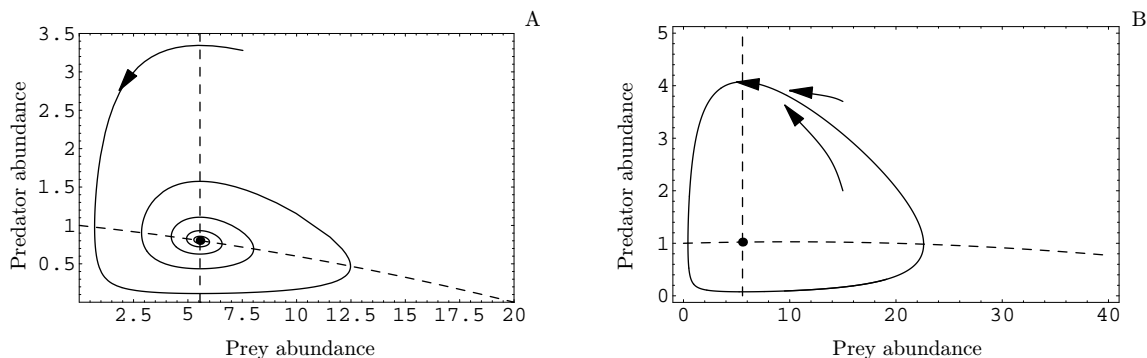
Figure 2.10: Prey-predator dynamics for the MacArthur–Rosenzweig model (2.23). Panel A shows the case where the carrying capacity is below the critical level $K_{crit}$ ($K = 20$) and the equilibrium is globally asymptotically stable. Panel B shows that for higher carrying capacities ($K = 70$) there exists a globally stable limit cycle along which prey coexist with predators. Dashed lines are isoclines. Parameters: $r = 1$, $\lambda = 1$, $e = 0.2$, $h = 0.02$, $m = 1$.

resource is relatively constant in the environment, i. e., this resource does not undergo population dynamics. This effectively means that uptake of the alternate resource by consumers is exactly compensated by resource production. This simplification is justified for many arthropod consumers because they can rely on alternative food such as pollen or nectar, the availability of which is unlikely to be influenced by the consumption (van Rijn and Sabelis 1993; van Rijn and Tanigoshi 1999). The presence of the alternative resource influences the consumer per capita growth rate which, in turn, has consequences for the abundance and the dynamics of the primary resource population. A generic framework to describe the dynamics of this system is:

$$
\begin{aligned}
\frac{dR_1}{dt} &= r_1(R_1)R_1 - f_1(R_1, R_2)C \\
\frac{dC}{dt} &= C\left(e_1 f_1(R_1, R_2) + e_2 f_2(R_1, R_2) - m\right).
\end{aligned}
\tag{2.24}
$$

Here $r_1$ denotes the per capita resource 1 growth rate, $f_i$ is the functional response with respect to the corresponding resource type, $e_i$ is the proportionality constant that describes efficiency with which resources are converted to new consumers and $m$ is the consumer mortality rate. I assume that the functional responses are of the Holling type II and they are given by (2.16) and (2.17).

I start the analysis of model (2.24) under the assumption that the preferred resource undergoes density-independent dynamics, i. e., $r_1(R_1) = r_1$. If consumers are non-adaptive foragers (i. e., $u_2$ is independent of resource one density in (2.16)) and (2.17)), condition (2.20) for local asymptotic stability of the corresponding resource 1–consumer equilibrium

$$
R_1 = \frac{m + R_2 \left(mh_2 u_2 - e_2\right)\lambda_2}{\left(e_1 - mh_1\right)\lambda_1}, \quad C = \frac{r_1 \left(e_1 + R_2 \left(e_1 h_2 u_2 - e_2 h_1\right)\lambda_2\right)}{\left(e_1 - mh_1\right)\lambda_1}
\tag{2.25}
$$

cannot be satisfied because the functional response for the first resource does not satisfy stability
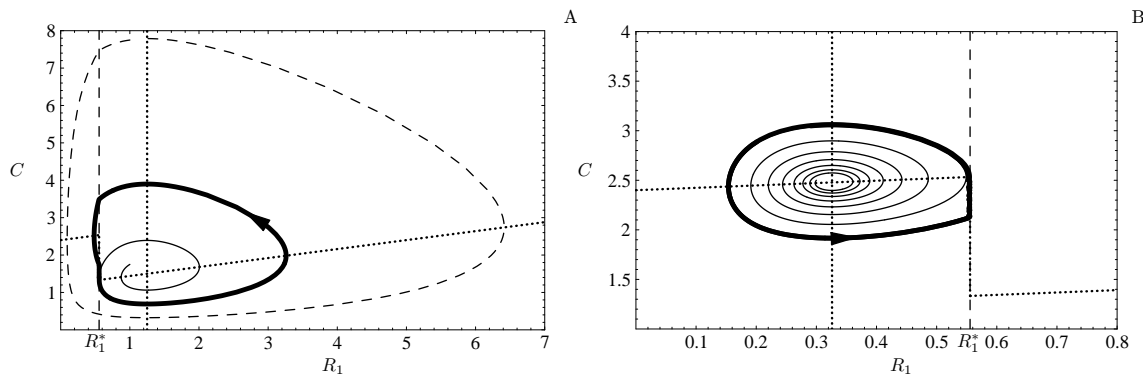
Figure 2.11: Resource–consumer phase plane with consumer and resource isoclines (dotted lines) for optimal diet model. When consumer mortality rate is above the profitability of the alternative resource ($m > e_2/h_2$) then the equilibrial resource 1 density is above the switching density (Figure A, $m = 1$). For low consumer mortality rates the equilibrial resource 1 density is below the switching density (Figure B, $m = 0.4$). In both cases consumer switching behavior leads to the emergence of a locally stable limit cycle (heavy line) and an unstable limit cycle (shown in Figure A as a dashed cycle). Parameters: $R_2 = 5, r_1 = 1.2, e_1 = 1, e_2 = 0.1, h_1 = 0.2, h_2 = 0.2, \lambda_1 = 1, \lambda_2 = 1$. Figure A after van Baalen et al. (2001).

condition (2.20) as

$$\frac{df_1(R_1, R_2)}{dR_1} - \frac{f_1(R_1, R_2)}{R_1} = -\frac{h_1 R_1 \lambda_1^2}{(h_1 R_1 \lambda_1 + h_2 R_2 u_2 \lambda_2 + 1)^2} < 0.$$

Qualitatively, for small handling times trajectories diverge away from the equilibrium similarly as those shown in Figure 2.9B. Thus, additional food source does not stabilize predator-prey population dynamics with the Holling type II functional response. Moreover, the two species could not coexist indefinitely because there would be a sequence of times at which consumers or resource one would converge to zero.

Now I assume that consumers exhibit adaptive behavior, viz., they follow rules of optimal diet choice model (Section 1.10). This means that in (2.16) and (2.17), $u_2$ is a step function given by (1.43) on page 54. I will show that the discontinuity in the functional response leads to emergence of a limit cycle along which both species can coexist.

Because at $R_1 = R_1^* = \frac{e_2}{\lambda_1(e_1 h_2 - e_2 h_1)}$ the right handside of model (2.24) is discontinuous, solutions are understood in the Filippov sense (Appendix). To understand the consequences of the discontinuity in the functional response on prey–predator population dynamics I examine the system in phase space by plotting the consumer–resource isoclines and the population trajectories about the equilibrium. Because per capita consumer reproduction rate does not depend on consumer density, the consumer isocline is a vertical line (dotted vertical line in Figure 2.11). The discontinuity in the functional response translates into a discontinuity in the isocline for resource 1 at the switching density $R_1^*$—the density of resource 1 where the consumer includes the less profitable resource in its diet. This produces a piecewise linear (dotted skewed line in Figure 2.11)

resource isocline that is z-shaped. By including the less profitable resource, consumers are able to persist because they no longer drive the more profitable resource to critically low densities. The system will oscillate along a limit cycle (the heavy line cycle in Figure 2.11). Qualitatively, there are two possibilities with respect to consumer mortality rate and profitability of the alternative resource. If the consumer mortality rate ($m$) is high such that consumers are unable to exist on the less profitable resource alone (i. e., $m > e_2/h_2$) then the resource 1–consumer equilibrium is

$$R_1 = \frac{m}{(e_1 - mh_1)\,\lambda_1}, \;\; C = \frac{e_1 r_1}{(e_1 - mh_1)\,\lambda_1},$$

that is to the right of the switching density $R_1^*$ (Figure 2.11A), and consumers will be specialists on the preferred resource 1 at this (unstable) equilibrium.

If, on the other hand, consumer mortality rate is low relative to the profitability of the alternative resource 2 (i. e., $m < e_2/h_2$) t the corresponding equilibrium is to the left of the switching line and it is given by (2.25) where $u_2 = 1$. At this (unstable) equilibrium consumers will be predominantly generalists (Figure 2.11B). This analysis suggests an interesting prediction that as the predation risk increases (higher values of consumer mortality rate $m$), consumers should specialize on the more profitable resource type.

Numerical bifurcation analysis reveals (Figure 2.12), however, that the limit cycle shown by the heavy solid line in Figure 2.11 is not globally stable because another, unstable, limit cycle exists (the dashed line cycle in Figure 2.11A). When initial densities of consumers and resource 1 lie beyond the orbit of this unstable limit cycle, the corresponding orbit will spiral outward, thereby precluding indefinite species coexistence. This shows that although optimal diet choice promotes species coexistence, it does not lead to species permanence.

Now I examine bottom-up effects on system dynamics by assuming that resource 1 exhibits logistic growth (i. e., $r_1(R_1) = r_1(1 - \frac{R_1}{K_1})$). When resource limitation is strong, i. e., $K_1$ is small, then population dynamics are effectively stabilized (Figure 2.13A and C). In this case, consumers specialize on the preferred resource when predation mortality is high (Figure 2.13C). The reason for this is that the profitability of the alternative resource is low relative to the magnitude of predation mortality such that it is not worth eating the alternative resource. However, when predation mortality is reduced, the model predicts the topology switch from a linear chain to food web with two resources (Figure 2.13A) because it is now worthwhile to eat the alternative resource. Enriching the system by increasing the environmental carrying capacity $K_1$ (Figure 2.13B and D) causes the system to fluctuate due to the paradox of enrichment (see the Rosenzweig-MacArthur model in Section 2.5.2). So, enriching effectively relaxes bottom-up regulation and causes an increase in the degree of top-down control.
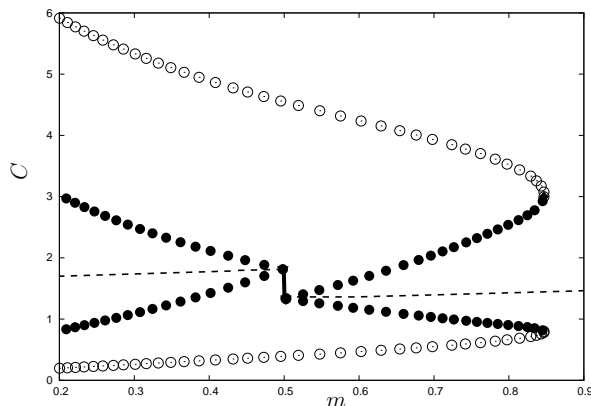
Figure 2.12: Bifurcation diagram of model (2.24) where predators behave as optimal foragers with respect to predator mortality rate $m$. Solid dots denote the stable limit cycle while open circles denote the unstable limit cycle. The dashed curve is the unstable interior equilibrium. Parameters correspond to those given in Figure 2.11.

## 2.6   Patchy environments

The original Lotka-Volterra model does not consider space explicitly. Instead, it assumes that populations are uniformly distributed in space. Spatial structure can be incorporated in the model either as a continuous variable which then leads to reaction-diffusion models (Britton 1986; Murray 1990), or as a discrete variable, which leads to patch models. A key question addressed by spatial prey-predator models is the effect of animal dispersal on the stability of prey-predator dynamics.

Here I start with a simple example that considers two spatial patches (Murdoch et al. 2003). In one patch prey are vulnerable to predation while the other patch is a complete refuge. I assume that up to $S$ prey can be in the refuge and both vulnerable and invulnerable prey reproduce at the same positive rate $r$. This means that the refuge is always fully occupied and animals born in the refuge must disperse to the open patch. Population dynamics in the open patch are described by the Lotka–Volterra model

$$
\frac{dR}{dt} = r(R + S) - \lambda RC,
$$

$$
\frac{dC}{dt} = (e\lambda R - m)C
$$

with equilibrium densities

$$
R^* = \frac{m}{e\lambda}, \;\; C^* = \frac{r}{\lambda} + \frac{re}{m}S.
$$

The recruitment of prey to the open patch makes the per capita prey growth rate $r(1 + S/R)$ in
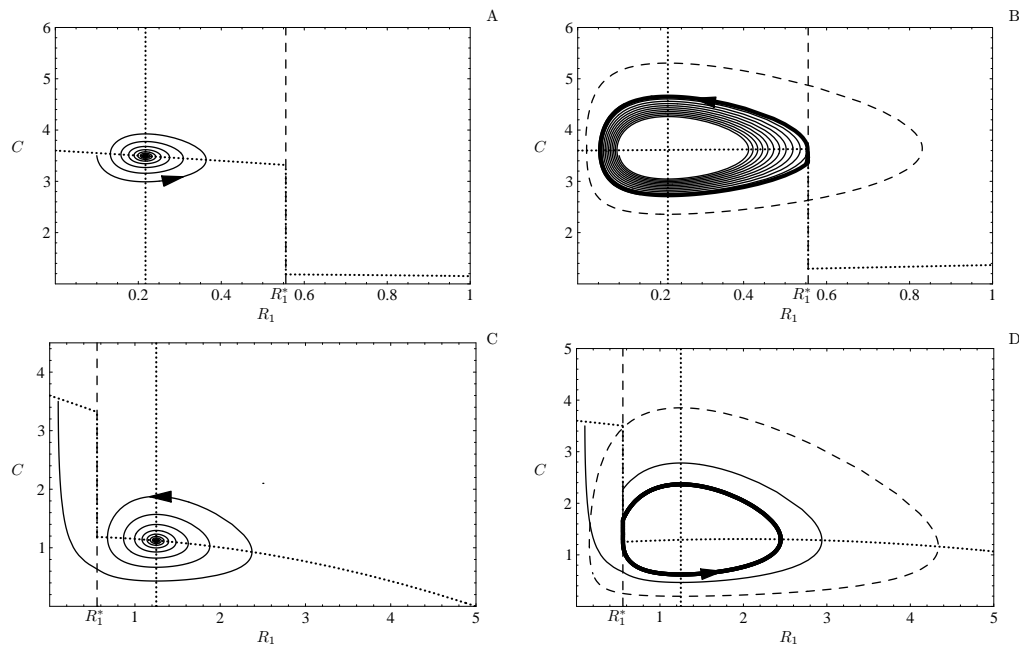
Figure 2.13: Phase plane analysis of model (2.24) where consumers behave as optimal foragers and prey growth is described by the logistic equation. Resource and consumer isoclines are shown as dotted lines. When consumer mortality rate is low ($m = 0.4$) then resource 1 equilibrium density is lower than is the switching density (Figures A and B). On contrary, for higher resource mortality rates the equilibrial resource 1 density is above the switching density (Figures C and D, $m = 1$). For low environmental productivities ($K = 5$ in Figures A and C) population densities are stabilized at an equilibrium. Enriching the environment ($K = 20$ in Figure B and $K = 9$ in Figure D) leads to the emergence of a locally stable limit cycle (heavy line) of smaller amplitude when compared with non-flexible consumers (dashed line cycle). Parameters: $R_2 = 10, r_1 = 1.2, e_1 = 1, e_2 = 0.1, h_1 = 0.2, h_2 = 0.2, \lambda_1 = 1, \lambda_2 = 1$. Figure D after Křivan and Schmitz (2003).

the open patch negatively density dependent (i. e., it decreases with increasing prey abundance $R$) similarly as in the case of the logistic growth. The stability conditions (2.18) and (2.19) hold and the above equilibrium is locally asymptotically stable, which supports the general conclusion from other theoretical studies that refugia that protect a constant number of prey have a strong stabilizing effect on prey–predator population dynamics (Maynard Smith 1974).

This example nicely illustrates stabilizing mechanism of asynchronous oscillations in population densities. In this example, the abundance of prey in the refuge is constant while the abundance of vulnerable prey varies due to demographic changes and recruitment of prey from the refuge. This asynchrony, then leads to the negative density dependent recruitment rate of prey to the vulnerable patch. While this mechanism is clear in this simple example, it is much less obvious in many models that consider space explicitly.

Now I consider a more complex prey–predator model in a heterogeneous environment consisting of $N$ patches. The simplest possible case assumes that all patches are identical and animal dispersal is unconditional (random). The question is whether animal dispersal can stabilize population dynamics that are unstable without dispersal. Because unconditional animal dispersal tends to equalize prey and predator abundance across patches, animal dispersal tends to synchronize animal population dynamics and the answer to the above question is negative. However, patch dependent dispersal rates and/or differences in local population dynamics can lead to asynchrony in local population dynamics, thus to negative density dependent recruitment rates that can stabilize prey–predator population dynamics on a global scale exactly as in the example with the refuge. Figure 2.14 shows the stabilizing effect of prey dispersal in a two-patch environment. Population dynamics are

$$
\begin{aligned}
\frac{dR_1}{dt} &= r_1 R_1 - \frac{\lambda_1 R_1}{1 + h_1 \lambda_1 R_1} C_1 + \varepsilon_2 R_2 - \varepsilon_1 R_1 \\
\frac{dC_1}{dt} &= \frac{e_1 \lambda_1 R_1}{1 + h_1 \lambda_1 R_1} C_1 - m_1 C_1 \\
\frac{dR_2}{dt} &= r_2 R_2 - \frac{\lambda_2 R_2}{1 + h_2 \lambda_2 R_2} C_2 + \varepsilon_1 R_1 - \varepsilon_2 R_2 \\
\frac{dC_2}{dt} &= \frac{e_2 \lambda_2 R_2}{1 + h_2 \lambda_2 R_2} C_2 - m_2 C_2
\end{aligned}
\tag{2.26}
$$

where $\varepsilon_i$ $(i = 1, 2)$ describes prey dispersal between patches. Without dispersal, the local prey–predator population dynamics are unstable due to the Holling type II functional response (Figure 2.14, left panel). Prey dispersal (Figure 2.14, right panel) can stabilize population dynamics at an equilibrium. Similarly, dispersal of predators (or both prey and predators) can (but does not necessarily) stabilize population densities. This mechanism is in the roots of deterministic metapopulation dynamics where populations can coexist on the global spatial scale despite local extinctions. The necessary conditions for such global stability are differences in patch or dispersal dynamics and
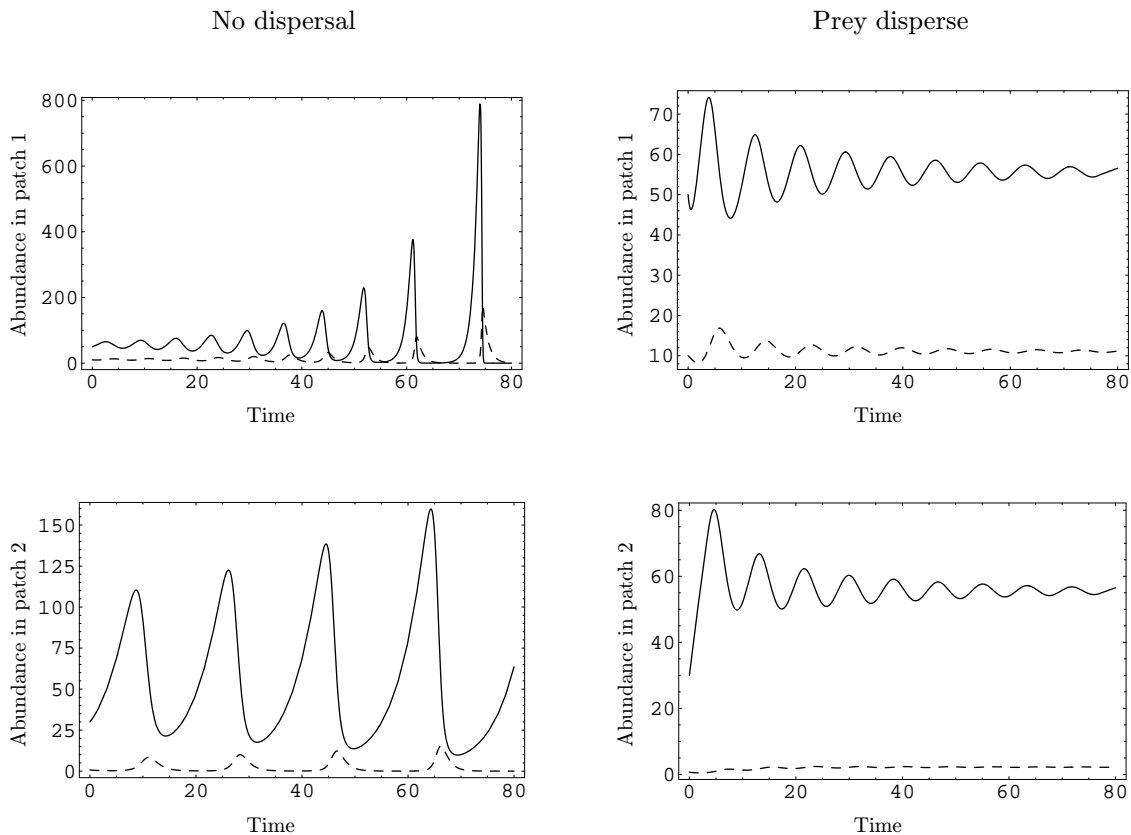
Figure 2.14:  This figure shows the stabilizing effect of dispersal in model (2.26).  The left panel shows prey (solid line) and predator (dashed line) dynamics in patch 1 (top panel) and patch 2 (bottom panel) without any dispersal ($\varepsilon_1 = \varepsilon_2 = 0$).  These dynamics assume the Holling type II functional response which excludes prey and predator coexistence in either patch.  The right panel shows the same system where prey disperse between patches ($\varepsilon_1 = \varepsilon_2 = 1$).  Parameters: $r_1 = 1$, $r_2 = 0.2$, $\lambda_1 = \lambda_2 = 0.1$, $e_1 = e_2 = 0.2$, $h_1 = h_2 = 0.02$, $m_1 = m_2 = 1$.

dispersal rates that are not too high to synchronize local patch dynamics.

## 2.7   Models of competition

The logistic growth is one possible description of intraspecific competition in which members of the same species compete for resources (e. g., habitats, food, sunlight, mates etc.).  Similarly, when two or more species share common resources, presence of one species can exert a negative effect on individuals of another species.  Competition among members of different species (or populations) is called interspecific competition.  The negative effect is manifested by a decrease in fitness that is related to the per capita population growth rate.

The following terms describe mechanisms by which competition occurs, which can generally be

divided into direct and indirect. These mechanisms apply equally to intraspecific and interspecific competition.

1. *Interference competition* - occurs directly between individuals via aggression etc. when the individuals interfere with foraging, survival, reproduction of others, or by directly preventing their physical establishment in a portion of the habitat. Male-male competition in red deer during rut is an example of interference competition within a species.

2. *Exploitation competition* - occurs indirectly through a common limiting resource which acts as an intermediate. For example the use of the resource(s) depletes the amount available to others.

3. *Apparent competition* - occurs indirectly between two species which are both preyed upon by the same predator. For example, species A and species B are both preys for predator C. The increase of species A will cause the decrease of species B because the increase of A's would increase the number of predator C's which in turn will hunt more of species B.

### 2.7.1   Lotka-Volterra model of competition

A direct extension of the logistic growth to two-species setting is called the Lotka–Volterra model of competition

$$
\begin{array}{rcl}
\frac{dM}{dt} & = & r_1 M \left( 1 - \frac{M}{K_1} - \alpha \frac{N}{K_1} \right) \\
\frac{dN}{dt} & = & r_2 N \left( 1 - \frac{N}{K_2} - \beta \frac{M}{K_2} \right).
\end{array}
\tag{2.27}
$$

When alone, both populations grow logistically. Parameters $\alpha$ and $\beta$ model interspecific competition, i. e., the negative effect of individuals of second species on individuals of the first species and vice versa. These interspecific competition are relative with respect to intraspecific competitions (measured as $1/K_i$). Thus, $\alpha = 1$ ($\alpha > 1$, $\alpha < 1$) means that the effect of second species on fitness of the first species is exactly the same (larger, smaller) as is the effect of the first species on its own fitness.

Besides the trivial equilibrium this model has one interior equilibrium

$$
(M^*, N^*) = \left( \frac{K_1 - \alpha K_2}{1 - \alpha \beta}, \frac{K_2 - \beta K_1}{1 - \alpha \beta} \right)
$$

and two equilibria with one species missing $(0, K_2)$, and $(K_1, 0)$. Graphical analysis based on position of isoclines gives the following predictions (Hofbauer and Sigmund 1998):

1. Species 1 outcompetes species 2 when $\alpha < \frac{K_1}{K_2}$ and $\frac{K_2}{K_1} < \beta$. All trajectories converge to $(K_1, 0)$.

2. Species 2 outcompetes species 1 if $\beta < \frac{K_2}{K_1}$ and $\alpha > \frac{K_1}{K_2}$. Trajectories converge to $(0, K_2)$.

3. Both species coexist if $\alpha < \frac{K_1}{K_2}$ and $\beta < \frac{K_2}{K_1}$. Trajectories converge to $(M^*, N^*)$.

4. If $\alpha > \frac{K_1}{K_2}$ and $\beta > \frac{K_2}{K_1}$ then there are two locally stable equilibria $(K_1, 0)$ and $(0, K_2)$ which results in bi-stability of model (2.27). The outcome of competition in this case depends on the sequence in which species arrive which is called "the priority effect". The species that arrives and establishes first survives the invasion of the other species.

The above analysis shows that only in the case where $\alpha\beta < 1$ the two species can coexist. This rule, called now the competitive exclusion principle, was formulated by Gause (1934). In the ecological literature it is rephrased that two species occupying the same niche cannot coexist. Ecological niche is a domain in the space of vitally important environmental factors within which the species existence is possible. Partial or complete overlap of ecological niches for two species leads to competition.

Using the niche concept we extend the 2-species competition model to $n$ species whose densities are $N_i$, $i = 1, \ldots, n$. Let us assume that resources can be characterized by a scalar (or vector) variable $x$ (e. g., the size of food etc.). Moreover, the amount of the resource at $x$ is $K(x)$. Ecological niche for consumer species $i$ is characterized by a probability density function $f_i(x)$ that describes the utilization of resource by individuals of this species. If the variance is small, the species $i$ is highly specialized on a particular food type. Large variance means low specialization, i. e., a wide niche.

The uptake of resource by species $i$ at the point $x$ is given by $f_i(x)N_i(t)$. Then $K(x) - \sum_{i=1}^{n} f_i(x)N_i$ is the free resource at $x$. The Lotka–Volterra competition model becomes

$$\frac{df_i(x)N_i}{dt} = r_i f_i(x) N_i \frac{K(x) - \sum_{i=1}^{n} f_i(x)N_i}{K(x)}.$$

Integrating this equation with respect to resource spectrum yields

$$\frac{dN_i}{dt} = r_i N_i \left( 1 - \frac{\sum_{j=1}^{n} \alpha_{ij} N_j}{K_i} \right) \tag{2.28}$$

where $K_i = \int K(x) f_i(x) dx$ is the total amount of resource consumed by the $i$th species and $\alpha_{ij} = \int f_i(x) f_j(x) dx$ is the coefficient of competition. In this sense the competition coefficient $\alpha_{ij}$ characterizes the niche overlap between two species. Existence of a positive equilibrium (all species present) of model (2.28) implies its global asymptotic stability in $R_+^n$.

PROPOSITION 19 *Let us assume that the positive interior equilibrium of model (2.28) exists. Then it is globally asymptotically stable in $R_+^n$.*

*Proof.* Let $N^* = (N_1^*, \ldots, N_n^*)$ be the positive interior equilibrium. Then function

$$V = \sum_{i=1}^{n} \frac{K_i}{r_i} (N_i - N_i^* \ln N_i)$$

is a Lyapunov function. This follows from the fact that

$$\frac{dV}{dt} = -\sum_{i,j=1}^{n} \alpha_{ij}(N_j^* - N_j)(N_i^* - N_i) = -\int \left(\sum_{i=1}^{n} f_i(x)(N_i^* - N_i)\right)^2 < 0$$

whenever $N \neq N^*$.

$\square$

For many extensions of the above proposition see, e. g., Takeuchi (1996), Hofbauer and Sigmund (1998).

### 2.7.2 Two-Species Competing in Two patches

Here I consider population dynamics of two competing species in a two-habitat environment. I compare two types of population dynamics. The first type assumes that animals do not move between habitats at all, while the second type of population dynamics assumes that at each time the distribution of animals follows the two-species IFD (see Section 1.9.1). These two cases can describe differences in population dynamics of competing sessile organisms versus those that are mobile.

First, let us assume individuals do not move between habitats. This leads to an elementary analysis of the population dynamics since the two-species dynamics in habitat 1 is completely independent of habitat 2. Thus, the dynamics in habitat $i$ are described by the Lotka–Volterra competition model

$$\begin{aligned}
\frac{dm_i}{dt} &= m_i r_i \left(1 - \frac{m_i}{K_i} - \frac{\alpha_i n_i}{K_i}\right), \quad i = 1, 2 \\
\frac{dn_j}{dt} &= n_j s_j \left(1 - \frac{n_j}{L_j} - \frac{\beta_j m_j}{L_j}\right), \quad j = 1, 2.
\end{aligned} \tag{2.29}$$

I remark that the per capita growth rates $1/m_i dm_i/dt$ and $1/n_i dn_i/dt$ are the fitness functions $V_i$ and $W_i$, see formulas (1.35) on page 48. Suppose that at each habitat both species coexist at the stable population equilibrium

$$m_i^* = \frac{K_i - \alpha_i L_i}{1 - \alpha_i \beta_i}, \quad n_i^* = \frac{L_i - \beta_i K_i}{1 - \alpha_i \beta_i}, \quad i = 1, 2.$$

The corresponding prey and predator distributions are $p_i = m_i^*/(m_1^* + m_2^*)$ and $q_i = n_i^*/(n_1^* + n_2^*)$.

Second, let us consider dispersing animals whose spatial distributions $p(M, N) = (p_1(M, N), p_2(M, N))$ and $q(M, N) = (q_1(M, N), q_2(M, N))$ of species 1 and 2, respectively, track the IFD at the current population numbers $N$ and $M$. Population dynamics for overall species densities $M$ and $N$ are then given by the following model

$$\begin{aligned}
\frac{dM}{dt} &= M \left(p_1 V_1(p_1 M, q_1 N) + p_2 V_2(p_1 M, q_1 N)\right) \\
\\
\frac{dN}{dt} &= N \left(q_1 W_1(p_1 M, q_1 N) + q_2 W_2(p_1 M, q_1 N)\right).
\end{aligned} \tag{2.30}$$

There are two conditions that an equilibrium of (2.30) must satisfy. First, as the distribution corresponds to the IFD for any population numbers, when both species occupy both patches we have $V_1 = V_2$ and $W_1 = W_2$. Moreover, at the population equilibrium $M^*$ and $N^*$, the right handside of (2.30) must equal zero which gives $V_1 = V_2 = W_1 = W_2 = 0$, exactly as at the equilibrium of the model without dispersal. Thus, the interior equilibrium $M^* = m_1^* + m_2^*$, $N^* = n_1^* + n_2^*$, $p_i^* = m_i^*/M^*$, $q_i^* = n_i^*/N^*$ in model (2.29) where animals do not move between patches is also the interior equilibrium of model (2.30) where both species disperse and their distribution corresponds to the IFD. The interesting question now is how the stability of the model without dispersal (2.29) compares to the model where animals disperse (2.30). We know that the model without dispersal is globally asymptotically stable in both habitats if and only if $1 - \alpha_1\beta_1 > 0$ and $1 - \alpha_2\beta_2 > 0$. However, there is no relation between these inequalities and inequality (1.36) on page 51 that determines whether distribution $(p^*, q^*)$ is IFD for the population equilibrium densities $M^*$ and $N^*$ when animals do disperse. Thus, it is easy to construct examples which show that there exists a stable population equilibrium for the model without dispersal (2.29) under which the corresponding species distribution is not stable with respect to small spatial spatial perturbations, i. e., it does not correspond to the IFD. Such an example requires two conditions hold: (i) none of the two species can go globally extinct ($\alpha_i < K_i/L_i$ and $\beta_i < L_i/K_i$ for $i = 1, 2$) and condition (1.36) on page 51 holds. Figure 2.15 shows such a case. The upper panel corresponds to the model (2.29) where animals do not disperse and the corresponding animal population equilibrium and distribution are

$$M = N = 11, \quad p_1 = 10/11, \quad q_1 = 1/11. \tag{2.31}$$

However, for the model which assumes dispersal, this spatial distribution at the population equilibrium is not stable with respect to small spatial perturbations (because condition (1.36) on page 51 holds). As we request that at the population equilibrium the corresponding population distribution corresponds to an IFD, (2.31) is not an equilibrium of model (2.30). In fact, for the above equilibrium population densities there exists two IFD distributions ($p = 1, q = 0$ and $p = 0, q = 1$). To make some predictions for population dynamics. we need to analyze all other population equilibria of model (2.30). In addition to the point (2.31), there are seven candidate points for equilibria (Table 2.1; Abrams et al. 2007). However, as it is clear from payoffs at these population numbers, none of the corresponding distribution is a 2-species IFD. This is because at these population distribution the patch where one (both) species are missing has a higher payoff than the occupied patch. We conclude, that model (2.30) has no equilibrium and, consequently, as species cannot go globally extinct, there must be some fluctuations in their population numbers. as I will show now.

Table 2.1: Candidate equilibria of model (2.30) for parametrization corresponding to Figure 2.15.

| $M$ | $N$ | $p_1$ | $q_1$ | payoffs |
|---|---|---|---|---|
| 20 | 10 | $\frac{19}{20}$ | 0 | $V_1 = V_2 = W_2 = 0,\ W_1 > 0$ |
| 12 | 1 | $\frac{5}{6}$ | 1 | $V_1 = V_2 = W_1 = 0,\ W_2 > 0$ |
| 10 | 20 | 1 | $\frac{1}{20}$ | $V_1 = V_1 = W_2 = 0,\ V_2 > 0$ |
| 1 | 10 | 0 | 0 | $V_2 = W_2 = 0,\ V_1 > 0,\ W_1 > 0$ |
| 19 | 19 | 1 | 0 | $V_1 = W_2 = 0,\ V_2 > 0,\ W_1 > 0$ |
| 2 | 2 | 0 | 1 | $V_2 = W_1 = 0,\ V_1 > 0,\ W_2 > 0$ |
| 10 | 1 | 1 | 1 | $V_1 = W_1 = 0,\ V_2 > 0,\ W_2 > 0$ |

To model animal dispersal explicitly, I follow Křivan et al. (2008) (see also Abrams et al. 2007) who combined population dynamics (2.29) with distribution dynamics (1.34) on page 47. This leads to the following model

$$
\begin{aligned}
\frac{dm_i}{dt} &= m_i V_i(m_i, n_i) + \nu(\textstyle\sum_{j=1}^{n} I_{ij}(m,n)m_j - m_i),\ \ i = 1,2 \\
\frac{dn_i}{dt} &= n_i W_i(m_i, n_i) + \xi(\textstyle\sum_{j=1}^{n} J_{ij}(m,n)m_j - m_i),\ \ i = 1,2.
\end{aligned}
\tag{2.32}
$$

In analogy to Section 1.9, $\nu$ and $\xi$ are positive parameters that characterize the relative time scale between population and dispersal processes.

Numerical simulations of model (2.32) with best response distributional dynamics reveal that the stable equilibrium for the population dynamics (Figure 2.15, top panel, no dispersal, $\nu = \xi = 0$) is destabilized when individuals start to disperse (Figure 2.15, middle, $\nu = \xi = 0.01$), leading to periodic cycling in both animal distribution and abundance. As the dispersal process becomes even faster with respect to the population dynamics time scale (Figure 2.15, bottom panel, $\nu = \xi = 0.1$), animal distribution fluctuates wildly (see also Abrams et al. 2007).

In summary, the instability of the interior NE for the dispersal dynamics suggests the combined population/dispersal dynamics will also be unstable at the population equilibrium, especially as the rate of dispersal relative to the population dynamics increases. Moreover, since the boundary IFDs do not correspond to stable population equilibria, we do not expect the combined system to approach an equilibrium solution (and this is illustrated in Figure 2.15, middle and bottom panels). That is, unless the population equilibrium corresponds to an IFD, the game-theoretic perspective predicts non-convergent system behavior. This conclusion contrasts markedly with the single species results of Section 1.7 where I showed that dispersal dynamics cannot destabilize population dynamics.

Species distributions $p_1$, $q_1$         Total population dynamics $M$, $N$
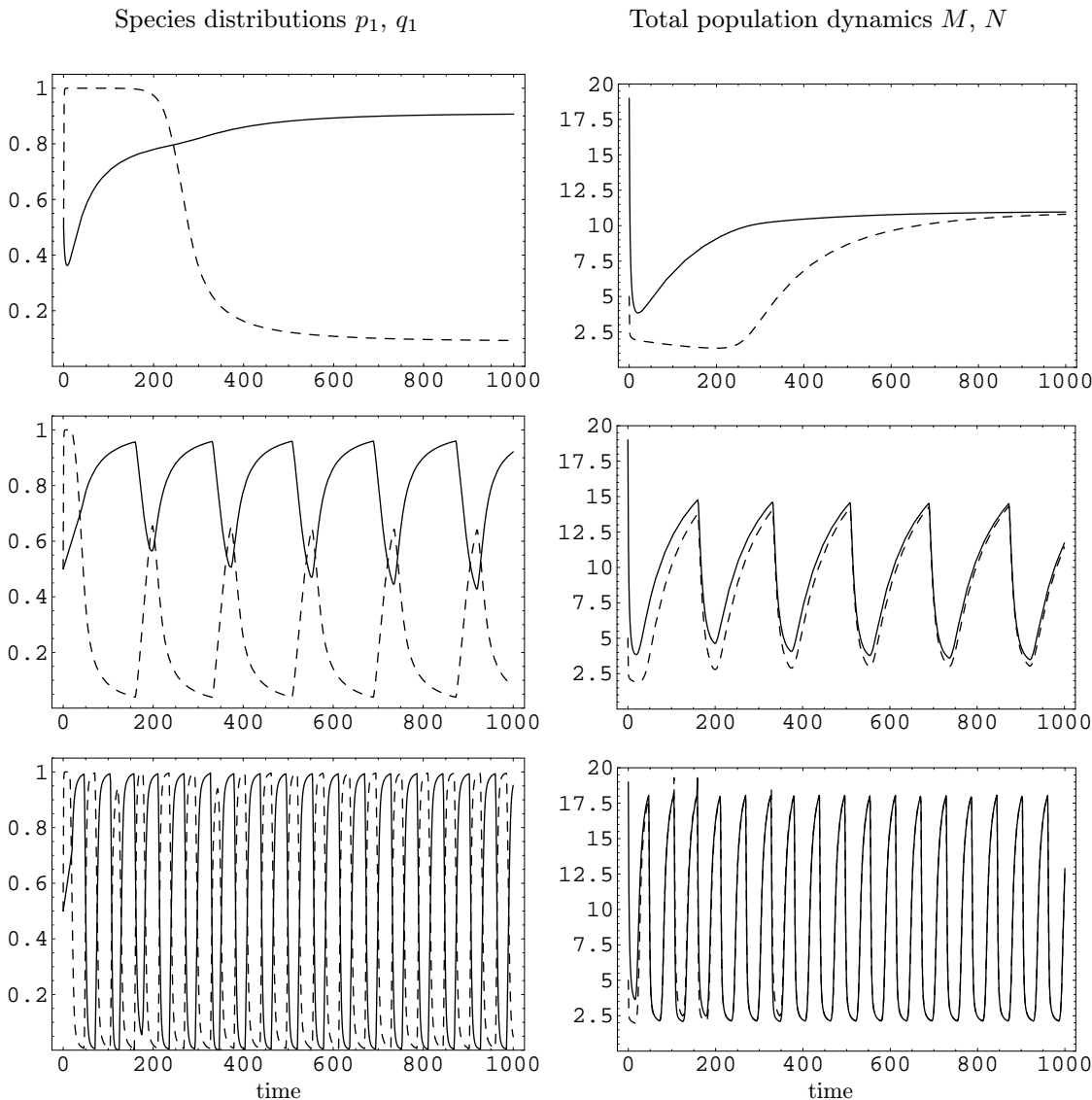


Figure 2.15: Dependence of combined dispersal and population dynamics (see model (2.32)) on dispersal and population time scales. The left panel shows animal distribution ($p_1$-solid line, $q_1$-dashed line) and the right panel shows total animal abundance ($M$-solid line, $N$-dashed line). The upper panel illustrates population dynamics with no animal dispersal ($\nu = \xi = 0$). Here, the system approaches the population equilibrium $M = N = 10$ even though the corresponding interior NE is not an IFD at these densities. The middle panel assumes low animal dispersal ($\nu = \xi = 0.01$) and the bottom panel assumes faster dispersal dynamics ($\nu = \xi = 0.1$). In both these panels, the system appears to be evolving to a limit cycle with the population switching quickly in the bottom panel between the two unstable boundary NE where the two species are segregated into separate patches. Other parameters are $r_1 = 1$, $r_2 = 0.1$, $s_1 = 0.1$, $s_2 = 1$, $K_1 = 19$, $K_2 = 2$, $L_1 = 2$, $L_2 = 19$, $\alpha_1 = 9$, $\alpha_2 = 0.1$, $\beta_1 = 0.1$, $\beta_2 = 9$.

### 2.7.3  Exploitation competition. Tilman's $R^*$ rule

The Lotka–Volterra competition model does not consider resource dynamics. Here I consider competition by two species for a resource that undergoes population dynamics. In particular, I consider competition in chemostat (abbreviated from Chemical environment is static) which is a bioreactor to which fresh medium continuously flows and the culture liquid is continuously removed so that the culture volume is constant. By changing the rate with which medium is added to the bioreactor the growth rate of the microorganism can be easily controlled. I assume that the resource level $R$, without consumers, is kept at a constant level $R = 1$. Competition for the resource in chemostat is described by the following model

$$
\begin{aligned}
\frac{dR}{dt} &= 1 - R - \frac{m_1 N_1 R}{a_1 + R} - \frac{m_2 N_2 R}{a_2 + R} \\
\frac{dN_1}{dt} &= \frac{m_1 N_1 R}{a_1 + R} - N_1 \\
\frac{dN_2}{dt} &= \frac{m_2 N_2 R}{a_2 + R} - N_2.
\end{aligned}
\tag{2.33}
$$

Here the consumption of the resource is described by the Monod function $\left(\frac{mR}{a+R}\right)$ which has the same form as the Holling type II functional response in ecology.

The distinctive feature of this model is the fact that no interior equilibrium exists. There are two equilibria with one consumer missing:

$$
(R_1^*, 0, N_2^*) = \left(\frac{a_1}{m_1 - 1}, 0, 1 - \frac{a_1}{m_1 - 1}\right),
$$

$$
(R_2^*, N_1^*, 0) = \left(\frac{a_2}{m_2 - 1}, 1 - \frac{a_2}{m_2 - 1}, 0\right).
$$

The following proposition, called Tilman's $R^*$ rule in ecology, states that the species that can indefinitely survive at the lower value of the resource wins the competition (Tilman 1982; Tilman 1988).

PROPOSITION 20 (WALTMAN (1983)) *Let $m_1, m_2 > 1$ and $0 < \frac{a_1}{m_1 - 1} < \frac{a_2}{m_2 - 1} < 1$. Then $\lim_{t \to \infty} R(t) = \frac{a_1}{m_1 - 1}$, $\lim_{t \to \infty} N_1(t) = 1 - \frac{a_1}{m_1 - 1}$ and $\lim_{t \to \infty} N_2(t) = 0$ for every solution of (2.33).*

*Proof.* Introducing $S = 1 - R - N_1 - N_2$ transforms system (2.33) to

$$
\begin{aligned}
\frac{dS}{dt} &= -S \\
\frac{dN_1}{dt} &= N_1 \left(\frac{m_1(1 - N_1 - N_2 - S)}{1 + a_1 - N_1 - N_2 - S} - 1\right) \\
\frac{dN_2}{dt} &= N_2 \left(\frac{m_2(1 - N_1 - N_2 - S)}{1 + a_2 - N_1 - N_2 - S} - 1\right).
\end{aligned}
$$

As $S(t) = S(0)e^{-t} \Rightarrow S(t) \to 0$, the above transformation reduces 3D system to 2D system

$$
\begin{aligned}
N_1' &= N_1 \left( \frac{m_1(1 - N_1 - N_2)}{1 + a_1 - N_1 - N_2} - 1 \right) \\
N_2' &= N_2 \left( \frac{m_2(1 - N_1 - N_2)}{1 + a_2 - N_1 - N_2} - 1 \right).
\end{aligned}
$$

Straightforward analysis of this system leads to the result.

$\square$

### 2.7.4 Apparent competition

Here I consider two resource species $R_1$ and $R_2$ that interact indirectly through a shared consumer $C$. A prototype of such a food web can be modeled by the following system of equations

$$
\begin{aligned}
\frac{dR_1}{dt} &= r_1 R_1 - f_1(R_1, R_2)C \\[2mm]
\frac{dR_2}{dt} &= r_2 R_2 - f_2(R_1, R_2)C \\[2mm]
\frac{dC}{dt} &= C \left( e_1 f_1(R_1, R_2) + e_2 f_2(R_1, R_2) - m \right).
\end{aligned}
\tag{2.34}
$$

Similarly to the exploitative competition, the next proposition shows that one resource will be always outcompeted.

PROPOSITION 21 *Let the functional responses $f_1$ and $f_2$ satisfy*

$$
\frac{f_1(R_1, R_2)}{f_2(R_1, R_2)} = \frac{\lambda_1 R_1}{\lambda_2 R_2}.
\tag{2.35}
$$

*Then the resource with the lower value of $r_i / \lambda_i$ is always outcompeted in model (2.34).*

*Proof.* Transformation of (2.34) to cylindrical coordinates $(\rho, \phi, C)$ given by $R_1 = (\rho \cos \phi)^{\lambda_1}$ and $R_2 = (\rho \sin \phi)^{\lambda_2}$ gives the following equation for $\phi$:

$$
\frac{d\phi}{dt} = \frac{1}{2} \left( \frac{r_2}{\lambda_2} - \frac{r_1}{\lambda_1} \right) \rho \sin(2\phi).
\tag{2.36}
$$

It follows that for $r_1/\lambda_1 > r_2/\lambda_2$, $\phi$ tends to zero which implies that the second species is outcompeted by the first species while for $r_1/\lambda_1 < r_2/\lambda_2$ it tends to $\pi/2$ which implies that the first species is outcompeted by the second species.

$\square$

Condition (2.35) holds not only for the linear functional response, but also for two-species Holling type II functional responses in a homogeneous environment $f_i = \lambda_i R_i / (1 + h_1 \lambda_1 R_1 + h_2 \lambda_2 R_2)$.

In the ecological literature competition between two prey species that share a common predator is referred to as predator mediated apparent competition (Holt 1977). If predation is the only regulatory mechanism of prey exponential growth apparent competition will always lead to exclusion of one prey for population dynamics modelled by Lotka–Volterra type differential equations with either a linear or Holling type II functional response. If prey growth is density dependent then both prey species can survive with predators for an appropriate range of parameters (Holt 1977). Thus, in classical models of population ecology, prey density dependence (bottom-up regulation) relaxes the strength of apparent competition making indefinite coexistence of both prey species possible.

## 2.7.5 Parker's matching principle when resources undergo population dynamics

Here I consider a fixed consumer population size while resource densities are treated dynamically. This extends the Parker's matching principle from section 1.5.2 to situations where not all resources are immediately consumed when they enter the system so there is no resource standing stock. Here I relax the assumption on zero standing resource stock keeping fixed consumer abundance.

If there are $n$ patches and resources ($R_i$, $i = 1, \cdots, n$ ) undergo population dynamics, their dynamics in patch $i$ are

$$\frac{dR_i}{dt} = r_i(R_i) - f_i(R_i)p_i C$$

where $r_i$ and $f_i$ are the resource growth rate and the functional response, respectively. As before, $p_i$ is the proportion of consumers in patch $i$ and $C$ is the (fixed) consumer density.

Following derivation of the Parker's matching principle I will assume that consumer payoff in any occupied patch is equal to the individual consumption rate (i. e., $V_i = f_i(R_i)$), that each patch has a resource carrying capacity $K_i$ (i. e., $r_i(K_i) = 0$) and that the resource dynamics converges to an equilibrium $R_i^*$ in each patch. Then, in each occupied patch, $R_i^*$ is a decreasing function of patch density. At this resource equilibrium $r_i(R_i) - f_i(R_i)p_i C = 0$ and derivation of this equality with respect to $p_i$ is

$$\frac{\partial(r_i(R_i) - f_i(R_i)p_i M)}{\partial R_i}\frac{dR_i}{dp_i} - f_i(R_i)C = 0.$$

As $\frac{\partial(r_i(R_i) - f_i(R_i)p_i M)}{\partial R_i}$ is negative at the stable equilibrium, $dR_i/dp_i < 0$ at the equilibrium. Thus, the resource level $R_i^*$ decreases as $p_i$ increases and individual consumer payoff in patch $i$ is a decreasing function of $p_i$. That is, the consumers are playing a habitat selection game (Section 1.5). Since $V_i = f_i(R_i^*) = r_i(R_i^*)/(p_i^* C)$ at equilibrium, the IFD of this habitat selection game is a $p^* \in S_n$ such that $r_i(R_i^*)/(p_i^* C) = r_j(R_j^*)/(p_j^* C) = V^*$ for all occupied patches $i$ and $j$. Furthermore, individual consumer payoff in any unoccupied patch $k$ is $V_k = f_k(K_k) \leq V^*$. In

particular, at the equilibrium,

$$\frac{p_i^*}{p_j^*} = \frac{r_i(R_i^*)}{r_j(R_j^*)}$$

for those patches that are occupied, which is a generalized Parker's matching law (Lessells 1995).

## 2.7.6 The Lotka–Volterra model of apparent competition when consumers are adaptive foragers

In this section I study the consumer distribution when resource-consumer dynamics are described by the Lotka–Volterra model in a two patch environment

$$
\begin{aligned}
\frac{dR_1}{dt} &= r_1 R_1 - u_1 \lambda_1 R_1 C \\
\frac{dR_2}{dt} &= r_2 R_2 - u_2 \lambda_2 R_2 C \\
\frac{dC}{dt} &= (e_1 \lambda_1 R_1 - m_1) u_1 C + (e_2 \lambda_2 R_2 - m_2) u_2 C.
\end{aligned}
\tag{2.37}
$$

In the model, the strategy $u_i$ ($i = 1, 2$, $0 \leq u_i \leq 1$, $u_1 + u_2 = 1$) specifies the proportion of an average consumer's lifetime that is spent feeding in patch $i$. I also assume, without loss of generality, that the intrinsic resource growth rate in patch 1 is higher than that in patch 2 ($r_1 > r_2$).

Proposition 21 shows that for fixed values resource population with the lower ratio $r_i/(\lambda_i u_i)$ goes extinct due to apparent competition (see Section 2.7.4). Thus, the three populations cannot coexist indefinitely if consumer preferences for either resource are fixed.

Now I assume that consumers are omniscient and they instantaneously move to the better patch. In Section 1.5, for fixed resource and consumer densities, the resulting consumer distribution was called the IFD. There is one important distinction between the above model and the model considered in Section 1.5, because now consumer fitness does not directly depend on consumer density. The relation is indirect, because consumer density influences resource density which, in turn, influences consumer fitness. Thus, for fixed resource densities the optimal strategy of a consumer that maximizes its fitness measured as the per capita consumer population growth rate is

$$
u_1(R_1, R_2) \in
\begin{cases}
\{1\} & \text{if } e_1 \lambda_1 R_1 - m_1 > e_2 \lambda_2 R_2 - m_2 \\[2mm]
\{u \mid 0 \leq u \leq 1\} & \text{if } e_1 \lambda_1 R_1 - m_1 = e_2 \lambda_2 R_2 - m_2 \\[2mm]
\{0\} & \text{if } e_1 \lambda_1 R_1 - m_1 < e_2 \lambda_2 R_2 - m_2
\end{cases}
\tag{2.38}
$$

and

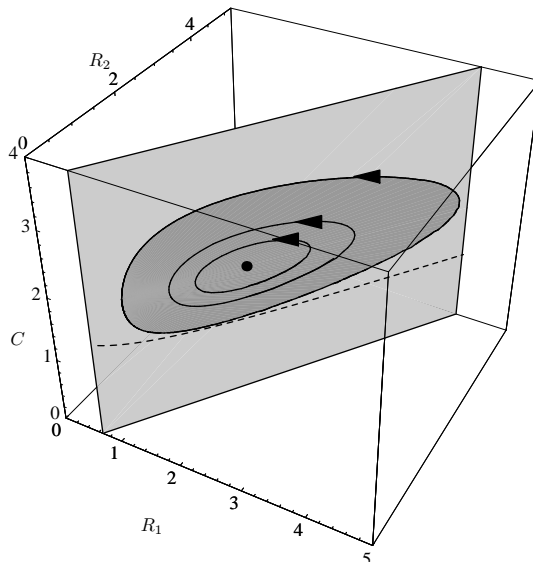$$u_2(R_1, R_2) = 1 - u_1(R_1, R_2).$$

Figure 2.16: A long term dynamics of model (2.37) which is driven by the adaptive consumer patch choice is shown in $(R_1, R_2, C)$ phase density space. All trajectories converge to the global attractor (dark shaded area) which lies in the IFD plane along which consumers fitness in both patches is the same. Population dynamics along this set are described by a family of cycles centered at the neutrally stable equilibrium. As $m_1 > m_2$, the attractor is bounded from below by the dashed line $C = \frac{r_1 - r_2}{\lambda_1} + \frac{r_2(m_1 - m_2)}{e_1 \lambda_1^2 R_1}$. Parameters: $r_1 = 1.5, r_2 = 0.5, m_1 = 0.3, m_2 = 0.2, \lambda_1 = 1, \lambda_2 = 1, e_1 = 0.15, e_2 = 0.1$.

Thus, model (2.37) with consumer strategy (2.38) extends the concept of the IFD to situation where resources undergo population dynamics. This model can be fully analyzed as the following proposition shows.

PROPOSITION 22 (BOUKAL AND KŘIVAN (1999)) *Trajectories of model (2.37) with optimal consumer strategy given by (2.38) converge to a global attractor that is located in the discontinuity plane* $e_1 \lambda_1 R_1 - m_1 = e_2 \lambda_2 R_2 - m_2$. *The attractor is formed by trajectories of*

$$
\begin{aligned}
\frac{dR_1}{dt} &= \frac{R_1(m_1 - m_2 - e_1 \lambda_1 R_1)(\lambda_1 \lambda_2 C - r_1 \lambda_2 - r_2 \lambda_1)}{e_1 \lambda_1 R_1(\lambda_1 + \lambda_2) + \lambda_2(m_2 - m_1)} \\
\frac{dC}{dt} &= (e_1 \lambda_1 R_1 - m_1)C
\end{aligned}
\tag{2.39}
$$

*that satisfy*

$$
C \geq \frac{r_1 - r_2}{\lambda_1} + \frac{r_2(m_1 - m_2)}{e_1 \lambda_1^2 R_1}
$$

*and*

$$
C \geq \frac{e_1 \lambda_1 R_1(r_2 - r_1) + r_2(m_2 - m_1)}{\lambda_2(e_1 \lambda_1 R_1 + m_2 - m_1)}.
$$

*On the attractor, the optimal consumer strategy is*

$$u_1 = \frac{r_1 e_1 \lambda_1 R_1 + (m_1 - m_2 - e_1 \lambda_1 R_1)(r_2 - \lambda_2 C)}{C((\lambda_1 + \lambda_2)e_1 \lambda_1 R_1 + \lambda_2(m_2 - m_1))}.$$

I remark that trajectories of model (2.39) in the plane $e_1 \lambda_1 R_1 - m_1 = e_2 \lambda_2 R_2 - m_2$ are closed curves centered on the equilibrium point

$$R_1^* = \frac{m_1}{e_1 \lambda_1}, \quad R_1^* = \frac{m_2}{e_2 \lambda_2}, \quad C^* = \frac{r_2 \lambda_1 + r_1 \lambda_2}{\lambda_1 \lambda_2}, \tag{2.40}$$

which is neutrally stable exactly as in the case of the classical Lotka–Volterra prey-predator model (Figure 2.16). For the case where $m_2 < m_1$, the global attractor is shown in Figure 2.16 as the dark shaded area.

Proposition 22 shows that consumers will drive resources to levels at which both patches will provide consumers with the same fitness which is the condition for the IFD. Then, consumers will spend a proportion $u_1$ of their life in patch one and proportion $u_2$ in patch 2, so that the fitness will stay the same in both patches. The mechanism leading to this outcome is as follows. Assume, first that the fitness of consumers that use resource patch 1 is higher than the fitness of consumers using resource patch 2 only. Because consumers are assumed to be omniscient, this leads immediately to a redistribution in which all consumers end up in the better patch. This redistribution causes a decrease of resource population growth in patch 1 while resources in patch 2 are no longer limited by their consumers. Consequently, payoff in the consumer free patch will increase in time faster than payoff in the occupied patch. Thus, consumers will again redistribute themselves to maximize fitness. Eventually the redistribution process results in a consumer distribution among patches in which the net fitness of consumers among both patches is identical.

When mortality rates are the same in both patches ($m = m_1 = m_2$), population dynamics on the attractor are given by

$$\begin{aligned}
\frac{dR_1}{dt} &= R_1 \left( \frac{r_1 \lambda_2 + r_2 \lambda_1}{\lambda_1 + \lambda_2} - \frac{\lambda_1 \lambda_2}{\lambda_1 + \lambda_2} C \right) \\
\frac{dC}{dt} &= C(e_1 \lambda_1 R_1 - m)
\end{aligned}$$

and consumer distribution on the attractor is

$$\frac{u_1}{u_2} = \frac{r_1 - r_2 + \lambda_2 C}{r_2 - r_1 + \lambda_1 C}.$$

At the population equilibrium $R_1^* = \frac{m}{e_1 \lambda_1}$ and $C^* = \frac{r_1 \lambda_2 + r_2 \lambda_1}{\lambda_1 \lambda_2}$ the consumer distribution is

$$\frac{u_1^*}{u_2^*} = \frac{r_1 \lambda_2}{r_2 \lambda_1}.$$

When the $\lambda$'s are identical, we recover the Parker's input matching rule (Section 1.5.2) which states that at the population equilibrium consumers distribute themselves among the patches in direct
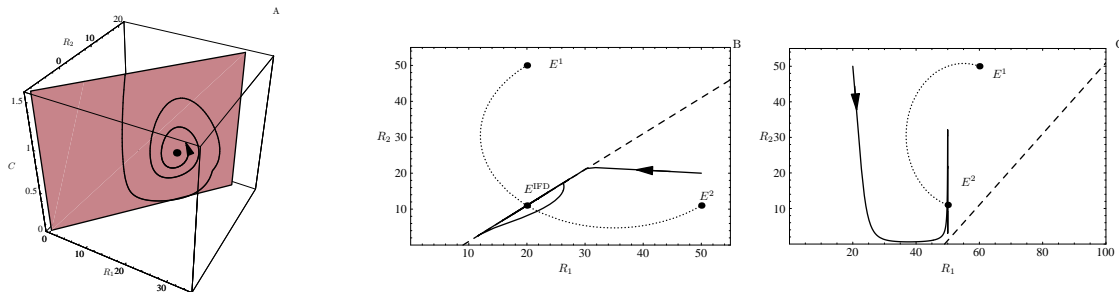
Figure 2.17: Trajectories of model (2.37) with bottom-up control which are driven by the optimal patch choice. For low consumer mortality rates in patch 1 ($m_1 < e_1\lambda_1 K_1$, $m_1 = 2$), the trajectory converges to an equilibrium $E^{\mathrm{IFD}}$ at which the consumer population splits across both patches (Figure A shows a trajectory in the 3D phase space while Figure B shows the projection of same trajectory to the resource 1–resource 2 phase space). When consumer mortality rate is high enough so that patch 1 cannot support consumers at positive levels ($m_1 > e_1\lambda_1 K_1$, $m_1 = 6$), all consumers will be in patch 2 (Figure C). The dashed line is projection of the IFD plane to the resource 1–resource 2 density phase space. $E^1$ is the equilibrium of the linear food chain consisting of resource 1, consumers and predators. As consumers include resource 2 in their diet, the equilibrium moves along the dotted curve toward $E^2$ which corresponds to complete diet shift of consumers to resource 2. Parameters: $r_1 = 0.5, r_2 = 0.4, \lambda_1 = 1, \lambda_2 = 1, K_1 = 50, K_2 = 50, e_1 = 0.1, e_2 = 0.1, m_2 = 1.1$.

proportion to resource supply rate. If the system does not coincide with the resource–consumer equilibrium, the IFD will fluctuate over time as population densities fluctuate along a population cycle.

I now extend previous analysis to consider the effects of adding bottom-up control to our consumer–resource system by making the assumption that resource population dynamics in the system described by model (2.37) are logistic, i. e., $r_i(R_i) = r_i(1 - R_i/K_i)$.

Once again, there are two "pure" strategies for consumers (i. e., stay in patch 1 only, or stay in patch 2 only) with the corresponding equilibria

$$E^1 = (R_1, R_2, C) = \left(\frac{m_1}{e_1\lambda_1}, K_2, \frac{r_1(e_1\lambda_1 K_1 - m_1)}{e_1 K_1 \lambda_1^2}\right)$$

and

$$E^2 = (R_1, R_2, C) = \left(K_1, \frac{m_2}{e_2\lambda_2}, \frac{r_2(e_2 K_2\lambda_2 - m_2)}{e_2 K_2 \lambda_2^2}\right).$$

The population trajectories of model (2.37) with density dependent resource growth tend to converge on the first equilibrium whenever resource densities are such that the consumer fitness in patch 1 is higher than that in patch 2, i. e., when resource densities are in the lower right triangle of the resource 1–resource 2 phase space ($e_1\lambda_1 R_1 - m_1 > e_2\lambda_2 R_2 - m_2$, Figure 2.17B); otherwise densities converge to the second equilibrium. However, if the above equilibria are positive, equilibrium $E^1$ lies in that part of the phase space in which consumers maximize fitness when they are in patch 2 ($e_1\lambda_1 R_1 - m_1 < e_2\lambda_2 R_2 - m_2$) and equilibrium $E^2$ lies in the part of the phase space

where consumer fitness is maximized in patch 1 $(e_1\lambda_1 R_1 - m_1 > e_2\lambda_2 R_2 - m_2)$. This situation leads to a dynamical tension because it prevents the population trajectories from reaching their expected equilibria. Numerical analyses of population dynamics of this system indicates that the trajectories will converge to a new equilibrium point on the IFD plane

$$
\begin{aligned}
R_1^{\text{IFD}} &= \frac{m_1}{e_1\lambda_1}, \\
R_2^{\text{IFD}} &= \frac{m_2}{e_2\lambda_2}, \\
C^{\text{IFD}} &= \frac{r_1(e_1\lambda_1 K_1 - m_1)}{e_1 K_1 \lambda_1^2} + \frac{r_2(e_2 K_2 \lambda_2 - m_2)}{e_2 K_2 \lambda_2^2}
\end{aligned}
$$

exactly as in the case of no density dependence considered in the previous section. This equilibrium point lies at the intersection of the IFD plane $e_1\lambda_1 R_1 - m_1 = e_2\lambda_2 R_2 - m_2$ (shown as the dashed line in Figure 2.17B) with a curve which is obtained by varying consumer patch preference $u_1$ from zero to one (see dotted line in Figure 2.17B). This allows to calculate that the IFD distribution of consumers at this equilibrium is

$$
\frac{u_1^*}{u_2^*} = \frac{r_1 e_2 \lambda_2^2 K_2 (e_1\lambda_1 K_1 - m_1)}{r_2 e_1 \lambda_1^2 K_1 (e_2\lambda_2 K_2 - m_2)}.
$$

The IFD population equilibrium will not be reached whenever consumer mortality rate in patch 1 is so high that the level of productivity in patch 1 is not sufficient to support consumers at positive densities $(K_1 < m_1/(e_1\lambda_1))$. In this case, all consumers will end up in patch 2 (Figure 2.17C).

The above analysis shows that manipulating resource carrying capacities and/or predation mortality on consumers will cause changes in food web topology. If the level of predation mortality is high relative to resource carrying capacity in a patch, i. e., $K_i/m_i$ low, then the system will not persist if both patches have low values of $K_i/m_i$. Alternatively, if both values are high, consumers will use both resource patches. In the other cases, only the patch with the higher $K_i/m_i$ will be used.

## 2.8 Both consumers and predators behave adaptively

Following Křivan (1997), I consider now the case where both species disperse. Suppose the predators with population density $C$ use strategy $v = (v_1, v_2)$ $(v_1 + v_2 = 1)$ and prey with density $R$ use strategy $u = (u_1, u_2)$ $(u_1 + u_2 = 1)$. The corresponding population dynamics are

$$
\begin{aligned}
\frac{dR}{dt} &= (r_1 - \lambda_1 v_1 C) u_1 R + (r_2 - \lambda_2 v_2 C) u_2 R \\
\frac{dC}{dt} &= (e_1 \lambda_1 u_1 R - m_1) v_1 C + (e_2 \lambda_2 u_2 R - m_2) v_2 C.
\end{aligned}
\tag{2.41}
$$

When both prey and predators maximize their fitness at fixed densities $R$ and $C$ we recover the predator-prey habitat selection game studied in Section 1.9.2. There we computed, for each fixed prey and predator density, the corresponding IFD distribution that is also a weak ESS. Here we continue to assume that dispersal is very fast when compared with population dynamics so that as the population numbers change, the species distribution tracks these changing prey and predator numbers.

Let us first consider the case $r_1 > r_2$ and $m_1 > m_2$. From Section 1.9.2 we know there are two thresholds for animal distribution, $R^* = \frac{m_1 - m_2}{e_1 \lambda_1}$ and $C^* = \frac{r_1 - r_2}{\lambda_1}$. For $R < R^*$ animal distribution is $(u_1, v_1) = (1, 0)$ and the corresponding population dynamics are

$$
\begin{aligned}
\frac{dR}{dt} &= r_1 R \\
\frac{dC}{dt} &= -m_2 C.
\end{aligned}
\tag{2.42}
$$

Clearly, all solutions that start in this region will enter the part of the phase space where $R > R^*$. For $R > R^*$ and $C < C^*$ the animal distribution is $(u_1, v_1) = (1, 1)$ and the corresponding population dynamics are

$$
\begin{aligned}
\frac{dR}{dt} &= (r_1 - \lambda_1 C) R \\
\frac{dC}{dt} &= (-m_1 + e_1 \lambda_1 R) C.
\end{aligned}
\tag{2.43}
$$

For $R > R^*$ and $C > C^*$ the animal distribution is $(u_1, v_1) = (\frac{r_1 - r_2 + \lambda_2 C}{(\lambda_1 + \lambda_2) C}, \frac{m_1 - m_2 + e_2 \lambda_2 R}{(e_1 \lambda_1 + e_2 \lambda_2) R})$ and population dynamics are

$$
\begin{aligned}
\frac{dR}{dt} &= \left( \frac{r_1 \lambda_2 + r_2 \lambda_1}{\lambda_1 + \lambda_2} - \frac{\lambda_1 \lambda_2}{\lambda_1 + \lambda_2} C \right) R \\
\frac{dC}{dt} &= \left( -\frac{e_1 \lambda_1 m_2 + e_2 \lambda_2 m_1}{e_1 \lambda_1 + e_2 \lambda_2} + \frac{e_1 \lambda_1 e_2 \lambda_2}{e_1 \lambda_1 + e_2 \lambda_2} R \right) C.
\end{aligned}
\tag{2.44}
$$

Systems (2.43) and (2.44) are Lotka–Volterra prey–predator models with respective equilibria

$$
\begin{aligned}
E^{(2.43)} = (R^{(2.43)}, C^{(2.43)}) &= \left( \frac{m_1}{e_1 \lambda_1}, \frac{r_1}{\lambda_1} \right) \\
E^{(2.44)} = (R^{(2.44)}, C^{(2.44)}) &= \left( \frac{e_1 \lambda_1 m_2 + e_2 \lambda_2 m_1}{e_1 \lambda_1 e_2 \lambda_2}, \frac{r_1 \lambda_2 + r_2 \lambda_1}{\lambda_1 \lambda_2} \right).
\end{aligned}
$$

Both of these equilibria are in the region $R > R^*$ and $C > C^*$. Boukal and Křivan (1999) proved that trajectories converge to a global attractor that is formed by solutions of model (2.44) that are in the region $R > R^*$ and $C > C^*$ of the phase space. For $m_1 > m_2$ the attractor is shown as the shaded area in Figure 2.18. If $m_1 < m_2$ then the two thresholds are $R^* = \frac{m_2 - m_1}{e_2 \lambda_2}$ and $C^* = \frac{r_1 - r_2}{\lambda_1}$ and the attractor is bounded by these two tresholds analogously with the case where $m_1 < m_2$.
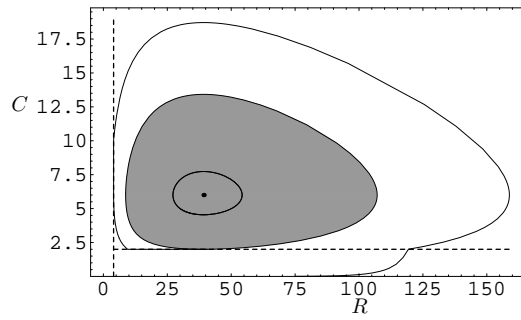
Figure 2.18: Dynamics of the patch model (2.41) where both predators and prey behavior is adaptive. In this figure $m_1 > m_2$, and trajectories converge to a global attractor (shaded area).

## 2.9 APPENDIX

### 2.9.1 Existence and uniqueness of Filippov solutions

Here I review some results on existence and uniqueness of solutions of differential equations with discontinuous right-hand sides. I considered dynamics of interacting populations that are described by a differential equation

$$x'(t) = f(x(t), u(t)) \tag{2.45}$$

where $x \in R^n$, $f : R^n \times R^m \mapsto R^n$, and $u$ is a control from a given set $U \subset R^m$ of admissible controls. Together with (2.45) there is given a set-valued map $S$ that associates to any $x$ a subset $S(x)$ of $U$. I will assume that the map $S$ is set-valued only along a manifold $M$ of a lower dimension. The map $S$ defines a feedback map that associates to every state $x$ a set of corresponding controls, i. e.,

$$u(t) \in S(x(t)). \tag{2.46}$$

Solutions of (2.45), (2.46) are couples $(x(t), u(t))$ where $x$ is an absolutely continuous function that satisfies (2.45) almost everywhere and $u$ is a measurable function that satisfies (2.46) everywhere (Aubin and Cellina 1984; Deimling 1992; Filippov 1988). Under some weak assumptions (continuity of $f$, upper semicontinuity of $S(x)$), the above model is equivalent with differential inclusion

$$x' \in F(x) := f(x, S(x)) \tag{2.47}$$

in the sense that for every solution $x(t)$ of (2.47) there exists a measurable function $u(t)$ such that (2.45) holds (Filippov 1962; Aubin and Cellina 1984).

The above system can be seen either as a differential inclusion or, equivalently, as a Filippov solution of a differential equation with a discontinuous right-hand side, see (Filippov 1988). Indeed, the above system is equivalent to the following differential

inclusion

$$x' \in F(x) := f(x, S(x)), \tag{2.48}$$

see (Aubin and Cellina 1984). Since $S$ is single-valued with the exception of points belonging to the set $M$ that has a lower dimension, (2.45) is a single-valued differential equation at points that do not belong to the set $M$. The right-hand side of (2.45) cannot be continuously defined at points of $M$, thus I may consider (2.45) as a differential equation with a discontinuous right-hand side. The Filippov solution of such an equation is then defined as a solution of (2.48), see (Filippov 1988). I give here two existence results that apply in several cases of practical interest.

PROPOSITION 23 (AUBIN AND CELLINA (1984),FILIPPOV (1988)) *Let $f : \mathbf{R}^n \times U \to \mathbf{R}^n$ be a continuous map which is linear in u. If the strategy map S has closed graph and non empty*

*convex values, then for any initial condition $(t_o, x_o)$ there exist a (strictly) positive $T$, an absolutely continuous $x : [t_o, t_o + T] \rightarrow \mathbf{R}^n$ and a bounded measurable $u : [t_o, t_o + T] \rightarrow U$ that satisfy (2.45),(2.46).*

In several cases solutions of (2.48) are uniquely defined despite the non-uniqueness in the right handside. In general, right uniqueness follows from one-sided Lipschitz condition, namely

$$\langle f_1 - f_2, x_1 - x_2 \rangle \leq L \|x_1 - x_2\|^2, \quad \text{for every } f_i \in F(x_i), \ \ i = 1, 2,$$

where $L$ is a Lipschitz constant and $\langle \cdot, \cdot \rangle$ stands for the scalar product in $\mathbf{R}^n$, see (Filippov 1988). This condition may not be easy to verify, but if I assume that $M$ splits $\mathbf{R}^n$ into two parts that I denote by $G_1$ and $G_2$, then right uniqueness follows from Proposition below. I denote by $u_i$ the unique value of the control $u$ in $G_i$. Let $f_i(x)$ denote the unique value of (2.45) for $x \in G_i$ ($i = 1, 2$). For $x$ such that $x \in M$, $f_1(x)$ denotes the limit of $f_1$ at the point $x$ from the region $G_1$ and similarly for $f_2$. By $n(x)$ I denote the normal vector to $M$ at $x$ oriented from $G_2$ towards $G_1$.

If $f$ is not linear in $u$ the existence and uniqueness of solutions of (2.45) may still be proved. For $x \in M$ I assume that $S(x)$ is an interval with the endpoints $u_i$.

PROPOSITION 24 (FILIPPOV (1988)) *Let $M$ be a $C^2$ manifold, $f$, $\frac{\partial f}{\partial u}$, $u_i \in C^1$ and*

$$\frac{\partial \langle n, f(x, u) \rangle}{\partial u} \neq 0 \ \text{ for all } \ u \in S(x).$$

*If for each $t \in \mathbf{R}_+$ at each point $x \in M$ at least one of the inequalities $\langle n(x), f_2(t, x) \rangle > 0$ or $\langle n(x), f_1(t, x) \rangle < 0$ is fulfilled, then for each initial condition there exists a unique solution of (2.48).*

Since Proposition 24 does not require the map $f(x, u)$ to be linear in $u$ it may be applied to (1.9). Thus using the above Propositions I get that for any initial condition there exists an unique solution of (1.9) and (2.6) which satisfy $u_i \in S_i(x)$.

# Bibliography

Abrams, P., R. Cressman, and V. Křivan. 2007. The role of behavioral dynamics in determining the patch distributions of interacting species. American Naturalist 169:505–518.

Aubin, J.-P., and A. Cellina. 1984. Differential inclusions. Springer-Verlag, Berlin, Germany.

Banks, C. J. 1957. The behavior of individual coccinellid larvae on plants. Animal Behaviour 5:12–24.

Bélisle, C., and J. Cresswell. 1997. The effects of a limited memory capacity on foraging behavior. Theoretical Population Biology 52:78–90.

Belovsky, G. E., and O. J. Schmitz. 1994. Plant defenses and optimal foraging by mammalian herbivores. Journal of Mammalogy 75:816–832.

Berec, L., and V. Křivan. 2000. A mechanistic model for partial preferences. Theoretical Population Biology 58:279–289.

Berec, M., V. Křivan, and L. Berec. 2006. Asymmetric competition, body size and foraging tactics: testing an ideal free distribution in two competing fish species. Evolutionary Ecology Research 8:929–942.

Binmore, K. 1992. Fun and Games. D. C. Heath, Lexington, Massachusetts.

Blanckenhorn, W. U., C. Morf, and M. Reuter. 2000. Are dung flies ideal-free distributed at their oviposition and mating site? Behaviour 137:233–248.

Boukal, D., and V. Křivan. 1999. Lyapunov functions for Lotka-Volterra predator-prey models with optimal foraging behavior. Journal of Mathematical Biology 39:493–517.

Britton, N. F. 1986. Reaction-diffusion equations and their applications to biology. Academic Press, London, UK.

Brown, J. S. 1998. Game theory and habitat selection. Pages 188–220, *in* L. A. Dugatkin and K. R. Hudson, eds. Game theory & animal behavior. Oxford University Press, New York, NY, USA.

Brown, J. S., and B. P. Kotler. 2004. Hazardous duty pay and the foraging cost of predation. Ecology Letters 7:999–1014.

Brown, J. S., and P. A. Alkon. 1990. Testing values of crested porcupine habitats by experimental food patches. Oecologia 83:512–518.

Brown, J. S., and T. L. Vincent. 1987. A theory for the evolutionary game. Theoretical Population Biology 31:140–166.

Brown, J. S., B. P. Kotler, and A. Bouskila. 2001. Ecology of fear: Foraging games between predators and prey with pulsed resources. Ann. Zool. Fennici 38:71–87.

Bulmer, M. 1994. Theoretical evolutionary ecology. Sinauer, Sunderland.

Cardinale, B. J., J. J. Weis, A. E. Forbes, K. J. Tilmon, and A. R. Ives. 2006. Biodiversity as both a cause and consequence of resource availability: a study of reciprocal causality in a predator-prey system. Journal of Animal Ecology 75:497–505.

Charnov, E. L. 1976. Optimal foraging: attack strategy of a mantid. American Naturalist 110:141–151.

Charnov, E. L., and G. H. Orians. 1971. Optimal foraging: Some theoretical considerations. http://hdl.handle.net/1928/1649.

Cressman, R. 1992. The stability concept of evolutionary game theory: a dynamic approach (Lecture notes in biomathematics, no 94). Springer-Verlag, Berlin, Germany.

Cressman, R. 1996. Frequency-dependent stability for two-species interactions. Theoretical Population Biology 49:189–210.

Cressman, R. 2003. Evolutionary Dynamics and Extensive Form Games. The MIT Press, Cambridge MA.

Cressman, R., and J. Hofbauer. 2005. Measure dynamics on a one-dimensional continuous trait space: theoretical foundations for adaptive dynamics. Theoretical Population Biology 67:47–59.

Cressman, R., and V. Křivan. 2006. Migration dynamics for the ideal free distribution. The American Naturalist 168:384–397.

Cressman, R., V. Krivan, and J. Garay. 2004. Ideal free distributions, evolutionary games, and population dynamics in multiple-species environments. American Naturalist 164:473–489.

Dall, S. R. X., B. P. Kotler, and A. Bouskila. 2001. Attention, 'apprehension' and gerbils searching in patches. Ann. Zool. Fennici 38:15–23.

Dawkins, R. 1976. The selfish gene. Oxford University Press, Oxford.

Deimling, K. 1992. Multivalued differential equations. DeGruyter, Basel.

Diffendorfer, J. E. 1998. Testing models of source-sink dynamics and balanced dispersal. Oikos 81:417–433.

Doncaster, C. P., J. Clobert, B. Doligez, L. Gustafsson, and E. Danchin. 1997. Balanced dispersal between spatially varying local populations: An alternative to the source-sink model. American Naturalist 150:425–445.

Elliott, N. C., and R. W. Kieckhefer. 2000. Response by coccinellids to spatial variation in cereal aphid density. Population Ecology 42:81–90.

Evans, E. W. 2003. Searching and reproductive behaviour of female aphidophagous ladybirds (Coleopptera: Coccinellidae): a review. European Journal of Entomology 100:1–10.

Evans, E. W., and T. R. Toler. 2007. Aggregation of polyphagous predators in response to multiple prey: ladybirds (Coleoptera: Coccinellidae) foraging in alfalfa. Population Ecology 49:29–36.

Filippov, A. F. 1962. On certain questions in the theory of optimal control. SIAM J. Control and Optimization 1(1):76–84.

Filippov, A. F. 1988. Differential equations with discontinuous righthand sides. Kluwer Academic Publishers, Dordrecht.

Fraser, D. F., and F. A. Huntingford. 1986. Feeding and avoiding predation hazard: the behavioral response of the prey. Ethology 73:56–68.

Frazer, B. D. 1988. Coccinellidae. Pages 217–230, *in* A. K. Minks and P. Harrewijn, eds. Aphids; Their Biology, Natural Enemies and Control, Volume B. Elsevier, Amsterdam.

Fretwell, D. S., and H. L. Lucas. 1970. On territorial behavior and other factors influencing habitat distribution in birds. Acta Biotheoretica 19:16–32.

Gause, G. F. 1934. The struggle for existence. Williams and Wilkins, Baltimore.

Gause, G. F., N. P. Smaragdova, and A. A. Witt. 1936. Further studies of interaction between predators and prey. The Journal of Animal Ecology 5:1–18.

Gilpin, M. E. 1975. Group selection in predator-prey communities. Princeton University Press, Princeton, NJ, USA.

Hanson, J., and L. Green. 1989. Foraging decisions: Prey choice by pigeons. Animal Behaviour 37:429–443.

Harper, D. G. C. 1982. Competitive foraging in mallards: 'ideal free' ducks. Animal Behaviour 30:575–584.

Hastings, A. 1983. Can spatial variation alone lead to selection for dispersal? Theoretical Population Biology 24:244–251.

Hodek, I., and A. Honěk. 1996. Ecology of Coccinellidae. Kluwer, Dordrecht.

Hofbauer, J., and K. Sigmund. 1998. Evolutionary games and population dynamics. Cambridge University Press, Cambridge.

Holbrook, S. J., and R. J. Schmitt. 1988. The combined effects of predation risk and food reward on patch selection. Ecology 69:125–134.

Holling, C. S. 1966. The functional response of invertebrate predators to prey density. Memoirs of the Entomological Society of Canada 48:5–88.

Holt, R. D. 1977. Predation, apparent competition, and the structure of prey communities. Theoretical Population Biology 12:197–229.

Holt, R. D. 1985. Population dynamics in two-patch environments: Some anomalous consequences of an optimal habitat distribution. Theoretical Population Biology 28:181–208.

Holt, R. D., and M. Barfield. 2001. On the relationship between the ideal-free distribution and the evolution of dispersal. Pages 83–95, *in* J. C. E. Danchin, A. Dhondt and J. Nichols, eds. Dispersal. Oxford University Press.

Honěk, A. 1980. Population density of aphids at the time of settling and ovariole maturation in *coccinella septempunctata* [*col. : coccinellidae*]. Entomophaga 25:427–430.

Honěk, A. 1982. Factors which determine the composition of field communities of adult aphidophagous Coccinellidae (Coleoptera). Zeitschrift für angewandte Entomologie 94:157–168.

Houston, A. I., and J. M. McNamara. 1988. The ideal free distibution whet competitive abilities differ: an approach based on statistical mechanics. Animal Behaviour 36:166–174.

Houston, A. I., and J. M. McNamara. 1999. Models of adaptive behaviour. Cambridge University Press, Cambridge, UK.

Houston, A. I., J. M. McNamara, and M. Milinski. 1995. The distribution of animals between resources - a compromise between equal numbers and equal intake rates. Animal Behaviour 49:248–251.

Hugie, D. M., and T. C. Grand. 1998. Movement between patches, unequal competitors and the ideal free distribution. Evolutionary Ecology 12:1–19.

Hugie, D. M., and T. C. Grand. 2003. Movement between habitats by unequal competitors: effects of finite population size on ideal free distributions. Evolutionary Ecology Research 5:131–153.

Ives, A. R., P. Kareiva, and R. Perry. 1993. Response of a predator to variation in prey density at three hierarchical scales: lady beetles feeding on aphids. Ecology 74:1929–1938.

Ives, P. M. 1981. Estimation of Coccinellid numbers and movement in the field. Canadian Entomologist 113:981–997.

Jackson, A. L., E. Ranta, P. Lundberg, V. Kaitala, and G. D. Ruxton. 2004. Consumer-resource matching in a food chain when both predators and prey are free to move. Oikos 106:445–450.

Kennedy, M., and R. D. Gray. 1993. Can ecological theory predict the distribution of foraging animals? A critical analysis of experiments on the ideal free distribution. Oikos 68:158–166.

Kotler, B. P., J. S. Brown, A. Bouskila, S. Mukherjee, and T. Goldberg. 2004. Foraging games between gerbils and their predators: Seasonal changes in schedules of activity and apprehension. Israel Journal of Zoology 50:255–271.

Kotler, B. P., L. Blaustein, and J. S. Brown. 1992. Predator facilitation: the combined effect of snakes and owls on the foraging behavior of gerbils. Ann. Zool. Fennici 29:199–206.

Krebs, J. R., J. T. Erichsen, M. I. Webber, and E. L. Charnov. 1977. Optimal prey selection in the great tit (*Parus major*). Animal Behaviour 25:30–38.

Křivan, V. 1997. Dynamic ideal free distribution: Effects of optimal patch choice on predator-prey dynamics. American Naturalist 149:164–178.

Křivan, V. 2007. The Lotka-Volterra predator-prey model with foraging-predation risk trade-offs. American Naturalist 170:771–782.

Křivan, V., and E. Sirot. 2002. Habitat selection by two competing species in a two-habitat environment. American Naturalist 160:214–234.

Křivan, V., and I. Vrkoč. 2000. Patch choice under predation hazard. Theoretical Population Biology 58:329–340.

Křivan, V., and O. J. Schmitz. 2003. Adaptive foraging and flexible food web topology. Evolutionary Ecology Research 5:623–652.

Křivan, V., R. Cressman, and C. Schneider. 2008. The Ideal Free Distribution: A review and synthesis of the game theoretic perspective. Theoretical Population Biology 73:403–425.

Lessells, C. M. 1995. Putting resource dynamics into continuous free distribution models. Animal Behaviour 49:487–494.

Lima, S. L. 1998a. Nonlethal effects in the ecology of predator-prey interactions. Bioscience 48:25–34.

Lima, S. L. 1998b. Stress and decision making under the risk of predation: Recent developments from behavioral, reproductive, and ecological perspectives. Stress and Behavior 27:215–290.

Losos, J. B., T. W. Schoener, R. B. Langerhans, and D. A. Spiller. 2006. Rapid temporal reversal in predator-driven natural selection. Science 314:1111–1111.

Lotka, A. J. 1926. Elements of physical biology. Williams and Wilkins, Baltimore.

Mangel, M., and C. W. Clark. 1988. Dynamic modeling in behavioral ecology. Princeton University Press, Princeton, NJ, USA.

Maynard Smith, J. 1974. Models in ecology. Cambridge University Press, Cambridge, UK.

Maynard Smith, J. 1982. Evolution and the theory of games. Cambridge University Press, Cambridge, UK.

Maynard Smith, J., and G. R. Price. 1973. The logic of animal conflict. Nature 246(2):15–18.

McNamara, J. M., and A. I. Houston. 1987. Partial preferences and foraging. Animal Behaviour 35:1084–1099.

McPeek, M. A., and R. D. Holt. 1992. The evolution of dispersal in spatially and temporally varying environments. The American Naturalist 140:1010–1027.

Milinski, M. 1979. An evolutionarily stable feeding strategy in sticklebacks. Zeitschrift für Tierpsychologie 51:36–40.

Milinski, M. 1988. Games fish play: making decisions as a social forager. Trends in Ecology and Evolution 3:325–330.

Milinski, M., and G. A. Parker. 1991. Competition for resources. Pages 137–168, *in* J. R. Krebs and N. B. Davies, eds. Behavioural ecology: An evolutionary approach. Oxford.

Mooij, W. M., R. E. Bennetts, W. M. Kitchens, and D. L. DeAngelis. 2002. Exploring the effect of drought extent and interval on the florida snail kite: interplay between spatial and temporal scales. Ecological Modelling 149:25–39.

Morris, D. W. 2003. Shadows of predation: habitat-selecting consumers eclipse competition between coexisting prey. Evolutionary Ecology 17:393–422.

Murdoch, W. W. 1969. Switching in general predators: Experiments on predator specificity and stability of prey populations. Ecological Monographs 39:335–354.

Murdoch, W. W., C. J. Briggs, and R. M. Nisbet. 2003. Consumer-Resource Dynamics. Princeton University Press, Princeton, New Jersey.

Murray, J. D. 1990. Mathematical biology. Springer-Verlag, Berlin.

Osawa, N. 2000. Population field studies on the aphidophagous ladybird beetle *harmonia axyridis* (coleoptera: Coccinellidae): resource tracking and population characteristics. Population ecology 42:115–127.

Parker, G. A. 1978. Searching for mates. Pages 214–244, *in* J. R. Krebs and N. B. Davies, eds. Behavioural ecology: an evolutionary approach. Blackwell, Oxford.

Parker, G. A. 1984. Evolutionarily stable strategies. Pages 30–61, *in* J. R. Krebs and N. B. Davies, eds. Behavioural ecology: An evolutionary approach. Blackwell, Oxford, UK.

Parker, G. A., and R. A. Stuart. 1976. Animal behavior as a strategy optimizer: Evolution of resource assessment strategies and optimal emigration thresholds. The American Naturalist 110:1055–1076.

Peacor, S. D., and E. E. Werner. 2001. The contribution of trait-mediated indirect effects to the net effects of a predator. Proceedings of the National Academy of Sciences of the USA 98:3904–3908.

Preisser, E. L., D. I. Bolnick, and B. M. F. 2005. Scared to death? the effects of intimidation and consumption in predator-prey interactions. Ecology 86:501–509.

Pulliam, H. R., and B. J. Danielson. 1991. Sources, sinks, and habitat selection - a landscape perspective on population-dynamics. The American Naturalist 137:S50–S66.

Pulliam, H. R., and T. Caraco. 1984. Living in groups: Is there an optimal group size? Pages 122–147, *in* J. R. Krebs and N. B. Davies, eds. Behavioural ecology: An evolutionary approach. Blackwell, Oxford.

Růžička, Z., and R. Zemek. 2007. Deterrent effects of larval tracks on conspecific larvae in *cycloneda limbifer*. BioControl xx:xxx–xxx.

Rechten, C., M. Avery, and A. Stevens. 1983. Optimal prey selection: why do great tits show partial preferences? Animal Behaviour 31:576–584.

Regelmann, K. 1984. Competitive resource sharing - a simulation-model. Animal Behaviour 32:226–232.

Relyea, R. A., and J. R. Auld. 2004. Having the guts to compete: how intestinal plasticity explains costs of inducible defences. Ecology Letters 7:869–875.

Rosenzweig, M. L. 1971. Paradox of enrichment: Destabilization of exploitation ecosystems in ecological time. Science 171:385–387.

Rosenzweig, M. L., and R. H. MacArthur. 1963. Graphical representation and stability conditions of predator-prey interactions. The American Naturalist 97:209–223.

Selten, R. 1980. A note on evolutionarily stable strategies in asymmetrical animal conflicts. Journal of theoretical Biology 84:93–101.

Shevitz, D., and B. Paden. 1994. Lyapunov stability theory of nonsmooth systems. IEEE Transaction on Automatic Control 39:1910–1914.

Sih, A. 1998. Game theory and predator-prey response races. Pages 221–238, *in* L. A. Dugatkin and K. R. Hudson, eds. Game theory & animal behavior. Oxford University Press, New York, NY, USA.

Sinervo, B., and C. M. Lively. 1996. The rock-paper-scissors game and the evolution of alternative male strategies. Nature 380:240–243.

Sinervo, B., E. Svensson, and T. Comendant. 2000. Density cycles and an offspring quantity and quality game driven by natural selection. Nature 406:985–988.

Solomon, M. E. 1949. The natural control of animal populations. The Journal of Animal Ecology 18:1–35.

Stamps, J. A. 2001. Habitat selection by dispersers: integrating proximate and ultimate approaches. Pages 230–242, *in* J. Clobert, E. Danchin, A. A. Dhondt and J. D. Nichols, eds. Dispersal. Oxford University Press, Oxford.

Stephens, D. W., and J. R. Krebs. 1986. Foraging theory. Princeton University Press, Princeton, NJ, USA.

Sutherland, W. J. 1996. From individual behaviour to population ecology. Oxford University Press, Oxford.

Svirezhev, Y. M., and D. O. Logofet. 1983. Stability of biological communites. Mir Publishers, Moscow, USSR.

Takeuchi, Y. 1996. Global dynamical properties of Lotka-Volterra systems. World Scientific Publishing Company, Singapore.

Taylor, P. 1979. Evolutionarily stable strategies with two types of player. Journal of Applied Probability 16:76–83.

Taylor, P. D., and L. B. Jonker. 1978. Evolutionary stable strategies and game dynamics. Math. Biosci. 40:145–156.

Thomas, L. C. 1986. Games, theory and applications. Ellis Horwood Limited, Chichester, UK.

Tilman, D. 1982. Resource competition and community structure. Princeton University Press, Princeton, NJ, USA.

Tilman, G. D. 1988. Plant strategies and the dynamics and structure of plant communities. Princeton University Press, Princeton, NJ, USA.

Tregenza, T. 1994. Common misconceptions in applying the ideal free distribution. Animal Behaviour 47:485–487.

Turchin, P., and P. Kareiva. 1989. Aggregation in *aphis varians:* an effective strategy for reducing predation risk. Ecology 70:1008–1016.

van Baalen, M., V. Křivan, P. C. J. van Rijn, and M. Sabelis. 2001. Alternative food, switching predators, and the persistence of predator-prey systems. The American Naturalist 157:512–524.

van der Werf, W., E. W. Evans, and J. Powell. 2000. Measuring and modelling the dispersal of *coccinella septempunctata* (Coleoptera:Coccinellidae) in alfalfa fields. European Journal of Entomology 97:487–493.

van Rijn, P. C. J., and L. Tanigoshi. 1999. The contribution of extrafloral nectar to survival and reproduction of the predatory mite *Iphiseius degenerans* on *Ricinus communis*. Experimental & Applied Acarology 23:281–296.

van Rijn, P. C. J., and M. W. Sabelis. 1993. Does alternative food always enhance biological control? The effect of pollen on the interaction between western flower thrips and its predators. Bulletin IOBC/VPRS 16:123–125.

Vincent, T. L., and J. S. Brown. 2005. Evolutionary Game Theory, Natural Selection and Darwinian Dynamics. Cambridge University Press, Cambridge, UK.

Volterra, V. 1926. Fluctuations in the abundance of a species considered mathematically. Nature 118:558–560.

Waltman, P. 1983. Competition models in population biology. Society for Industrial and Applied Mathematics, Philadelphia, USA.

Weibull, J. W. 1995. Evolutionary game theory. The MIT Press, Cambridge.

Weisser, W. W. 2001. The effects of predation on dispersal. Pages 180–188, *in* J. Clobert, E. Danchin, A. A. Dhondt and J. D. Nichols, eds. Dispersal. Oxford University Press, Oxford.

Werner, E. E., and J. F. Gilliam. 1984. The ontogenetic niche and species interactions in size-structured populations. Annual Review of Ecology and Systematics 15:393–425.

Werner, E. E., and S. D. Peacor. 2003. A review of trait-mediated indirect interactions in ecological communities. Ecology 84:1083–1100.

Wikelski, M., and C. Thom. 2000. Marine iguanas shrink to survive el nino - changes in bone metabolism enable these adult lizards to reversibly alter their length. Nature 403:37–38.

Yalden, D. W. 2000. Shrinking shrews. Nature 403:826–826.